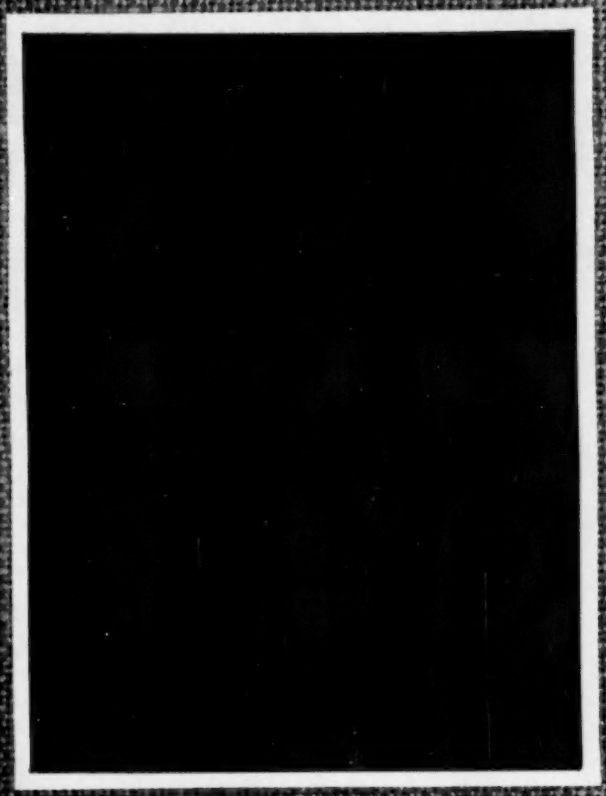

one of a series

"WE USED TO COOL THE BEER IN THE NITRITE BUCKET."

This came from one who spent an undergraduate summer in the dyehouse. Alas! Many summers have passed since a batch of D&D colors caused him an anticipatory thirst. Now, what with dashpots and helipots, he has little time during the working day for suds pots. Which brings us to a more pertinent question than you may at first recognize: Did you know that Wallerstein has as good a name in beer as in textiles? One Wallerstein enzyme protects beer against chill haze, and another Wallerstein biochemical minimizes the effect of O_2 on the brew's flavor. That cold bottle our friend drew from the bucket so long ago...that cool glass you hope to make friends with after the reports are done tonight...had you suspected they owe so much to Wallerstein?

Here you were thinking that all we make is Rapidase® and Serizyme®! Why, the enzymes we make are used in everything from tanning compounds to chocolate milk amplifiers. Not that we are suggesting a flavored fiber, mind, but we have shelves full of commercial, development and experimental enzymes that might be put to use by you in some untrodden avenue of textile research. The purity of these enzymes ranges from AR grade on down. If you care to tell us a bit about your requirements, perhaps we could send you one or two to look at.

WALLERSTEIN COMPANY
Division of Baxter Laboratories, Inc.
Staten Island 3, N.Y.

Interested in Cellase,™ a high potency cellulase? Write Dept. R-7.

TEXTILE RESEARCH JOURNAL

Volume 31 — *July 1961* — Number 7

Editor:
Richard K. Toner

Production Editor:
Dorothy Dana Hollmann

Advisory Board

Herbert J. Ball
Earl E. Berkley
John Boulton
C. H. Fisher
Walter J. Hamburger
Milton Harris
R. M. Hoffman
Harold P. Lundgren
Herman Mark
Edward R. Schwarz
George Switlyk
Helmut Zahn

TEXTILE RESEARCH JOURNAL, published monthly at Prince and Lemon Streets, Lancaster, Pa., is devoted to the interest of research in textile and allied industries. It is published by Textile Research Institute.

Manuscripts and communications should be sent to the Publications Department, P.O. Box 625, Princeton, N. J.

Second-class postage paid at Lancaster, Pa.

Subscription rates: $25.00 per year; additional for postage, 50 cents to Canada, $1.00 to all other countries. Single copies, $2.50 each.

Contents copyright © 1961 by Textile Research Institute. Advertising rates supplied on request.

IN THIS ISSUE

Graft Polymerization of Acrylamide onto Cotton Fabric for Further Treatments. *H. Kamogawa and T. Sekiya* 585

Isocyanate Modification of Wool in Dimethyl Sulfoxide. *N. H. Koenig* 592

Thermal Neutron Irradiation of Cotton. *Florine A. Blouin, Jett C. Arthur, Jr., Rollin S. Orr, and Vega J. Ott* 597

Converting the Fibrograph to Automatic Direct-Reading Operation. *P. R. Ewald and Smith Worley, Jr.* 602

The Effect of Blending Cottons of Dissimilar Fiber Properties upon Spinning Performance and Yarn Quality. *William T. Waters and Joe Phillips* 608

The Supercontraction of Sound and Weathered Keratin Fibers. *O. A. Swanepoel* 618

Relaxation Shrinkage of Wool Fabrics: Its Release with Regain and Time. *K. Baird* 624

Measurement of the Modulus of Dynamic Elasticity of Staple Fibers. *H. G. Weyland* 629

The Load–Extension Properties of Warp Knitted Fabrics. *D. L. Cook and P. Grosberg* 636

Softness of Cotton Yarns as Affected by Fiber and Yarn Properties. *Edith Honold and James N. Grant* 643

The Molecular Structure and Mechanical Properties of Polyethylene Terephthalate Fibers. *I. M. Ward* 650

Dimensional Changes in Multicomponent Systems of Fabrics. A Theoretical Study. *Joel Lindberg* 664

LETTERS TO THE EDITOR

Further Simplifications of the Vibraweigh Method. *G. F. Bush* 670

Some Aspects of the Wash-and-Wear Problem. *Joel Lindberg* 671

Effects of Buffers on Formaldehyde-Curing of Amidoximate Hydrochloride of Partially Cyanoethylated Cotton. *Michiharu Negishi, Heihachiro Itō, and Toshiyuki Kuramochi* 673

BOOK REVIEWS 676

IN COMING ISSUES 678

REPRINT REQUESTS SHOULD BE DIRECTED TO THE AUTHORS
SEE ARTICLES FOR ADDRESSES

JULY 1961
VOL. 31 NO. 7

TEXTILE RESEARCH JOURNAL

Graft Polymerization of Acrylamide onto Cotton Fabric for Further Treatments

H. Kamogawa and T. Sekiya

The Textile Research Institute of the Japanese Government, 4 Sawatari, Kanagawa, Yokohama, Japan

Abstract

Effects of variables in the graft polymerization of acrylamide onto cotton fabric using ceric ammonium nitrate as catalyst have been investigated. Trials to impart a durable creaseproofing effect to the polyacrylamide-grafted fabric by the incorporation of cross-links between graft chains of different cellulose molecules by means of a methylene-bisamide linkage (–$CONHCH_2HNOC$–) have been made. A sharp maximum is found in the values of the apparent amount of grafting plotted against the pH values of treating solutions; correlations of effects of these variables with the mechanism of polymerization are described. Data are presented to explain the formation of a chemical bond between cellulose and polyacrylamide by means of solubility characteristics in cuprammonium solution. Data on durability to acid extraction and alkaline laundering, as well as on mechanical properties of the aftertreated fabrics, the most excellent of which is obtained by the acid-cure of methylolated polyacrylamide-grafted fabric alone, or particularly with adipamide, are also given.

Introduction

It is well known that cellulosic materials such as cotton and viscose rayon can be grafted with various vinyl polymers either by high energy irradiation or by chemical initiators. Mino and Kaizerman [3] reported that ceric salts, including ceric ammonium nitrate, could initiate graft polymerization of acrylamide and other monomers to polyvinylalcohol. They stated that ceric salts could also initiate graft polymerization onto cellulose, although details were not given.

Our present investigation is concerned with this problem, and the study has been further extended to include the secondary treatment of polyacrylamide-grafted cotton with various reactive compounds, including formalin and methylol derivatives of urea, ethyleneurea, melamine, and adipamide. Methylol derivatives of polyacrylamide-grafted cotton have also been prepared for further treatment with compounds having excellent reactivity with methylolamide groups (—$CONHCH_2OH$) of the grafted cotton, such as adipamide, urea, ethyleneurea, melamine, and glycerol, or for cross-linking alone.

One purpose of these procedures is to impart a durable, wrinkle-resistant finish to cotton fabric by combining the wrinkle-resistant finish achieved by the usual procedures with the durable finish achieved by graft polymerization. Another aim of the study is to alleviate strength losses caused by the usual wrinkle-resistant finishes (e.g., by dimethylolethyleneurea) by means of grafting followed by cross-linking between graft chains.

Experimental

Materials

Commercial acrylamide (AM) from American Cyanamid Co. was recrystallized twice with benzene-acetone; reagent grade ceric ammonium nitrate (Ce^{IV}) was used as received. Adipamide ($H_2NOC-(CH_2)_4CONH_2$) was synthesized from adipic acid and phosphorus trichloride by a usual procedure (m.p. 220° C.). Methylol derivatives of urea, melamine, etc., were prepared in aqueous solutions by the usual methylolation reaction with formalin by base catalysis. Other reagents were used as received. Cotton poplin (40's) employed in the treatments was desized and scoured.

Graft Polymerization of Acrylamide

A typical procedure for the graft polymerization of acrylamide onto cotton fabric is as follows. An approximately 10-g. sample of the desized and scoured cotton fabric was impregnated with AM-monomer and ceric ammonium nitrate by immersing the fabric in a 100-ml. aqueous solution. The pH values of the treating bath were adjusted by addition of acid. The polyacrylamide (PAM)-grafted fabric thus produced was extracted with hot water by means of a Soxhlet extractor for 8 hr. to remove water-soluble materials, such as AM-monomer, ungrafted surface polymer, and cerium compounds. The apparent amounts of grafting were determined by the Kjeldahl procedure.

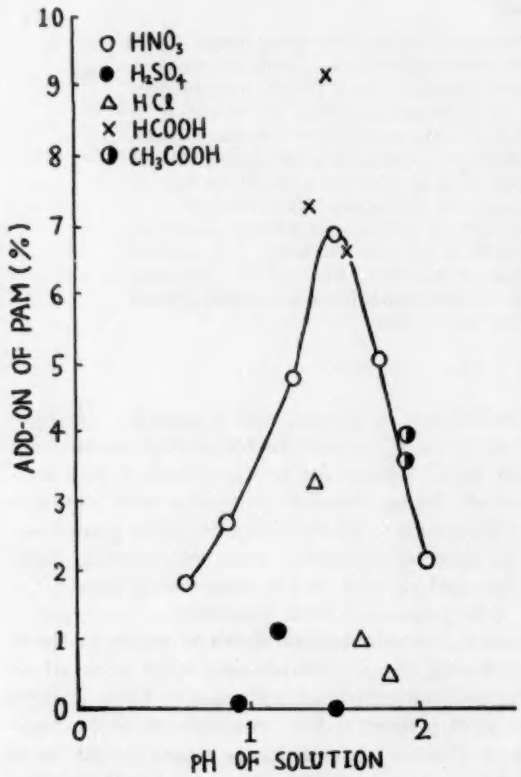

Fig. 1. Variation of polymer add-on with the kinds and amount of acids added. All experiments were carried out at 25° C. for 30 min. with 5% monomer and 0.1% Ce^{IV} concentration.

Methylolation of the PAM-Grafted Cotton Fabric

The following is given as typical of the procedures used to prepare methylolated PAM-grafted fabrics by base catalysis. An approximately 100-g. piece of fabric was immersed for 1 hr. at 25° C. in a 10% aqueous HCHO solution, the pH value of which was regulated with sodium hydroxide to about 11 [1]. The methylolated fabric thus formed was neutralized with acetic acid, scoured with water to remove free HCHO, and air dried.

Secondary Treatments

PAM-grafted or PAM-grafted and subsequently methylolated fabrics were padded with aqueous solutions of an acid catalyst, such as ammonium chloride, and cross-linking materials, such as formalin, dimethylolethyleneurea, trimethylolmelamine, adipamide, and glycerol. The fabrics were then dried, cured, and scoured by the usual procedure.

Testing Methods

Crease resistance of the treated fabric was determined with the Monsanto Wrinkle Recovery Tester. Elmendorf tear strength and Custom Universal abrasion resistance (edge) were also deter-

TABLE I. Effect of Ce^{IV} Concentration upon Polymer Add-On*

Ce^{IV} concentration, %	pH of treating bath†	Add-on of PAM, %	Solution polymerization
0.02	1.9	1.36	None
0.05	1.8	0	None
0.10	1.8	5.03	Slight
0.15	1.7	5.96	Slight
0.20	1.7	6.07	Slight

* All experiments were carried out for 30 min. at 25°C. with 5% AM concentration.

† 0.1% conc. HNO_3 was added to each treating bath.

mined. With some samples, tensile strength and elongation at break were measured with the Instron.

Results and Discussion

Effect of Variables in the Graft Polymerization of Acrylamide onto Cotton Fabric

As illustrated in Figure 1, the kinds of acids added as well as the pH values of the treating baths affect considerably the apparent amount of PAM grafted. A plausible mechanism for the graft polymerization may be given as follows.

$$[Ce^{IV}X_6] + \text{Cell}{=}\underset{\underset{OH}{|}}{C}{-}H \rightleftharpoons \text{Complex} \xrightarrow{K_i} \text{Cell}{=}\underset{\underset{OH}{|}}{C}\cdot + Ce^{III} + H^+ \quad (1)$$

$$\text{Cell}{=}\underset{\underset{OH}{|}}{C}\cdot + M \longrightarrow \text{Cell}{=}\underset{\underset{OH}{|}}{C}{-}M\cdot \xrightarrow{K_p} \text{graft polymer} \quad (2)$$

where M represents AM monomer and X may be a negative ion such as OH, NO_3, or a water molecule.

The appearance of a maximum when the amount of grafting is plotted against the pH values of the treating solutions in the case of the addition of nitric acid can be attributed to a somewhat peculiar feature of the termination reaction of polymer radicals. In a redox system of ceric nitrate-3-chloro-1-propanol, it was found that the rate of polymerization is independent of Ce^{IV} concentration [4]. This fact may possibly indicate that the termination reaction takes place as follows.

$$R\cdot + [Ce^{IV}X_6] \xrightarrow{K_t} \text{dead polymer} + Ce^{III} + H^+ \quad (3)$$

where R· represents a polymer radical.

In this case, however, the relationship between the amount of grafting and Ce^{IV} concentration is the usual one, as shown in Table I. Since the usual termination by radical recombination is strictly limited in the case where the graft polymer molecules have only slight mobility, a possible explanation of this phenomenon lies in assuming that the termination of either radicals formed from ceric salt and cellulose molecule or their end products is accelerated by their contact with oxygen in the air. Therefore, at lower ceric ion concentrations, oxygen is more effective in terminating the reaction than ceric salt, causing lower values of add-on of polymer; at higher concentrations, this relation is reversed and almost constant values are obtained, unless solution polymerization is initiated. The pH dependence in Figure 1 might be interpreted as due to the fact that rate constants of both initiation (K_i) and termination (K_t) are affected by the amount of acid added. It may be that, at higher pH values than about 1.5, increase of K_i with addition of acid is more rapid than that of K_t, while this relation is reversed at lower values.

TABLE II. Effect of AM-Concentration upon Polymer Add-On*

AM concentration, %	Ce^{IV} concentration, %	PAM add-on, %	Solution polymerization
2	0.1	0	None
5	0.1	4.55	None
10	0.1	5.03	Slight
15	0.1	16.9	Considerable
10	0.15	15.9	Considerable

* All experiments were carried out for 30 min. at 25°C. pH values of the baths were regulated to 1.8 with nitric acid.

Differences in add-on of polymer depending on the kinds of acid added can be attributed to the formation of complex compounds among ceric ion, acid anion, and other substances described above. Dependence of the amount of add-on of polymer upon monomer concentration, temperature, and time of polymerization are usual, as shown in Tables II, III, and IV. The amount of grafting appears to increase with higher values of these variables, although, with higher temperature and AM concentration, considerable solution polymerization can be observed in the treating bath.

Solubility Test for Grafting

PAM-grafted cotton samples (uncured) were dissolved in cuprammonium solution, in which both

TABLE III. Effect of Time of Polymerization upon Polymer Add-On*

Ce^{IV} concentration, %	Time of polymerization, min.	Add-on of PAM, %	Solution polymerization
0.1	10	0.92	None
0.1	20	4.50	Slight
0.1	30	5.03	Slight
0.05	30	0	None

* All experiments were carried out at 25°C. with 5 % AM concentration. The pH values of the baths were regulated to 1.7 with nitric acid.

TABLE IV. Effect of Temperature of Polymerization upon Polymer Add-On*

Temperature of polymerization, °C.	pH of treating bath	Add-on of PAM, %	Solution polymerization
25	1.7	5.03	Slight
50	1.7	4.55	Considerable
70	1.6	11.3	Considerable

* All experiments were carried out at 5% AM—and 0.1% Ce^{IV}—concentration for 30 min. pH values of treating baths were regulated with nitric acid.

cellulose and AM homopolymer are soluble. Upon acidification, however, the cellulose became insoluble, and its N-content was determined. Data in Table V represent proof of grafting. The fact that a nitrogen content about 4 times as large as that for a physical mixture of cellulose and polyacrylamide were obtained for Samples 2 and 3 is a good indication that a chemical bond between acrylamide and cellulose exists. The fact that the grafted cellulose dissolved completely seems to exclude the possibility that extensive cross-linking took place.

Creaseproofing Effect of Secondary Treatments

As has already been shown by various investigators, vinyl polymer-grafted cellulosic fibers such as cotton and viscose rayon have many interesting properties depending upon the kinds of polymers grafted. Among these are increase in elongation at break, decrease in moisture regain, and elevation of abrasion resistance. However, these usually require a comparatively large amount of grafted polymer (usually more than 20%). A marked improvement in crease resistance by such procedures has not yet been reported.

Our next concern was to treat PAM-grafted or PAM-grafted and subsequently methylolated fabrics with various reactive compounds which might enter into reaction with $—CONH_2$ or $—CONHCH_2OH$ groups of the grafted cotton and impart such favorable properties as durable crease resistance and dimensional stability to the fabric. Table VI shows the results. It can be seen from this Table that methylolated PAM-grafted fabric, acid-cured, as well as HCHO-cured PAM-grafted fabric, has excellent crease resistance. The possible mechanisms for the reactions which take place during the curing stage are presented in Figures 2 and 3.

TABLE V. Solubility Characteristics of Graft Polymers and Physical Mixture in Cuprammonium Solution*

Expt.	Material	PAM content, % Original	PAM content, % Material recovered on acidification of solution
1	Physical mixture	14.1	2.01
2	Graft	8.86	9.12
3	Graft	11.3	8.09

* Polyacrylamide (PAM), cellulose, and grafted material are all soluble in cuprammonium, but upon acidification, cellulose and grafted material become insoluble.

The formation of the three kinds of linkages, (A), (B), and (C), represented in the figures, may be the main cause of the creaseproofing effect obtained, although the possibility of some occurrence of ether linkage ($—CH_2OCH_2—$) should be taken into consideration.

The effects of other materials, such as hexamethylenediamine HCl-salt (HD·HCl), dimethylolethyleneurea (DMEU), dimethylolurea (DMU), dimethyloladipamide (DMADPAM), trimethylolmelamine (TMML), ethylene urea, adipamide, glycerol, etc., also may be attributed to the formation of similar cross-links between two grafted polymer chains, between a cellulose molecule and a graft polymer, or between two cellulose chains. The effect of cross-linking upon crease resistance can be ascertained by the fact that aftertreatment of PAM-grafted cotton with monofunctional compounds such as benzaldehyde (BZAL) and methylolstearamide (MSTAM) scarcely improves this property.

Data in Table VI also show that, of all three kinds of finishing methods, the third for methylolated

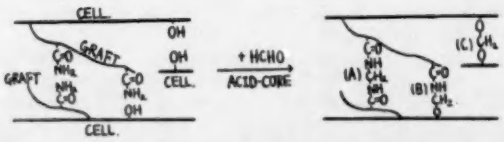

Fig. 2. Schematic representation of cross-linking of PAM-grafted cellulose with formaldehyde.

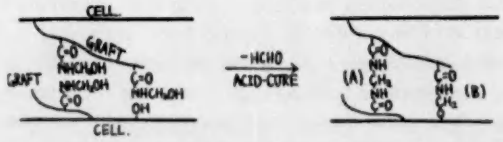

Fig. 3. Schematic representation of cross-linking of methylolated PAM-grafted cellulose by acid-cure.

PAM-grafted fabric is the best from the standpoints of both crease resistance and strength, since the formation of the (C) linkage by free HCHO may be prevented to a considerable extent. It must be also noted that cross-links with comparatively longer chains such as adipamide and hexamethylenediamine are particularly effective in obtaining wrinkle-resistant finishes with comparatively minor losses of strength.

Table VII gives the effect of the kind of acid catalyst used and the amount of add-on of polymer upon the mechanical properties of methylolated PAM-grafted fabrics. It can be readily recognized that relatively strong catalysts like ammonium chloride are required for a satisfactory finish. It can also be seen that too much deposit of PAM onto the fabric adversely affects the creaseproofing effect.

Durability of the Treatment

An experiment was next designed to evaluate the effects of laundering and acid extraction upon crease resistance and the amount of add-on of polymer as determined by nitrogen analysis. It is evident from Table VIII that several aftertreated samples endure the acid extraction as well as severe alkaline launderings at boiling temperature very well, while the

TABLE VI. Subsequent Utilization of Grafted Cotton for Cross-Linking*

Treating bath	Crease angle, deg.	Abrasion resistance, cycles	Tear strength, Kg.	Tensile strength, Kg.	Elongation at break, %
		(1) Original fabric			
Water alone	73	186	1.18	20.0	12.1
5% HCHO and 0.1% NH_4Cl†	147	55	0.39	9.6	5.4
5% HD·HCl and 5% HCHO	96	22	0.15	5.2	5.6
5% DMEU and 0.1% NH_4Cl	126	79	0.62	13.7	9.2
5% DMU and 0.1% NH_4Cl	124	84	0.66	14.6	7.5
5% DMADPAM and 0.1% NH_4Cl	70	94	1.26	<20.0	<12.2
5% TMML and 0.1% NH_4Cl	120	146	0.78	20.0	10.8
5% BZAL and 0.1% HD·HCl†‡	70	90	1.13	<20.0	<11.3
5% MSTAM and 0.1% HD·HCl‡	82	158	1.36	<20.0	<12.0
		(2) PAM-grafted fabric (add-on of PAM, 5.96%)			
Water alone	76	125	1.11	20.0	13.5
5% HCHO and 0.1% NH_4Cl†	142	49	0.45	8.9	8.8
5% HD·HCl and 5% HCHO	94	57	0.13	8.8	9.4
5% DMEU and 0.1% NH_4Cl	119	148	0.73	17.1	9.9
5% DMU and 0.1% NH_4Cl	130	98	0.53	17.5	12.2
5% DMADPAM and 0.1% NH_4Cl	73	123	1.01	20.0	14.9
5% TMML and 0.1% NH_4Cl	119	110	0.73	20.0	12.0
5% BZAL and 0.1% HD·HCl†‡	75	136	0.99	20.0	13.6
3% MSTAM and 0.1% HD·HCl‡	84	129	1.15	<20.0	<16.8
		(3) Methylolated PAM-grafted fabric			
Water alone	80	123	1.06	20.0	16.2
0.1% NH_4Cl	132	94	0.73	14.9	13.1
2% Ethyleneurea and 0.1% NH_4Cl	102	101	0.89	18.0	15.3
2% Urea and 0.1% NH_4Cl	101	125	0.98	19.4	14.9
2% Adipamide and 0.1% NH_4Cl	130	105	0.77	18.2	14.8
2% Melamine and 0.1% NH_4Cl	86	113	0.99	20.0	17.9
2% Glycerol and 0.1% NH_4Cl	138	80	0.68	14.7	15.1
3% Stearamide and 0.1% HD·HCl‡	118	95	0.80	16.3	12.8
3% Cetyl alcohol and 0.1% HD·HCl‡	107	94	0.93	18.1	15.0
2% Hexamethylene-diamine(HD)	87	90	0.93	19.1	16.9
10% HD and 10% HCHO (two baths)**	131	117	0.73	—	—

* Treatments consisted of padding to 100% wet pickup and oven drying for 10 min. at 80° C. followed by curing for 10 min. at 130° C.

† Curing alone.

‡ Dioxane solution.

** Fabric with 10.8% of PAM add-on was used.

creaseproofing brought about by the usual procedures, with the exception of HCHO-curing, is almost completely lost after acid extraction, as for instance in the case of dimethylolethyleneurea. As shown above, the kinds of linkages it is plausible to consider responsible for cross-linking of the grafted cellulose molecule can be classified in the following three categories: (A) —$CONHCH_2HNOC$— (a methylene linkage between two amide groups); (B) —$CONHCH_2O$— (a methylene linkage between an amide and an alcohol); (C) —OCH_2O— (a methylene linkage between two alcohol groups). In acidic media, the stabilities of these linkages are in the sequence

$$(A) > (C) > (B)$$

while they are all more stable in basic media. Therefore, during the acid extraction described above, some of (B) linkages may possibly be destroyed, causing some lowering of crease resistance of the HCHO-cured, PAM-grafted fabric or the methylolated, PAM-grafted, and subsequently acid-cured one in spite of their complete retention of amide groups, and also causing considerable loss of commonly used reactant type resins such as dimethylolethyleneurea. This interpretation is strengthened by the fact that the methylolated PAM-grafted

TABLE VII. Acid-Cure of Methylolated PAM-Grafted Cotton

Add-on of polymer, % of PAM	Crease angle, deg.	Tear strength, Kg.	Tensile strength, Kg.	Elongation at break, %
	(1) NH_4Cl catalyst, 0.1%			
1.82	114	0.41	14.0	8.89
2.67	111	0.48	15.2	9.09
4.77	135	0.40	11.6	10.99
6.88	127	0.43	10.0	8.4
7.58	142	0.38	—	—
9.28	151	0.36	10.4	11.4
16.9	92	0.57	13.5	10.8
	(2) $(NH_4)_2HPO_4$ catalyst, 0.1%			
1.82	85	0.79	<20.0	<11.3
6.88	90	0.88	<20.0	<13.4
9.28	92	0.78	19.2	16
16.9	73	0.69	20.0	17

TABLE VIII. Durability of the Aftertreatments under Acid and Alkaline Conditions

Treating bath	Original		After acid extraction*		After alkaline laundering†	
	Crease angle, deg.	Add-on of polymer, %	Crease angle, deg.	Add-on of polymer, %	Crease angle, deg.	Add-on of polymer, %
			(1) Original fabric			
5% HCHO and 0.1% NH_4Cl	147	—	137	—	143	—
5% HD·HCl and 0.1% NH_4Cl	96	—	94	—	76	—
5% DMEU and 0.1% NH_4Cl	126	3.45	88	0.80	108	3.12
5% DMU and 0.1% NH_4Cl	124	4.23	73	0.41	95	2.77
5% TMML and 0.1% NH_4Cl	120	3.97	71	1.35	88	2.36
			(2) PAM-grafted fabric			
Water alone	75	10.8	76	12.5	67	5.65
5% HCHO and 0.1% NH_4Cl	132	12.0	101	13.8	127	11.0
5% DMEU and 0.1% NH_4Cl	114	—	73	—	108	—
5% DMADPAM and 0.1% NH_4Cl	84	—	74	—	58	—
5% HD·HCl and 5% HCHO	85	—	84	—	68	—
			(3) Methylolated PAM-grafted fabric			
0.1% NH_4Cl	111	2.92	100	3.13	112	3.17
0.1% NH_4Cl	135	3.39	93	3.50	129	—
0.1% NH_4Cl	142	8.27	115	7.38	141	7.84
0.1% NH_4Cl	149	10.8	109	13.5	133	10.6
5% Ethyleneurea and 0.1% NH_4Cl	125	10.8	98	—	104	—
5% Glycerol and 0.1% NH_4Cl	148	10.8	98	—	134	—
5% Adipamide and 0.1% NH_4Cl	127	10.8	129	—	116	—

* Fabrics were immersed in 0.1 *N* HCl for 1 hour at 60° C.

† A rather severe laundering test in which fabrics were boiled in an alkaline solution containing 0.5% soap and 0.2% soda ash for 5 hours.

sample, acid-cured in conjunction with adipamide, best retains crease resistance after the acid extraction, presumably owing to the formation of the (A) linkage between the methylolamide group of the grafted cellulose and the amide group of adipamide, thus decreasing the ratio of the (B) linkages with respect to the (A) ones. In the case of urea, melamine, hexamethylenediamine, or their HCHO-derivatives, on the other hand, the methylene linkages formed are more or less amine-like; their stabilities are inferior to amide, causing a marked destruction of linkages by both acid extraction and alkaline launderings at the boil.

Data in Table VIII also show that free amide groups (—$CONH_2$) are more susceptible to alkaline hydrolysis than methyleneamide groups (—$CONH \cdot CH_2$—), since, for the PAM-grafted fabric which had not been subjected to any aftertreatment, alkaline laundering resulted in a considerable loss in the apparent amount of add-on of PAM, indicating that the nitrogen content decreased due to the hydrolytic decomposition of the amide group [2].

Summary and Conclusions

Graft polymerization of acrylamide onto cotton fabric using Ce^{IV} compounds as catalyst proceeded at a comparatively rapid rate even at room temperature. The optimum pH range for obtaining the maximum amount of add-on of polyacrylamide was about 1.4–1.6 at 25° C. Although there was not found any visible peculiarity in the effect of Ce^{IV} concentration upon add-on of polyacrylamide, initiation through complex formation and termination by Ce^{IV} compounds appear to be the main mechanism of the polymerization. A comparatively large part of the polyacrylamide produced without and within the fiber may possibly be grafted to the cellulose molecule, since values for apparent polyacrylamide content nearly similar to those for original fabrics were obtained for samples recovered upon acidification of their cuprammonium solutions.

Of all the aftertreatments investigated, the acid cure of methylolated polyacrylamide-grafted fabric alone or in conjunction with adipamide offered the best durability to both acid extraction and alkaline launderings, presumably due to the formation of a durable methylene-bisamide linkage between graft chains. HCHO-cure of the polyacrylamide-grafted fabric, as well as the original cotton, also brought about excellent durability to acid extraction. A disadvantage of this finish, however, was its poor strength as compared with the former, presumably due to the formation of short methylene cross-linkages between cellulose molecules by free HCHO.

A "durable" wrinkle-resistant finish, in the strict sense that the finish has the same life as the substrate, has not yet been attained. It is possible, however, that graft polymerization in combination with or followed by cross-linking may be a means of achieving such a finish in the future.

Literature Cited

1. Kamogawa, H., *Bull. Textile Research Inst. (Japan)* **40**, 33 (1957).
2. Kamogawa, H., Murase, R., and Sekiya, T., *Bull. Textile Research Inst. (Japan)* **54**, 35 (1960).
3. Mino, G. and Kaizerman, S., *J. Polymer Sci.* **31**, 242 (1958).
4. Mino, G., Kaizerman, S., and Rasmussen, E., *J. Polymer Sci.* **38**, 393 (1959).

Manuscript received November 1, 1960.

Isocyanate Modification of Wool in Dimethyl Sulfoxide

N. H. Koenig

Western Regional Research Laboratory,[1] Albany 10, California

Abstract

In the presence of hot dimethyl sulfoxide, a variety of monoisocyanates penetrate into and react chemically with wool. Dimethyl sulfoxide is superior to pyridine, the only other known reaction medium, in respect to cost, odor, and toxicity. Reaction is very rapid when the ratio of materials is 3 ml. of dimethyl sulfoxide, 2 ml. of phenyl isocyanate, and 1.2 g. of dry wool fabric; uptake of isocyanate is about 36% of the weight of the wool in only 10 min. at 105° C. Isocyanate-treated fabrics are more resistant to chemicals and to laundering shrinkage.

Introduction

The reactions of various proteins with organic isocyanates in hot pyridine were systematically studied by Fraenkel-Conrat [4]. Later, Farnworth [3], Moore [7], and Moore and O'Connell [8] chemically modified wool with isocyanates in pyridine; they obtained isocyanate uptakes (weight increases) as high as 45%. The treatment reduces fabric felting shrinkage and increases resistance to acids, alkalis, and oxidizing agents.

The present investigation shows that dimethyl sulfoxide can be advantageously substituted for pyridine as a medium for chemical modification of wool with isocyanates. In the presence of dimethyl sulfoxide, a variety of aromatic and aliphatic isocyanates react with wool, with uptakes up to about 60%.

Commercially, dimethyl sulfoxide is much more acceptable than pyridine. The sulfoxide costs only one-half as much, it has a much less offensive odor, and it is less toxic than pyridine. Further, dimethyl sulfoxide is a lesser fire hazard because its vapor pressure is lower. Still another advantage of dimethyl sulfoxide is its higher boiling point (189° C. as against 116° C. for pyridine); this permits rapid wool–isocyanate reactions in dimethyl sulfoxide at temperatures of 105° to 125° C. without pressure-tight equipment.

Because wool is firmly held together by disulfide cross-links, penetration is a key problem in attempts to chemically modify wool. Because the isocyanate molecules are too large to penetrate the keratin structure, liquid isocyanates by themselves do not react appreciably with wool. Likewise, the isocyanates do not react with wool in most non-hydroxylic solvents, since these solvents do not swell wool. On the other hand, low molecular weight hydroxylic wool-swelling solvents such as water and ethanol are unsuitable for internal chemical modification because isocyanates react vigorously with the active hydrogen atoms of these solvents. As an illustration, application of isocyanates to wool in phenol, cresol, or a petroleum fraction [2] results in a surface polymer deposit rather than internal chemical modification.

Both pyridine and dimethyl sulfoxide are suitable media for the reaction of isocyanates with wool. Generally, enough pyridine or dimethyl sulfoxide is present to serve as a liquid medium for isocyanate dispersion, heat transfer, and wool penetration. In the case of pyridine, Farnworth concluded from fiber diameter measurements that wool swells sufficiently in anhydrous pyridine at 70° C. to permit slow penetration of phenyl isocyanate. Also, according to a recent study [6] dimethyl sulfoxide at 85° to 105° C. swells (and supercontracts) wool. Since hot dimethyl sulfoxide does have the ability to swell wool and does not have active hydrogen atoms, it is an effective medium for wool–isocyanate reactions.

Experimental

Materials

The fabric used was undyed flannel, 7 oz./yd.[2], exhaustively extracted with ethyl ether followed by

[1] A laboratory of the Western Utilization Research and Development Division, Agricultural Research Service, U. S. Department of Agriculture.

ethanol. Dimethyl sulfoxide was a commercial grade, stated to be 99.9% pure. Most isocyanates were Eastman highest purity chemicals. *p*-Chlorophenyl, 2,5-dichlorophenyl, *p*-methoxyphenyl, and 2-biphenylyl isocyanates were Eastman practical grade. *n*-Butyl isocyanate was provided by the Carwin Company, North Haven, Connecticut, and *n*-octadecyl isocyanate by Mobay Chemical Company, St. Louis, Missouri.[2]

Application of Isocyanates

In the presence of dimethyl sulfoxide, isocyanates react with wool under a wide variety of conditions. It is generally desirable to dry the wool. Moisture in the wool or apparatus sometimes causes insoluble coatings on the fabric; it also wastes isocyanate. If the reagents are added successively, it is helpful to wet out the wool first with dimethyl sulfoxide. The isocyanate should then be distributed over the fabric and the combined reagents agitated briefly. For most uniform reaction, the reagents should be mixed prior to application. It is best to apply the mixture within an hour to avoid possible decomposition. To conserve reagents, the fabric is spread out flat in a tray or dish and enough liquid is added to just cover the fabric. Physical tests were made on 10 × 12-in. pieces of fabric. These swatches were rolled loosely and treated in 250-ml. graduated cylinders. Most samples were heated in an oven set under a hood. The procedure for extracting excess reagents may be varied in many ways as to mechanical action and solvent. However, hydroxylic solvents sometimes react with excess isocyanate to form troublesome deposits.

A very convenient procedure was adopted for treating most small wool samples (about 1.2 g. of dry fabric). This procedure, referred to as the "Petri dish technique," is as follows.

Cut fabric circles (about 85 mm. in diameter) to fit the bottom of a 100 × 15 mm. Petri dish set. Obtain the dry weight of the circles after drying them at 105° C. or by conditioning them and applying a moisture factor to the conditioned weight. Just prior to treatment, dry the fabric in an open Petri dish for 1 hr. at 105° C. Add the dimethyl sulfoxide and isocyanate to the fabric. Cover the sample with the Petri dish top and heat it in the oven or keep it at room temperature for a specified time. Rub the treated fabric under warm acetone at least twice and until no further surface deposit can be removed. Then extract the sample with ethanol overnight in a Soxhlet apparatus. Suspend the fabric by clips in an oven for 2 hr. at 105° C, then cool and weigh the dried fabric. Calculate percent uptake as one hundred times increase in dry weight divided by original dry weight.

Testing Methods

Chemical resistance. A piece of fabric, 0.4–0.5 g., is cut into 1 mm. strips to facilitate penetration. The strips are dried at 105° C. for 2 hr. prior to and 3 hr. after solubility treatments. The solubilities are expressed as percentage loss in weight on a dry basis.

a. Acid solubility. In 4 *M* HCl for 1 hr. at 65° C. [10].
b. Alkali solubility. In 0.1 *M* NaOH for 1 hr. at 65°C. [5].
c. Peracetic acid—ammonia solubility. At room temperature for 24 hr. in 2% peracetic acid followed by 24 hr. in 0.3% ammonia [1].

Fabric physical properties.

a. Breaking strength. On cut strips, ASTM method D 39-49.
b. Stiffness. Bending length and flexural rigidity by cantilever test, ASTM method D 1388-55T.
c. Crease recovery. Vertical strip test, ASTM method D 1295-53T.

Shrinkage. Four to 8 fabric circles are milled simultaneously in an Accelerotor [9] at 1780 r.p.m. for 2.0 min. with 200 ml. of 0.5% sodium oleate solution at 40° C.

Results and Discussion

Nature of Reaction

Evidence that dimethyl sulfoxide is not merely a solvent is given by the following experiment. Dry flannel (1.2 g.) was treated by the Petri dish technique with dimethyl sulfoxide (3 ml.) and phenyl isocyanate (2 ml.) for 1 hr. at 105° C. The uptake of isocyanate was 37%. The experiment was then repeated except that the following liquids were individually substituted for dimethyl sulfoxide: *n*-butyl acetate, *n*-butyl ether, *n*-butyl phosphate, N,N-dimethylaniline, *p*-dioxane, ethyl oxalate, methyl iso-

[2] Mention of specific companies does not imply endorsement by the Department of Agriculture over others of a similar nature not mentioned.

butyl ketone, pyridine, quinoline, toluene, and 2,2,4-trimethylpentane. In these experiments the increase in weight of the wool was only 2% to 4% except for pyridine, where the weight increase was 37%. Of the variety of organic solvents tested, only dimethyl sulfoxide and pyridine are suitable media for the wool–isocyanate reaction.

The reaction in dimethyl sulfoxide is similar to that in pyridine, i.e., the isocyanate adds to wool side chains that have reactive hydrogen atoms. Analytical data for phenyl isocyanate treatment (Table I), showing decrease in total nitrogen and sulfur, correspond to the postulated addition reaction. Table I also shows about 80% reduction in Van Slyke amino nitrogen, demonstrating chemical modification rather than surface deposition. It has been shown previously [6] that dimethyl sulfoxide alone does not affect the analytical values.

Treatment with Phenyl Isocyanate

Since phenyl isocyanate is a reactive, readily available liquid, it was used as a model compound in studying the principles of isocyanate reactions. The relative amounts of phenyl isocyanate to dimethyl sulfoxide were varied in experiments described in Table II. With the small total volume employed (5 ml.), there was an optimum ratio of phenyl isocyanate to dimethyl sulfoxide. Thus, in reactions interrupted in 5 min., the uptake was highest (12%) when the volume ratio of isocyanate to sulfoxide was 2 to 3, with 1.2 g. of wool. The 2 to 3 ratio also gave the highest uptake (33%) of the various samples after 10 min. in the oven.

The effect of temperature on reaction rate is illustrated in Table III. At room temperature, phenyl isocyanate reacted very slowly (8% uptake in 24 hr.). At 85° C., the reaction was essentially complete (36%) in 1 hr. or less. A temperature of 105° C. was very convenient for high uptakes—36% in 10 min. This is close to the maximum value, since the uptake was only 37% after 50 additional minutes. For reasons as yet unknown, occasional higher values, e.g., a 40% uptake in Table IV, were obtained at 105° C. An uptake of 41% was obtained in 15 min. in an oven at 135° C., but the wool is very susceptible to degradation at this temperature.

Chemical Resistance

Conditions for the reaction of various isocyanates, together with chemical solubilities of the modified fabrics, are summarized in Table IV. The reaction conditions cited are merely illustrative and were varied for experimental convenience. With the iso-

TABLE I. Analysis of Phenyl Isocyanate-Treated Fabric*

Sample	Total nitrogen, %	Amino nitrogen, %†	Total sulfur, %
Untreated wool			
exptl. values	16.6	0.29	3.49
Treated, 36.9% uptake			
exptl. values	15.4	0.06	2.68
theoretical values (calc.)	15.3	0.00	2.55

* All values are on a dry wool basis.
† Van Slyke method.

TABLE II. Effect of Ratio of Phenyl Isocyanate to Dimethyl Sulfoxide*

Phenyl isocyanate, ml.	Dimethyl sulfoxide, ml.	Uptake of phenyl isocyanate, %	
		in 5 min.	in 10 min.
4.0	1.0	4	11
3.0	2.0	6	25
2.0	3.0	12	33†
1.0	4.0	11	22

* Dry fabric circles (1.2 g.), in Petri dishes, treated with 5.0 ml. total of reagents and set in 105° C. oven for indicated time.
† Value for a sample run at the same time as the other 10-min. samples in Table II. Average of this sample and all other samples after 10 min. at 105° C. is 36% (Table III).

TABLE III. Effect of Temperature and Time on Uptake of Phenyl Isocyanate*

Temperature, °C.†	Reaction time, min.	Uptake, %
25	1,440	8
85	60	36
105	2	5
105	5	20
105	7	25
105	10	36‡
105	30	36
105	60	37
135	15	41

* Dry fabric circles (1.2 g.) were treated in a Petri dish with 3 ml. dimethyl sulfoxide followed by 2 ml. phenyl isocyanate.
† Temperature of room (25° C.) or oven. Actual sample temperature was below oven temperature for first several minutes.
‡ Average of 4 values: 33, 36, 37, 38.

TABLE IV. Solubilities of Wool Treated with Isocyanates (RNCO) in Dimethyl Sulfoxide (DSO)*

R in isocyanate	RNCO, ml.	DSO, ml.	Time, min.	Uptake, %	Peracetic acid-NH_2 solub., %	Acid solub., %	Alkali solub., %
Untreated wool	0	0	0	0	85	8	12
Phenyl	3	3	3	17	31	3	12
Phenyl	2	3	5	25	25	1	10
Phenyl†	10	10	5	40	17	1	6
o-Tolyl	2	3	60	35	30	2	15
m-Tolyl	2	3	30	39	5	1	4
p-Tolyl	2	3	30	33	10	1	2
o-Chlorophenyl	3	3	20	52	15	2	5
m-Chlorophenyl†	10	15	60	57	2	2	3
p-Chlorophenyl†	10‡	15	60	45	5	2	3
2,5-Dichlorophenyl	2‡	3	30	61	7	2	3
o-Methoxyphenyl	2	3	30	34	27	2	13
p-Methoxyphenyl	2	3	15	42	13	2	4
1-Naphthyl	4	4	15	49	19	0	3
2-Biphenylyl	4	6	30	43	13	1	8
n-Butyl	2	3	60	14	98	2	18
n-Octadecyl	2	3	36	36	7	1	5
Carbethoxymethyl	3	3	22	36	97	12	69

* Unless otherwise indicated, 1.2 g. dry wool fabric treated in 105° C. oven.
† Weight of dry wool, 4.0 g.
‡ Volume when liquified (m.p. 30° C.).

cyanates studied, high uptakes on a weight basis can be obtained with compounds of high molecular weight, e.g., 61% by weight uptake of 2,5-dichlorophenyl isocyanate.

In most cases, the modified wool products are more resistant to chemical attack, as determined by solubilities under acid, alkaline, and oxidizing conditions. All compounds except carbethoxymethyl isocyanate greatly increase the resistance to hot hydrochloric acid. Isocyanate treatment also greatly increases resistance to peracetic acid oxidation, except for the carbethoxymethyl and butyl derivatives. These same two compounds increase alkali solubility (decrease resistance to alkali), especially carbethoxymethyl isocyanate. *o*-Tolyl and *o*-methoxyphenyl isocyanate treatment may increase alkali solubility slightly, unlike the *m*- and *p*-tolyl and *p*-methoxyphenyl compounds. This "*ortho* effect" is being investigated further. All of the other isocyanates moderately decrease alkali solubility.

Physical and Shrinkage Properties

The physical properties of modified wools are illustrated with phenyl isocyanate-treated fabrics in Table V. Fabric breaking strength increases moderately with increasing uptake; the increased strength is probably related to the increase in fabric weight. Flexural rigidity is much greater at high uptakes.

TABLE V. Physical Properties of Phenyl Isocyanate-Treated Fabrics*

	Phenyl isocyanate uptakes, %			
	0†	13	23	34
Treatment conditions‡				
Isocyanate volume, ml.	0	15	20	30
Dimethyl sulfoxide volume, ml.	0	260	255	245
Treatment time, min.	0	15	20	30
Breaking strength, cut strip, lb.	34	39	44	49
Fabric weight, mg./cm.^{2}	20	25	30	36
Stiffness				
Bending length, cm.	1.55	1.67	1.62	1.70
Flexural rigidity, mg.-cm.	77	118	130	176
Crease recovery, %	80	82	82	83

* Average of 3 warp and 3 fill values.
† Untreated control fabric.
‡ Weight of dry fabric, 15–16 g.

The recovery from creasing is slightly improved by treatment. At low uptakes of isocyanate, the fabrics have a good hand and color; above 10% uptake most of the fabrics are more or less shrunk, harsh, and yellowed.

Typical data on felting shrinkage of isocyanate-modified fabrics are shown in Table VI. The amount

TABLE VI. Accelerotor Shrinkage of Isocyanate-Treated Fabrics

Isocyanate	Isocyanate uptake, %	Area shrinkage, %
None (untreated)	0	50
Phenyl	6	22
	11	15
	27	3
	36	0
o-Tolyl	34	0
o-Chlorophenyl	48	1
o-Methoxyphenyl	30	1
1-Naphthyl	9	19
	31	6
n-Butyl	11	14

of shrinkage decreases as uptake increases. At high isocyanate uptake, many of the fabrics are essentially shrinkproof in the accelerated laundering test. Part of this shrink resistance is a result of treatment shrinkage, which may be as high as 20% (in area) for high uptake samples.

Summary

Dry wool fabrics have been chemically modified with several aliphatic and aromatic monoisocyanates in hot dimethyl sulfoxide as a reaction medium. Isocyanates penetrate into the keratin structure and react with side chains of the wool molecule in either dimethyl sulfoxide or pyridine, but not in a variety of other organic liquids. Pyridine, however, has a repulsive odor and is also more expensive and more toxic than dimethyl sulfoxide.

With 1.2-g. dry wool circles in Petri dishes and 5 ml. of total reagents, the rate of isocyanate uptake is very rapid with 2 ml. of phenyl isocyanate and 3 ml. of dimethyl sulfoxide. Uptakes of 36% phenyl isocyanate are obtained in only 10 min. at 105° C. or in less than 1 hr. at 85° C. An uptake of 61% has been achieved with a high molecular weight compound, 2,5-dichlorophenyl isocyanate.

Fabrics treated with phenyl isocyanate have good mechanical strength and crease recovery, but fabric color, hand, and flexibility are more or less impaired. Fabrics modified by various isocyanates are generally more resistant to acid, alkali, and oxidizing environments; they also resist shrinkage when laundered.

Acknowledgments

I wish to thank Helen Kivela for skilled technical assistance. R. A. O'Connell and associates performed the physical tests; K. T. Williams' staff supplied analytical data. I am also indebted to H. P. Lundgren and W. L. Wasley for advice and encouragement.

Literature Cited

1. Alexander, P., Fox, M., Stacey, K. A., and Smith, F. L., *Biochem. J.* **52**, 177 (1952).
2. Barr, T., Capp, C. W., and Speakman, J. P., *J. Soc. Dyers Colourists* **62**, 338 (1946).
3. Farnworth, A. J., *Biochem. J.* **59**, 529 (1955).
4. Fraenkel-Conrat, H., Cooper, M., and Olcott, H. S., *J. Am. Chem. Soc.* **67**, 314 (1945).
5. Harris, M. and Smith, A. L., *J. Research Natl. Bur. Standards* **17**, 577 (1936).
6. Koenig, N. H. and O'Connell, R. A., TEXTILE RESEARCH JOURNAL **30**, 712 (1960).
7. Moore, J. E., TEXTILE RESEARCH JOURNAL **26**, 936 (1956).
8. Moore, J. E. and O'Connell, R. A., TEXTILE RESEARCH JOURNAL **27**, 783 (1957).
9. Stiegler, H. W., Glidden, H. E., Mandikos, G. J., and Thompson, G. R., *Am. Dyestuff Reptr.* **45**, 685 (1956).
10. Zahn, H. and Würz, A., *J. Textile Inst.* **45**, P88 (1954).

Manuscript received November 4, 1960.

Thermal Neutron Irradiation of Cotton[1]

Florine A. Blouin, Jett C. Arthur, Jr., Rollin S. Orr, and Vega J. Ott

Southern Regional Research Laboratory,[2] New Orleans, Louisiana

Abstract

Purified cotton samples were irradiated in a "pure" source of thermal neutrons in the dosage range of 5×10^{14} through 1×10^{17} neutrons per cm.^{2} Neutron irradiation produced chain cleavage, carboxyl groups, and reducing groups in the cotton cellulose. The water solubility of the cotton was not appreciably affected in this dosage range. The wet and dry strengths and the elongation of the cotton were decreased by neutron irradiation. The uniformity of strength along the fiber length was only slightly lowered. The reducing groups produced in the neutron-irradiated cotton were shown to be markedly different in degree of reaction with sodium chlorite, copper equivalence, and influence on alkali sensitivity from the reducing aldehyde groups produced by periodate oxidation of cotton cellulose. A close similarity between the effects of thermal neutron and gamma ray irradiation on cotton was observed.

Introduction

Although a number of studies have recently been published on the effects of various types of nuclear radiation on cotton cellulose [3, 16, 18, 20] only two laboratories have investigated the effects of neutron irradiation on cotton cellulose. Gilfillan and Linden [11] studied the effect of neutron irradiation on the strength of various types of yarns. At the neutron dosage used (2.3×10^{17} neutrons per cm.^{2}) the viscose and cotton yarns lost almost 100% of their original strength. Teszler et al. [19–21] made a more thorough study of the effects of neutron irradiation over a wide range of dosages on cotton and rayon. These workers examined such properties as tenacity, elongation, stiffness, modulus, cupriethylene diamine and cellulose nitrate viscosity, microscopic swelling characteristics, and dye affinities.

In both of the previous studies the samples were irradiated at the Brookhaven National Laboratory. In the positions in the reactor which were used, the radiation was composed of thermal neutrons plus a high percentage of fast neutrons and a high accompanying gamma ray flux [5]. The samples described in the present work were irradiated in the Materials Testing Reactor at the National Reactor Testing Station in a position which gave a very pure thermal neutron flux and which was specially shielded to eliminate the accompanying gamma radiation [17].

Experimental

Preparation of Samples

Raw Deltapine cotton was purified by extracting with hot ethanol and by boiling in a 1% sodium hydroxide solution [3]. The purified cotton was conditioned at 21° C. and 65% RH, resulting in a moisture content of 7.65%. Thirty-gram samples of the purified cotton were sealed into aluminum cylinders (440 ml.) in an atmosphere of air.

Irradiation of Samples

Six cylinders, each containing 30 g. of cotton, were sent to the National Reactor Testing Station, Idaho Falls, Idaho. Five of the samples were irradiated in the "thermal column" of the Materials Testing Reactor [17]. The accompanying gamma radiation was cut by four inches of lead. The cylinders were kept sealed for a period of 42 days after irradiation, after which time the cotton was removed for analysis. At this time the aluminum cylinders still showed detectable activation, and there was a measurable activity in the cotton samples which had received the two highest dosages.

Analyses of Irradiated Samples

The fluidity of the samples dispersed in cupriethylene diamine hydroxide was determined by the A.S.T.M. method [1]. The procedure for the dispersion

[1] Presented at the 138th National Meeting of the American Chemical Society, New York, N. Y., September 11–16, 1960.

[2] One of the laboratories of the Southern Utilization Research and Development Division, Agricultural Research Service, U. S. Department of Agriculture.

of the samples in the solvent was modified [3], and the values for the degree of polymerization of the samples were calculated using Conrad's constant of 190.5 [7].

The carboxyl content was determined by the calcium acetate titration method, as described by Davidson and Nevell [9]. One-gram samples were used.

The copper number of the irradiated samples was determined by Braidy's method, as described by Clibbens and Geake [6]. One-gram samples were used. The copper number is the weight of copper in grams which is reduced by 100 g. of sample.

The water solubility was determined by refluxing 1 g. of sample for 1 hr. in 100 ml. of distilled water and obtaining the dry weight of the residue.

The Pressley Index of the irradiated fibers was determined using the Pressley flat-bundle tester according to the A.S.T.M. method [2]. Five breaks were made per sample and a zero gauge (clamp spacing) was used.

The tenacity of the irradiated cotton in the wet and dry state at zero and at $\frac{1}{8}$-in. gauge (clamp spacing) and the elongation of the fibers at $\frac{1}{8}$-in. gauge were determined using the Stelometer, according to the method described by Orr et al. [15]. Seven breaks per sample were made. The standard or dry state refers to fibers conditioned at 21° C. and 65% RH. The fibers broken in the wet state had approximately a 50% moisture pickup.

Preparation of Samples for Chlorite Treatment

In order to better interpret the data from neutron-irradiated cotton samples treated with sodium chlorite, samples of gamma-ray-irradiated and periodate-oxidized cottons of comparable levels of oxidation were prepared and similarly treated with chlorite for conversion of aldehyde groups to carboxyl groups.

Two samples of purified cotton (10 g. each) were sealed in air in tall form weighing bottles (150 ml.) and irradiated with gamma rays from Southern Regional Research Laboratory's cobalt-60 source. The samples received a dosage of 0.99 and 1.99×10^7 roentgens at a dose rate of approximately 10^5 roentgens/hr.

Two samples of purified cotton were treated with a 0.008 *M* solution of potassium metaperiodate for 255 and 360 min. in the dark at room temperature. The oxygen consumption of the 360-min. sample was found to be 0.009 atoms of oxygen per glucose unit, using Müller and Friedberger's method for determination of the periodate ion concentration [8]. The samples were thoroughly washed and air dried.

Since in earlier work on the effects of gamma irradiation on cotton [4] it was found that a high percentage of the carboxyl groups (approximately 50%) produced during irradiation was removed on water-washing of the samples, the gamma-ray-irradiated, the periodate-oxidized, and the neutron-irradiated samples were water-washed (1 hr. reflux) in order that the data obtained before and after chlorite treatment might be on a more comparable basis.

The water-washed samples were analyzed by the methods previously described for determination of carboxyl content, reducing power, and fluidity.

Chlorite Treatment of Irradiated and Chemically Oxidized Samples

Water-washed samples of neutron-irradiated, gamma-ray-irradiated, and periodate-oxidized cottons were treated with sodium chlorite, according to the method of Davidson and Nevell [10]. These workers determined the experimental conditions necessary for maximum conversion of the aldehyde groups in periodate-oxidized cellulose to carboxyl groups by the sodium chlorite method. The samples were treated with a solution 0.2 *M* in sodium chlorite and 1 *M* in acetic acid for 72 hr. at room temperature. The samples were thoroughly washed and air dried and after a relatively short time analyzed by the previously described techniques for determination of carboxyl groups, reducing power, and fluidity.

Results and Discussion

Some of the physical and chemical properties of the cotton samples which were irradiated with thermal neutrons are given in Table I. On the basis of the properties examined, the structural changes which

TABLE I. Some Physical and Chemical Properties of Purified Cotton Irradiated with Thermal Neutrons

Dosage, neutrons/cm²	Degree of polymerization	Carboxyl groups, mmoles/g.	Copper number, g./100 g.	Water solubility, %	Pressley index, lb./mg.
0	4300	0.000	0.10	0.0	8.45
5×10^{14}	2800	0.002	0.16	—	8.22
5×10^{15}	1000	0.002	0.59	—	7.88
1×10^{16}	610	0.006	1.13	—	7.51
5×10^{16}	230	0.021	5.23	0.5	5.59
1×10^{17}	150	0.035	8.86	0.6	4.14

TABLE II. Some Mechanical Properties of Purified Cotton Irradiated with Thermal Neutrons

Dosage, neutrons/cm.²	Condition	Tenacity, g./tex		Elongation ⅛ in. gauge, %	Tenacity ratios		
		Zero gauge*	⅛ in. gauge†		⅛ in./ zero gauge	Wet/dry	
						Zero gauge	⅛ in. gauge
0	standard	32.7	20.5	7.6	0.63		
	wet	41.3	22.2	11.0	0.54	1.26	1.08
5×10^{14}	standard	33.0	21.3	7.5	0.65		
5×10^{15}	standard	30.0	19.6	7.7	0.65		
	wet	33.2	18.2	9.8	0.55	1.11	0.93
1×10^{16}	standard	29.3	17.8	7.2	0.61		
5×10^{16}	standard	19.3	10.8	5.7	0.56		
	wet	16.0	8.5	7.4	0.53	0.83	0.79

* Zero gauge ≅ 0.8 mm. "true" specimen length.
† ⅛ in. gauge ≅ 4.0 mm. "true" specimen length.

occurred on irradiation of cotton with thermal neutrons were the formation of carboxyl and reducing groups and the cleavage of the cellulose chains. The degree of polymerization (DP) of the irradiated samples, as measured by their fluidity in cupriethylene diamine hydroxide, showed a marked decrease as the irradiation dosage increased. The titratable acidity expressed as millimoles of carboxyl groups per gram of sample increased as the dosage of neutron irradiation increased. The copper number, which expresses the copper reducing power of the samples, increased rapidly with increased dosage. These same three properties were found to be similarly affected when purified cotton was irradiated with gamma rays [3].

The water solubility of the cotton was not appreciably affected in the dosage range of the neutron irradiation.

The strength of the fibers, as determined by the Pressley flat-bundle tester method, decreased as the irradiation dosage increased. The losses in strength produced by thermal neutron irradiation of cotton were comparable with the losses in strength produced by gamma irradiation of cotton at similar degrees of polymerization [3].

The results of a more thorough investigation of the mechanical properties of the neutron-irradiated samples are given in Table II. The tenacities of the irradiated samples, obtained using a zero and a ⅛-in. gauge under standard conditions and for three samples in the wet state, are given. The loss in strength was large only at the highest dosage used. The wet strength of the irradiated fibers decreased faster than the dry strength as dosage increased. The changes in elongation, using the ⅛-in. gauge, paralleled the changes in strength. The ratio of the tenacity values obtained with the ⅛-in. gauge to those obtained with the zero gauge gives a measure of the uniformity of strength along the fiber length. The results indicated that this uniformity was only slightly lowered by neutron irradiation. The lowering of the wet to dry strength ratio of the irradiated samples indicated that neutron irradiation of cotton reversed the effect of moisture on the strength of the fibers.

It was also noted that the losses in strength produced by neutron and gamma irradiation of cotton were markedly less than those produced by heat and acid degradation [22] of cotton at comparable degrees of polymerization. This is probably due to the more homogeneous nature of the interaction of nuclear radiation with cotton.

Although the copper number determination is a measure of the reducing-group content of a sample of oxidized cellulose, it is not generally considered to be stoichiometric in nature. However, a number of workers have recently shown, by comparing the copper number method with other methods of measuring aldehyde content, that a particular type of oxidized cellulose will reduce a fairly constant number of moles of copper per aldehyde group present in the cotton at various levels of oxidation [10, 12, 14]. They also found that the copper equivalents reduced per aldehyde group differed quite markedly in going from one type of oxidized cellulose to another. These variations in copper equivalence were attributed to differences in the type and position of the reducing groups present in the various types

of oxidized cellulose. Work with low-molecular-weight model reducing compounds by Lidman-Safwat and Theander [12] also indicated the importance of the structure of the reducing unit in relation to the amount of copper reduced. On the basis of these studies it was concluded that a comparison of the copper reducing power of an oxidized cotton and its aldehyde content measured by some other method could provide valuable information on the structure of the oxidized material. Two samples of the neutron-irradiated cottons under study were examined with this objective in view. Two other types of oxidized cottons were treated similarly for comparative purposes. Samples of neutron-irradiated, gamma-ray-irradiated, and periodate-oxidized cottons were first water-washed to remove any material that might otherwise be lost during the water-washing involved in later treatment. These samples were then analyzed for DP, carboxyl content, and copper number. The results are given in the first three columns of Table III.

Davidson and Nevell [10] made an extensive study of the optimum conditions for conversion of the aldehyde groups in periodate-oxidized cellulose to carboxyl groups by sodium chlorite solutions. The three types of cottons were treated under conditions similar to the optimum conditions devised by Davidson and Nevell and again analyzed for DP, carboxyl content, and copper number. These results are given in the last three columns of Table III.

The chlorite treatment indicated the presence of 0.040 and 0.060 mmoles of aldehyde groups which could be converted to acid groups per gram of neutron-irradiated cotton (difference between carboxyl content before and after chlorite treatment). In the gamma-ray-irradiated cottons of similar degrees of degradation, 0.035 and 0.047 mmoles of aldehyde groups of this type per gram of sample were indicated. In all four of these samples only 50%–60% of the reducing power was lost by conversion of these aldehyde groups to carboxyl groups. The aldehyde groups which were converted in these samples were found to have, on an average, a copper equivalence of 11. Treatment of the periodate samples gave a 90% loss in reducing power and a copper equivalence of approximately 5. These results are consistent with those of Davidson and Nevell on periodate-oxidized cellulose of this degree of oxidation but are not nearly as precise.

Some marked differences between the neutron- and gamma-irradiated cottons and the periodate-oxidized cottons were observed. This, at least, suggested something about the structure of the irradiated cottons. A large difference in copper equivalence between the aldehyde groups in the irradiated cottons and those in the periodate-oxidized cotton that were converted to acids by chlorite was noted. This indicated that the aldehydes in the irradiated cottons were probably not of the C_2 and C_3 type present in periodate-oxidized cottons. The high copper equivalence obtained with the irradiated cottons suggested that at least some of the aldehyde groups

TABLE III. Comparison of Some of the Chemical Properties of Neutron-Irradiated, Gamma-Ray-Irradiated, and Periodate-Oxidized Cottons before and after Treatment with Chlorite

Description of sample	Water-washed			Chlorite treated		
	Degree of polymerization	Carboxyl groups, mmoles/g.	Copper number, g./100 g.	Degree of polymerization	Carboxyl groups, mmoles/g.	Copper number, g./100 g.
Control	3600	0.000	0.10	2800	0.007	0.16
Neutron-irr. 5×10^{16} n./cm.^{2}	230	0.016	3.94	230	0.056	2.10
Neutron-irr. 1×10^{17} n./cm.^{2}	130	0.026	7.97	160	0.086	3.56
Gamma-ray-irr. 1×10^7 roentgens	240	0.015	4.09	240	0.050	1.60
Gamma-ray-irr. 2×10^7 roentgens	170	0.023	6.30	180	0.070	2.52
Periodate-oxid. 255 hr.	440	0.003	3.07	850	0.076	0.33
Periodate-oxid. 360 hr.	350	0.004	3.66	680	0.121	0.47

present in the irradiated cotton were similar to those present in dichromate-oxalic acid oxidized cellulose. A copper equivalence of 11 for these chemically oxidized cottons was obtained by Lidman-Safwat and Theander [12]. An equivalence of 16 was obtained by Nabar and Padmanabhan [14]. Both groups used analyses similar to those used in this present investigation in estimating copper equivalence. Other work on the oxidation of cellulose with dichromate in the presence of oxalic acid [13, 14] indicated that oxidation of the C_6 position to an aldehyde may be the predominant effect in this type of oxidation and thus be responsible for the high copper equivalence. Production of an aldehyde by dehydrogenation of the C_6 position of the anhydroglucose unit of cotton cellulose by nuclear radiation would be a logical product of activation of this carbon atom [4].

The high residual copper number of the irradiated cottons after chlorite treatment, as contrasted to almost complete loss of copper number by the periodate-oxidized cottons, indicated another marked difference between the two types of oxidized cottons. This high residual copper number indicated that a large portion of the reducing groups present in the irradiated cotton cellulose was of a type resistant to further oxidation with chlorite. This suggested the presence of either ketone groups or aldehyde groups of a highly resistant nature, possibly of the hemiacetal type.

Another marked difference between the periodate-oxidized cottons and the irradiated cottons was found in the effect of the chlorite treatment on the degree of polymerization, as measured in the strongly alkaline cupriethylene diamine hydroxide reagent. Periodate-oxidized cellulose is known to be extremely alkali-sensitive [8]. The DP measurements, made in an alkaline reagent like cupriethylene diamine, would be much lower than the true chain length due to chain cleavage at the oxidized units on exposure to this reagent. Conversion of the aldehyde groups in periodate-oxidized cellulose to carboxyl groups is accompanied by almost complete stabilization of the material toward alkalies [10]. This is reflected in Table III by a very large increase in the DP of the periodate-oxidized cottons after chlorite treatment. The irradiated cottons did not exhibit any large changes in DP after chlorite treatment, suggesting that at least that portion of the aldehyde groups which was converted to carboxyl groups did not produce alkali sensitivity in the irradiated cottons. This is consistent with the data of Teszler et al. [20], which indicated that neutron- and gamma-irradiated cottons were not alkali-sensitive.

When the DP changes obtained by Teszler et al. [20] on neutron-irradiated cotton are compared with the DP measurements reported in this work, it is found that the amount of chain cleavage at any particular neutron dosage is much less for the samples irradiated in the "purer" source of thermal neutrons. In fact, the low energy of thermal neutrons suggests that they could not directly, by energy transfer, produce a chemical change in the cellulose. The changes which did occur were probably secondary in nature and due to the higher energy nuclear radiation released when neutrons were captured by the individual atoms of the cellulose itself, by the atoms of the gaseous atmosphere in which the cotton was sealed, and/or to that released by activation of the aluminum and other trace metals of the containers in which the cottons were irradiated.

The suggestion of Teszler et al. [21], based on the dyeing characteristics of irradiated cottons, that neutron irradiation produces a strictly hydrolytic type degradation of cellulose, whereas gamma irradiation produces an oxidative degradation, was not substantiated by the present work. The data obtained here suggest a close similarity between the effects of gamma irradiation and thermal neutron irradiation on cotton, both types of irradiation producing an oxidative degradation.

Summary

Purified cotton samples were irradiated in a "pure" source of thermal neutrons in the dosage range of 5×10^{14} through 1×10^{17} neutrons per cm.^{2} Neutron irradiation produced chain cleavage, carboxyl groups, and reducing groups in the cellulose. The wet and dry strengths and the elongation of the cottons were decreased by neutron irradiation. The reducing groups produced in the neutron-irradiated cottons were shown to be markedly different from those in periodate-oxidized cottons. A close similarity between the effects of thermal neutron and gamma ray irradiation on cotton was observed.

Literature Cited

1. American Society for Testing Materials, ASTM Designation D539–53, Philadelphia, Pa.
2. American Society for Testing Materials, ASTM Designation D1445–57, Philadelphia, Pa.

3. Blouin, F. A. and Arthur, H. C., Jr., TEXTILE RESEARCH JOURNAL **28**, 198–204 (1958).
4. Blouin, F. A. and Arthur, J. C., Jr., *J. Chem. Eng. Data* **5**, 470–5 (1960).
5. Brookhaven National Laboratory, "Research Reactor Facility; Irradiation Services and Radioisotopes," Upton, N. Y., Associated Universities, Inc., U. S. Atomic Energy Commission, December 1955.
6. Clibbens, D. A. and Geake, A., *J. Textile Inst.* **15**, T27–38 (1924).
7. Conrad, C. M., Tripp, V. W., and Mares, T., *J. Phys. & Colloid Chem.* **55**, 1474–91 (1951).
8. Davidson, G. F., *J. Textile Inst.* **31**, T81–96 (1940).
9. Davidson, G. F. and Nevell, T. P., *J. Textile Inst.* **39**, T102–17 (1948).
10. Davidson, G. F. and Nevell, T. P., *J. Textile Inst.* **46**, T407–23 (1955).
11. Gilfillan, E. S. and Linden, L., TEXTILE RESEARCH JOURNAL **25**, 773–7 (1955).
12. Lidman-Safwat, S. and Theander, O., *Svensk Papperstidn.* **61**, 42–6 (1958).
13. Lindberg, B. and Theander, O., *Acta Chem. Scand.* **8**, 1870–4 (1954).
14. Nabar, G. M. and Padmanabhan, C. V., *J. Soc. Dyers Colourists* **69**, 295–7 (1953).
15. Orr, R. S., Weiss, L. C., and Grant, J. N., TEXTILE RESEARCH JOURNAL **25**, 939–46 (1955).
16. Pan, H.-P., Proctor, B. E., Goldblith, S. A., Morgan, H. M., and Naar, R. Z., TEXTILE RESEARCH JOURNAL **29**, 415–21 (1959).
17. Phillips Petroleum Co., Atomic Energy Division, "National Reactor Testing Station; Irradiation Services at the Materials Testing Reactor," Idaho Falls, Idaho, 1955.
18. Saeman, J. F., Millett, M. A., and Lawton, E. J., *Ind. Eng. Chem.* **44**, 2848–52 (1952).
19. Teszler, O. and Hefti, H., *Textil-Rundschau* **13**, 61–66 (1958).
20. Teszler, O., Kiser, L. H., Campbell, P. W., and Rutherford, H. A., TEXTILE RESEARCH JOURNAL **28**, 456–62 (1958).
21. Teszler, O., Wiehart, H., and Rutherford, H. A., TEXTILE RESEARCH JOURNAL **28**, 131–5 (1958).
22. TRIPP, V. W., Orr, R. S., Ziifle, H. M., and Conrad, C. M., TEXTILE RESEARCH JOURNAL **28**, 404–17 (1958).

Manuscript received November 7, 1960.

Converting the Fibrograph to Automatic Direct-Reading Operation

P. R. Ewald and Smith Worley, Jr.

United States Department of Agriculture, Cotton Quality Laboratories,[1] Knoxville, Tennessee

Introduction

Since 1935, when Hertel [2] started work on the curve-drawing Fibrograph that he subsequently introduced for measuring the length of cotton fibers [1], the instrument has evolved in a number of ways. In 1952, Tallant [5] showed how to add a servo drive to the manually operated first commercial model [7, 8]. Later on he made an improvement in the conversion [6]. To eliminate some of the possible errors in curve measurement, Rouse [4] modified another manual model of the instrument in 1958 to permit direct readings on dials.

Recently, Hertel [3] made a drastic revision in the Fibrograph principle to measure span-lengths of cotton fibers rather than upper half mean (UHM) and mean lengths as did the earlier instruments. Span-lengths are being measured with a commercial digital type Fibrograph now on the market.

Since these new concepts and instruments represent quite a departure from the conventional curve-drawing types of Fibrograph, research workers in cotton must be able to translate data from earlier work to correspond to data obtained by the new methods. Specifically, they must be able to relate span-length values with dial-type or curve-drawn mean and UHM values using identical optical systems and samples.

To compare the dial and span-length measurement methods with conventional curve-drawing methods, a Fibrograph already converted [5] from a manual model to an automatic curve-drawing model was modified further so that all measurements could be made on the same instrument. This paper describes relatively simple modifications which permit use of

[1] Agricultural Research Service, Crops Research Division, cooperating with the University of Tennessee Agricultural Experiment Station.

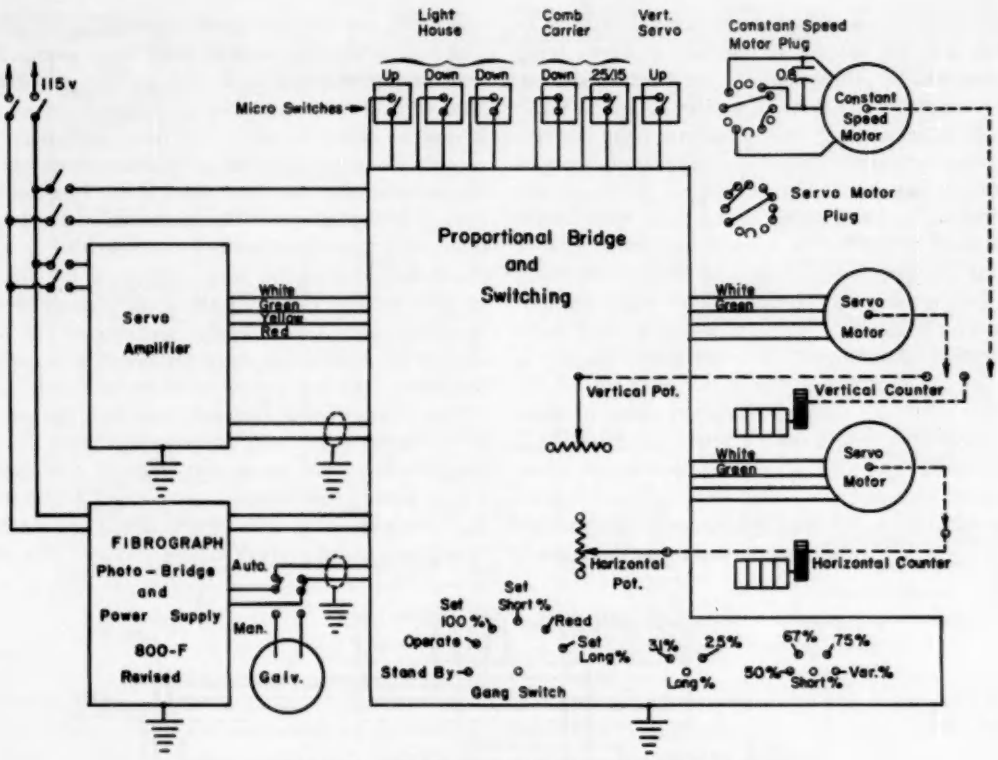

Fig. 1. General schematic diagram of conversion.

the same instrument as a manual, an automatic curve-drawing, or an automatic dial or digital-type Fibrograph according to the measurements needed.

Construction of Conversion

Automatic Curve Drawing

The original servo conversion [5] made the Fibrograph semi-automatic; i.e., it was necessary to raise the motors at the end of each run and to lower the comb carrier by hand. The operation was made fully automatic by attaching micro switches to the lighthouse and comb carrier to run the comb carrier back down when the lighthouse is raised at the end of a run and to serve as limit switches to prevent over-travel. Also, the outside hand knob shaft bearings were replaced with ball bearings to provide smoother operation, particularly because of the added weight of the motors on the bearings.

Automatic Dial or Digital Measuring

The conversion to a dial Fibrograph [4] was described for a manual operation. Automatic dial measurements are obtained when the instrument is set up for span-length measurements as described in the next paragraph. For specific aid in making dial-type readings, a mechanical click stop is built into the vertical drive counter shaft to give a positive indication when the comb carrier is at 0.15,[2] 0.25, 0.35, etc., in. The carrier may, of course, be set manually at any intermediate length as needed, and for automatic curve drawing or span-length measurement, the click stop is turned off.

Span-Length Measuring

Manual operation. Obtaining dial or digital span-length measurements from a Fibrograph requires only the attachment of counters to the comb carrier vertical drive to measure fiber length and to the card carrier horizontal balancing drive to measure the amount of fiber being scanned. If the proper gear ratios are used to drive the counters, the fiber

[2] Early-model Fibrographs will require a resetting of the comb carrier stop and may require modification of the lighthouse before readings can be taken at 0.15 in.

length being scanned will be measured directly in inches, and the amount or number of fibers being scanned will be proportional to the counter reading. For example, if the vertical counter is set on 0.15 ² or 0.25 in., depending on the starting point desired, then the horizontal counter is turned until the galvanometer balances. The reading on the horizontal counter is the 100% value. The short span length is obtained by setting the horizontal counter to such a value as 50%, 67%, or 75% of the starting value and then turning the vertical counter until the galvanometer balances. The vertical counter now reads the shorter span length. The horizontal counter is then set to such a value as 2.5% or 3.1% of the starting value and the operation is repeated to show the longer span length on the vertical counter.

Automatic operation. To make span-length measurements automatically, it is necessary to replace the vertical-drive, constant-speed motor with another servo motor that swings on the mounting shaft which supported the constant-speed, curve-drawing motor. The two motors are provided with plugs so that they may be interchanged depending on the job needed. The vertical-drive servo motor is arranged so that it may be raised to turn on a micro switch and to contact the drive knob of a ten-turn potentiometer for automatically standardizing current in a proportioning bridge circuit. The horizontal drive is also fitted with a ten-turn potentiometer to give an electrical indication in the bridge circuit of the amount of fiber on the combs at the start position before scanning, and subsequently, percentages of that amount for span-length determinations. A schematic diagram of the instrument is shown in Figure 1.

The proportioning bridge circuit, with the general wiring of the instrument, is shown in Figure 2. The potentiometers are an integral part of this bridge. Proportional predetermined percentages of the starting-point amount of fiber on the combs are obtained by a proportional tapped voltage divider. The total

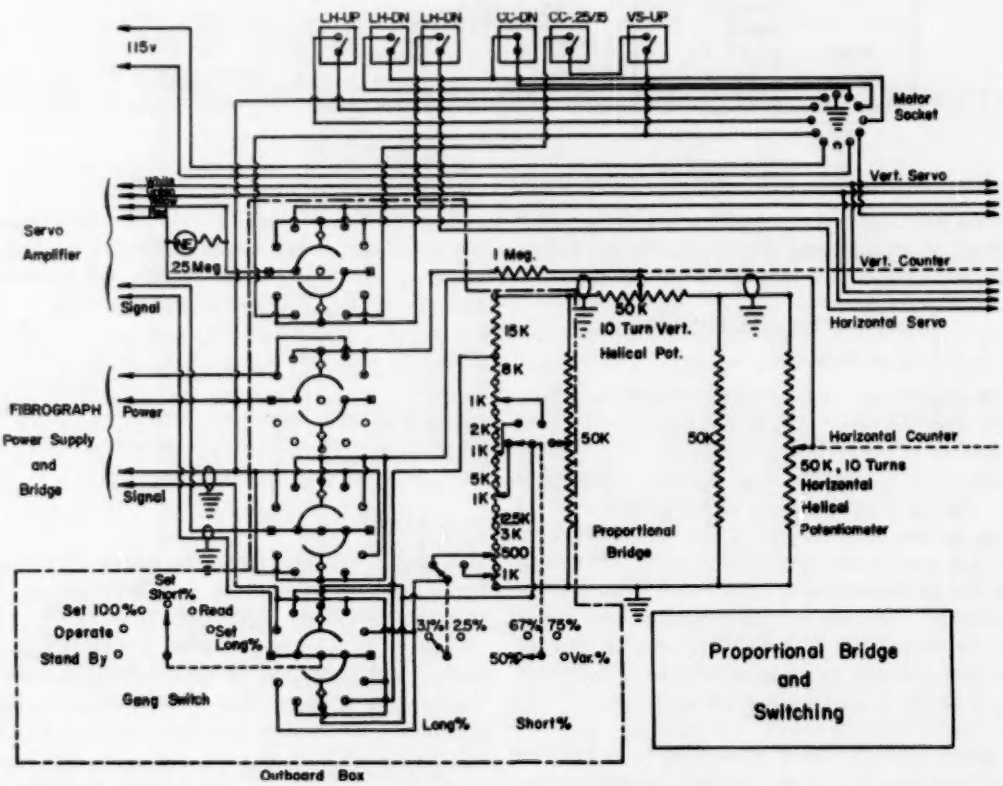

Fig. 2. General wiring diagram of conversion.

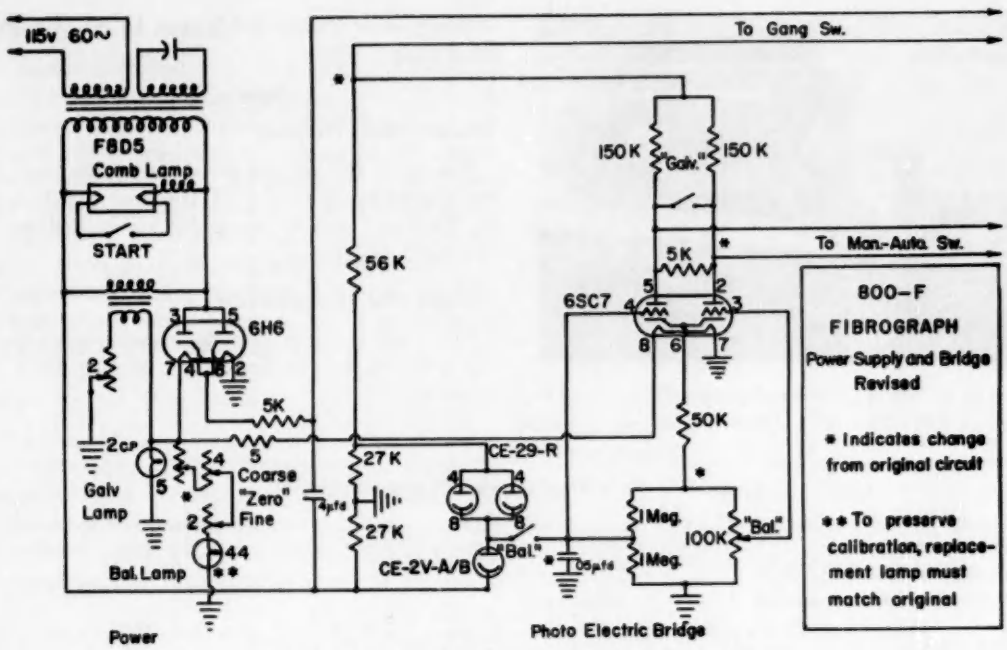

Fig. 3. Fibrograph wiring as revised from original.

resistance of this divider is set at 35 K ohms since a fully loaded pair of combs balances out at about 35 K ohms on the horizontal ten-turn potentiometer. A parallel, 50 K, continuously adjustable divider permits any desired percentage to be obtained. A 4-position switch selects the wanted "Short %" and a 2-position switch the "Long %" from the above dividers. Another 50 K resistance is put into the bridge to keep the circuit symmetrical. A 4-gang, 8-pole, 5-position switch is used by the operator to carry out the standardizing, percentage setting, and length readings needed for span-length measurements. In the conversion described, these switches and voltage dividers were mounted outboard for convenience of experimental change. It should be noted that where small signal voltages are handled by the gang switch, contacts are doubled for improved reliability. Also for all circuits carrying small voltages, shielded cable is employed. Other added elements are a neon light for the output of the servo amplifier to indicate when the bridge is not balanced and a micro switch positioned near the comb carrier so that it closes to permit standardizing only when the carrier is at the starting position of 0.25 or 0.15 in. as needed.

Conversion to span-length measurement operation is completed by tapping off bridge current from the Fibrograph power supply as shown in Figure 3, and adding a 1-megohm resistor to the proportional bridge to limit current to approximately the same value as that used for the photo-electric bridge of the original Fibrograph. Note that only lamp and bridge currents are drawn through the regulator transformer to insure circuit stability; motor currents are taken directly from the line. Changes made by the original servo conversion [3, 4] are also shown in Figure 3.

Completed Conversion

Table I shows the parts requirements for the construction described, with approximate costs. All time-and-material items can be easily made with hand tools except the drive wheels and knobs and ball bearing mounts, which require access to a lathe if they cannot be purchased or improvised.

The completely converted instrument is shown in Figure 4. One item not mentioned is the idler wheel seen on the horizontal drive. It keeps the horizontal motor raised out of the way of gears and the potentiometer. Changes have been made in the comb carrier to permit use of special combs and

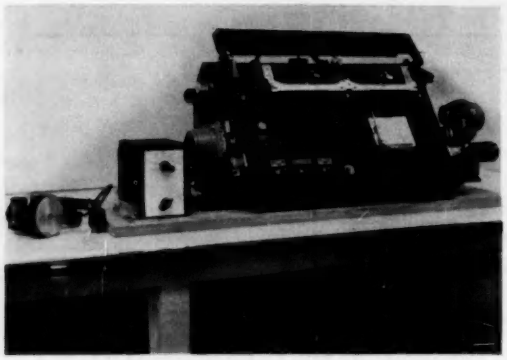

Fig. 4. Converted instrument.

drawing sliver clamps which must be the subject of other papers.

Operation

Manual Curve Drawing

The servo motors are raised out of the way, the servo amplifier is turned off, the gang switch is set to "Operate," and all operations are carried out as originally designed.

Manual Dial Measurements

Operation is the same as for manual curve drawing with the dial readings made directly from the counters.

TABLE I. Parts Requirements with Approximate Cost

	Approximate cost in dollars
Automatic Curve Drawer	
Original servo conversion	
1 ea. servo amplifier	152
1 ea. 27-RPM servo motor	53
1 ea. 6-RPM drive motor	30
1 ea. 0.05 ufd condenser, 50 K resistor, DPDT switch	2
2 ea. drive wheels, motor swing mounts	(time and materials)
Additional conversion	
2 ea. SPST N/O micro switches (closed when lighthouse is down)	4
1 ea. SPST N/O micro switch (closed when lighthouse is up)	2
1 ea. SPST N/C micro switch (open when comb carrier is down)	2
1 ea. DPST motor switch	1
2 ea. ball bearing for hand knobs	3
2 ea. mounts for ball bearings	(time and materials)
Automatic dial or digital measurements	
Manual Operation	
1 ea. counter, revolution, 3 or 4 digit clockwise shaft on right	10
1 ea. counter, revolution, 3 or 4 digit counterclockwise	10
1 ea. pair 2.5/1 brass drive gears for vertical counter	2
1 ea. pair 5/1 brass drive gears for horizontal counter	2
2 ea. angle brackets to mount counters	(time and materials)
1 ea. click stop for vertical counter	(time and materials)
Automatic Operation	
1 ea. 27-RPM servo motor	53
1 ea. set of 11 prong socket and 2 plugs	1
1 ea. SPST N/O micro switch (close when vertical servo is up)	2
1 ea. SPST N/O micro switch (close when carrier is at 0.25 or 0.15)	2
2 ea. 10-turn 50 K helical potentiometers	30
1 ea. set wire wound and variable voltage dividers as shown in Figure 1	15
1 ea. 4-gang, 8-pole, 5-position switch	3
1 ea. single-pole 4-position switch	1
1 ea. 1/25 watt neon and 0.25 meg. resistor	1
1 set hookup and shielded wire	2
1 ea. drive knob for vertical potentiometer	(time and materials)
1 ea. drive wheel for vertical servo	(time and materials)
1 ea. idler wheel for horizontal servo	(time and materials)
1 ea. idler wheel swing mount	(time and materials)

Automatic Curve Drawing

The constant-speed motor is plugged into its place, installed on the shaft, and the gang switch is set to "Operate." The instrument is stabilized as for manual curve drawing, the "Auto–Man." switch thrown to "Auto," and the zero reset if necessary. The Fibrograph then operates as a fully automatic model with the down position of the lighthouse causing the comb carrier to rise and the up position of the lighthouse causing the comb carrier to descend. The horizontal motor balances out in accord with the amount of fiber being measured at the moment.

Automatic Dial Measurements

Operation is the same as for automatic curve drawing except that the constant-speed motor is turned off and vertical comb-carrier settings are made by hand, using the click stop if desired. The horizontal motor is allowed to balance itself as before. Readings are then made directly from the counters.

Span-Length Measurements

The vertical servo motor is plugged into place and the instrument is standardized as for automatic curve drawing. With the combs inserted, the lighthouse is lowered and the horizontal servo allowed to balance. The gang switch then is turned to "Set 100%" and the vertical servo motor raised against the calibration potentiometer wheel until the vertical servo balances. The vertical servo is lowered into place and the gang switch is moved to "Set Short %." After the horizontal motor balances, the gang switch is moved to "Read," and when the vertical servo motor stops, the shorter span length is then read on the left counter for whatever value has been set on the 4-position switch. The gang switch is next moved to "Set Long %." When the horizontal motor stops the gang switch is returned to "Read," and when the vertical servo stops, the longer span length is read on the left counter. The lighthouse is then raised until the comb carrier descends, after which the gang switch is returned to the "Operate" position. The instrument is then ready for another cotton sample.

Acknowledgment

The authors wish to acknowledge the many helpful comments of Thomas Kerr on the problems of evaluating cotton length, which have led to the design of this conversion.

Literature Cited

1. American Society for Testing Materials, Committee D–13, "ASTM Standards on Testing Materials," Philadelphia 3, Pa. (October 1959), ASTM Designation D1447–54T, "Tentative Method of Test for Length of Cotton Fibers by Fibrograph."
2. Hertel, K. L., TEXTILE RESEARCH **10**, 510–525 (1940).
3. Hertel, K. L. and Craven, C. J., *Textile Inds.*, **124**, No. 7, 103–107 (1960).
4. Rouse, J. T., TEXTILE RESEARCH JOURNAL **28**, 505 (1958).
5. Tallant, J. D., TEXTILE RESEARCH JOURNAL **22**, 617–619 (1952).
6. Tallant, J. D., TEXTILE RESEARCH JOURNAL **28**, 815 (1958).
7. Witherspoon, Jack, *Elec. Mfg.* **40**, No. 6, 98–101 (Dec. 1947).
8. Witherspoon, Jack, *Textile Inds.* **113**, No. 1, 87–90 (1949).

Manuscript received October 28, 1960.

The Effect of Blending Cottons of Dissimilar Fiber Properties upon Spinning Performance and Yarn Quality

William T. Waters and Joe Phillips

School of Textile Technology, Auburn University, Auburn, Alabama

Abstract

The blending of cottons with dissimilar fiber properties has been investigated to determine its effect upon processing performance, spinning performance and yarn quality in medium and fine count yarns. In these trials, the effect of grade and cavitomic damage (SM and LM, Sp.), fiber fineness (3.4 and 5.5 Micronaire reading), staple length ($\frac{7}{8}$ in. and $1\frac{1}{16}$ in.) and fiber strength (70,000 lb./in.^{2} and 95,000 lb./in.^{2}) was evaluated. Cotton bales differing appreciably in the property being investigated but having other pertinent properties similar were used. For each trial, the 100% components of the property being investigated and three blends of these cottons were run. The effects of varying percentages of the different cotton fiber properties upon spinning performance and yarn quality are shown.

Introduction

While previous work has shown the effect of cotton's more important fiber properties upon processing performance and yarn quality, the yarn characteristics to be expected from predetermined blending have not been fully investigated. Today's trend of higher spindle speeds, new harvesting and ginning practices, larger packages, and the elimination of a number of prespinning processes has increased the stresses on cotton yarns during spinning, and in many cases has resulted in lower spinning performance and a lower spinnable limit. For this reason, cotton fiber properties and the planned blending of cottons according to these properties have become increasingly important.

In an effort to show the merits of precalculated blending of cotton, a systematic study of blends containing varying amounts of cotton with dissimilar fiber properties has been made using medium and fine count carded yarns. In these trials, the effect of blending cottons differing in grade and cavitomic damage, staple length, fineness, and strength has been investigated. A brief review of the literature on this subject follows.

In an analysis of a large number of samples, Mayne et al. [7] found that classer's grade had little relationship to yarn appearance grade. Samples varying from strict middling to strict low middling, very light spotted were found to show no appreciable difference in yarn appearance grade. The use of new ginning machinery and practices to offset the higher trash content of machine- and rough-picked cotton have created in many instances artificially higher grades which do not reflect the true spinning value of the cotton. Ross [9] shows that some new ginning practices increase the amount of fibers shorter than $\frac{1}{2}$ in., which results in increased ends down during spinning and lower yarn quality.

Fiori et al. [4] investigated the effect of blending extremely fine and coarse cottons and found that the blended sample spun as well as its corresponding control. Leitgeb and Wakeham [6] found that increasing fineness (lower Micronaire reading) resulted in increased yarn strength and lower end breakage rate. Regnery [8] also investigated this effect and found that blending by Micronaire fineness groups resulted in a more consistent day-to-day performance and that extremely low-Micronaire-reading (2.9) cotton tends to increase ends down in spinning.

The inferior quality of cotton containing excessive quantities of short fibers is described in four case histories by Wakeham [12]. These case histories demonstrate that improper drying during ginning, over-processing during cleaning, and microbiological attack (cavitoma) increase the amount of short fibers

during processing and result in greater waste, more uneven roving and yarn, lower spinning performance, and weaker yarns. The effect of short fiber content upon yarn properties and spinning performance was investigated by Tallant et al. [10, 11]. The results obtained indicate that increasing the amount of fibers less than $\frac{3}{4}$ in. in length brings about a lowering of yarn strength, evenness, appearance, and spinning performance.

Although it is generally accepted that fiber strength has a direct correlation with yarn strength, the effects found by Fiori et al. [3] demonstrate very clearly the importance of fiber strength. In comparison of a high strength cotton (96,000 lb./in.^{2}) with a medium strength cotton (80,000 lb./in.^{2}) it was found that the higher strength cotton produced stronger yarns and had little effect upon processing efficiency prior to spinning optimum twist, yarn elongation, and product evenness.

Waters et al. [13] investigated the relative effect of selected fiber properties and spinning processing variables on spinning performance. For the ranges studied, spinning tension, spinning twist, and short fibers affected spinning performance most and in the order named, while fiber fineness lower than a 4.0 Micronaire reading had the least effect. Fineness above a 4.0 Micronaire reading, fiber strength, and spinning draft, on the other hand, had an intermediate effect on spinning performance.

Experimental Method

Cotton

The primary objective of this work was to evaluate the blending of cottons with extreme properties. Many bale samples from the 1959 crop were tested to choose cottons which were average in major fiber properties with the exception of the one property being evaluated. The fiber properties of samples from bales chosen for this work are shown in Table I. Although these bales do not represent the greatest possible extremes in the properties being investigated, it is felt that they are representative of the extremes common in mills. The bales from Alabama are certified DPL 15 variety grown in the Harpersville, Alabama, area. During ginning, these bales went through one Moss-Gordon Lint Cleaner. The history of the remaining bales is not known; however, all bales were checked for short fiber content.

Preblending Procedure

In order to decrease the variation of properties within a bale, each bale was preblended and rebaled at Lummus Gin Company. The following machinery was used: four Lummus Blending Feeders, Pepper Shaker (similar to a Superior Cleaner), Lint Comber (saw tooth type roll), Superjet Cleaner, and Pepper Shaker.

Design of Experiment

To insure accurate and unbiased data and to exclude errors which are normally encountered in experimental work, the Forward Doolittle method [5] was used for design of experiment and computation of regression lines. In each investigation of a particular property, such as fineness, the two component cottons were run 100% and in three blends. Two independent replicates were made for each sample. From the raw data, lines of regression were computed, and calculated points are plotted for

TABLE I. Fiber Properties of Samples from Bales Selected

Designation	Classification	Micronaire reading	Pressley strength (0 in. gauge), 1,000 lb./in.^{2}	Fibrograph (UHM), in.	Probable damage by cavitoma*	Growth area
Control	SM, $1\frac{1}{16}$ in.	4.3	80.6	1.05	No	Alabama
Low grade, cavitomic†	LM, Sp. $1\frac{1}{32}$ in.	4.3	79.6	1.05	Yes	Alabama
Coarse, mature	SM, $1\frac{1}{32}$ in.	5.5	79.1	1.03	No	Alabama
Fine, immature	Sm, $1\frac{1}{16}$ in.	3.1	81.2	1.06	No	Tennessee
Short staple	Sm, $\frac{7}{8}$ in.	4.5	81.0	0.86	No	Texas
Strong staple‡	M+, $1\frac{1}{16}$ in.	4.4	97.7	1.10	No	California
Weak staple	M, $1\frac{1}{16}$ in.	4.1	68.9	1.06	No	Georgia

* ITT pH indicator method.

† Cavitoma damage as evidenced by high pH, microscopic analysis, and comparison of short fiber content before and after passage through Shirley Analyzer.

‡ Acala variety.

TABLE II. Fiber Properties of Various Bales after Preblending and Partial Cleaning at Lummus Gin Company

Property	Control	Low grade, cavitomic	Coarse, mature	Fine, immature	Short staple	Strong staple	Weak staple
1. Fibrograph fiber length							
a. Upper half mean, in.	1.03	0.99	1.00	1.04	0.85	1.07	1.02
b. Mean, in.	0.76	0.70	0.75	0.70	0.59	0.78	0.70
c. Uniformity ratio, %	73	71	76	67	70	73	72
d. Short fiber index, %	13	21	13	16	23	15	16
2. Micronaire reading	4.3	4.2	5.4	3.4	4.6	4.4	4.0
3. Tensile strength							
a. Pressley (0 in. gauge; 1,000 lb./in.^{2})	81.6	81.5	79.0	78.7	84.4	94.8	70.9
b. Pressley ($\frac{1}{8}$ in. gauge; P.I.)	3.38	2.88	3.21	3.36	3.02	3.86	2.88
c. Stelometer ($\frac{1}{8}$ in. gauge; g./tex)	17.5	15.0	17.2	16.3	15.1	19.5	15.7
4. Elongation at break, % (Stelometer, $\frac{1}{8}$ in. gauge)	8.2	6.7	8.4	8.5	6.7	7.8	9.0

presentation of results. Variance was analyzed to determine the significance of the blend variable and the reliability of the data and experiment design.

Processing Procedure

Approximately 100 lb. of raw cotton were processed into 1.10 (520 tex) and 2.50 (240 tex) hank roving for each sample, using conventional machinery. In view of the cleaning during preblending, opening and cleaning were done with only a Blending Feeder and a Superior Cleaner. Blends were made at finisher picking from four breaker picker laps.

The respective rovings were spun into 22/1 (26 tex) and 50/1 (12 tex) yarn on a Roberts M-1 Spinning Frame for evaluation of yarn quality. In addition, each sample was evaluated for spinning performance using the U. S. D. A. accelerated ends down method (84 spindle hr.) [2]. This method is based upon the fact that finer yarn numbers spun from the same cotton under similar conditions and organization will produce a greater number of spinning end breakages. For any one test, a series of four yarns of increasing fineness are spun holding the variables of spindle speed, twist multiplier, and relative traveler size constant. The total number of ends down per 84 spindle hr. is then plotted against yarn count. The point where this trend line intersects an arbitrary number of end breakages (20 in this work) is designated as the spinnable limit. Plots on both regular and logarithmic graph paper facilitate drawing the best fitting curve. It should be understood that this method of evaluating spinning performance is much faster and more sensitive to differences in fiber properties than a conventional ends down test because of the fine counts being spun. It is designed to determine the spinning capabilities of a particular cotton, and may or may not be similar to regular ends down performance in view of the processing variables being used. For example a shorter staple cotton or cotton containing an excessive amount of short fibers might spin at a satisfactory ends down level with optimum yarn twist and spindle speed, but the capabilities of these cottons in a finer yarn, at lower twist and higher spindle speed are not as great as those of a longer staple cotton or cotton with a lower short fiber content. All processing evaluations were conducted at a constant relative humidity of 58%.

Testing Procedure

All tests were conducted at standard conditions using recommended ASTM test methods [1]. Fiber strength and elongation properties were measured from both raw stock and finisher drawing sliver using the Pressley and Stelometer testers at zero and $\frac{1}{8}$-in. gauges. Fiber fineness and maturity properties were measured on the Micronaire and Arealometer, and fiber length properties were determined by means of the Servo-Fibrograph. The percentage of fibers shorter than $\frac{1}{2}$ in. but longer than $\frac{3}{16}$ in. was also determined on the Servo-Fibrograph as a measure of short fiber content. Card web neps were

counted using the N. C. State template method with nep counts being taken periodically throughout the entire carding of a sample. Evenness (%CV) of finisher drawing sliver, roving, and yarn was measured by the Uster Evenness Tester. Evaluation of yarn quality consisted in measuring evenness, skein strength, single strand strength and elongation at break (Uster), and yarn appearance.

Results and Discussion

The properties of fiber from the various bales after preblending and partial cleaning at Lummus Gin Company are shown in Table II. These figures represent truer values for the bale properties since the bales are now more homogeneous. In general, the properties appear similar to those obtained from the original bale samples. One notable exception to this is the low-grade, cavitomic-damaged bale. It is evident that preblending and cleaning (lint comber) have significantly lowered the staple length and increased the number of short fibers. This is a characteristic of cavitomic damaged cotton. The results obtained for the different blend trials are presented separately to show the effect of grade and cavitoma, fineness, staple length, and strength upon performance.

Grade and Cavitomic Damage

The grade of cotton purchased by a mill is usually dictated by cost, the amount of waste that can be tolerated, and yarn quality. Analysis of trash content at several stages of processing shows the lower grade cotton to have only about 1% more actual trash than the higher grade and most of the blends to be only slightly higher in trash content. A comparison of actual trash content and yarn appearance indicates that lower grades can be blended with only small increases in actual waste and no appreciable differences in yarn appearance grade. However, as is the case with the bale mentioned above, properties other than grade may be present which would be detrimental to yarn quality, such as cavitomic damage and lower fiber strength at $\frac{1}{8}$-in. gauge.

The blending of increased amounts of lower grade cotton was found to give only a slight increase in product unevenness but a large increase in neps (see Figure 1). Since both cottons are similar in fineness, it appears that the increase in neps is largely due to the effect of field damage and cavitoma. The increase in neps at carding did not appreciably lower yarn appearance, however.

Fiber properties were measured from finisher drawing sliver in order to give a better prediction of yarn quality. In examining this data (Table III), it is seen that increased amounts of the lower grade cotton give an increase in short fiber content and a decrease in fiber strength at the $\frac{1}{8}$-in. gauge. Using the normal classification of grade, staple, and Pressley (0 gauge), the lower quality of this cotton due to cavitoma and low $\frac{1}{8}$-in. gauge strength would not have been predicted.

The effect of lower grade cotton upon spinnable limit is shown in Figure 2; analysis of variance showed this effect to be significant at the 99% level. This relationship is a linear one in which spinnable limit decreases in direct proportion to the amount of

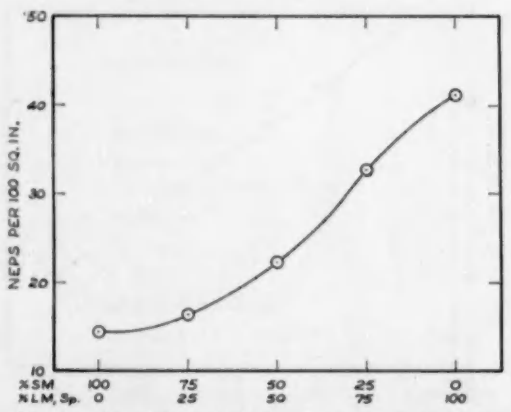

Fig. 1. The effect of blending a lower grade cotton (cavitomic-damaged) upon card web neps.

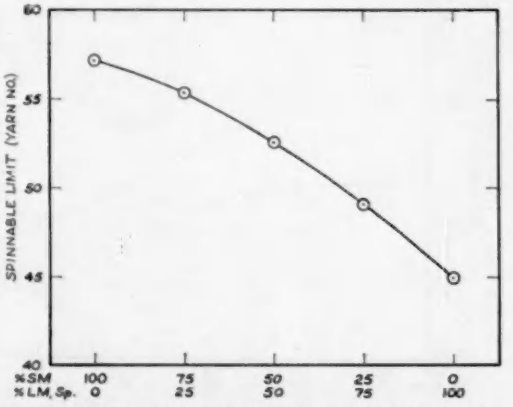

Fig. 2. The effect of blending cottons differing in grade and cavitomic damage upon spinnable limit (USDA Accelerated Ends Down Test).

TABLE III. Fiber Properties from Finisher Drawing Sliver of Blends Containing Varying Amounts of Strict Middling and Low Middling Spotted Cotton*

Property	100% SM	75% SM 25% LM, Sp.	50% SM 50% LM, Sp.	25% SM 75% LM, Sp.	100% LM, Sp.
1. Fiber length (Fibrograph)					
a. Upper half mean, in.	1.06	1.06	1.06	1.05	1.06
b. Mean, in.	0.79	0.78	0.75	0.73	0.71
c. Uniformity ratio, %	75	73	71	69	67
d. Short fiber index, %	13.0	14.8	16.6	18.2	17.8
2. Micronaire reading	4.4	4.4	4.4	4.3	4.3
3. Tensile strength					
a. Pressley (0 in. gauge; 1,000 lb./in.²)	80.0	80.8	80.0	80.2	80.7
b. Pressley ($\frac{1}{8}$ in. gauge; P.I.)	3.54	3.25	3.14	3.10	3.08
c. Stelometer ($\frac{1}{8}$ in. gauge; g./tex)	17.4	16.4	15.6	15.3	15.0
4. Elongation at break, % (Stelometer, $\frac{1}{8}$ in. gauge)	9.4	8.2	7.7	7.0	6.4

* Low Middling, Spotted Cotton is also cavitomic damaged.

lower grade cotton blended. The lowering of spinnable limit is probably not due to the lower grade of the cotton in this case but more likely to the increased amount of short fibers.

The blending of a lower grade, cavitomic-damaged cotton with a higher, undamaged grade was found to have an appreciable effect upon yarn strength, particularly in blends containing 50% or more of the lower grade. This effect is shown in Figure 3. Analysis of variance in the results indicates a significant effect at the 99% confidence level.

Here again, the effect is not due to grade but to the increasing amounts of short fibers and the decreasing fiber strength at $\frac{1}{8}$-in. gauge. Plots of yarn strength versus fiber strength ($\frac{1}{8}$-in. gauge) and short fiber index show a definite relationship among these properties.

It was also noticed from the data that increased proportions of the lower grade cotton gave slightly more uneven yarn and a lower elongation to break. The increased amount of short fibers and the lower elongation to break of the lower grade cotton seem to offer a reasonable explanation for these effects.

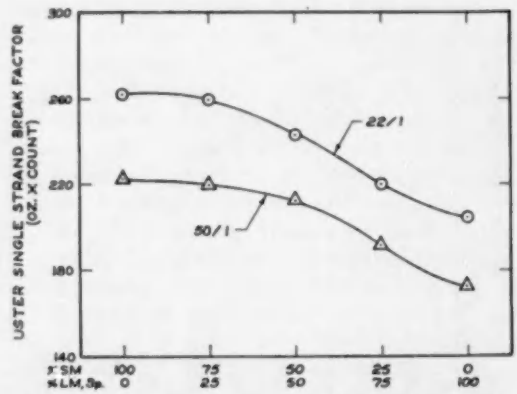

Fig. 3. The effect of blending a lower grade, cavitomic-damaged cotton with a higher grade cotton upon yarn strength.

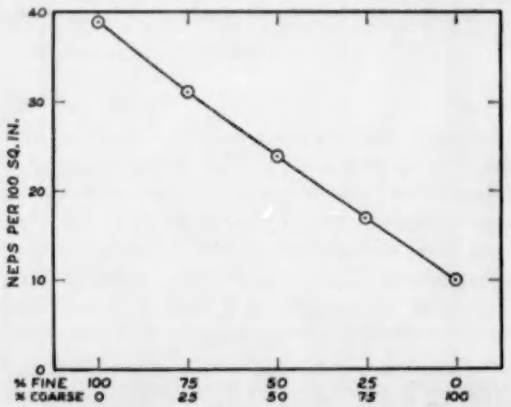

Fig. 4. The effect of blending coarse (5.5 μg./in.) and fine (3.4 μg./in.) cotton upon card web neps.

From previous work in this field and the results obtained here, it appears that differences of two or three grades as such will not have a very great effect upon yarn quality and appearance if other fiber properties are normal. However, the lower grade cottons are more commonly damaged, and their lower fiber properties (e.g., excessive short fibers and lower fiber strength at ½-in. gauge) can drastically lower spinning performance and yarn quality. The blending of up to 25% lower grade or damaged cotton appears to be acceptable from the point of view of processing performance and yarn quality. In addition it should offer savings in raw material costs and a means of running damaged cotton on hand.

Fiber Fineness

With the introduction of the Micronaire, it has become common practice in most mills to measure the "Micronaire fineness" of all bales and to blend according to this property. This practice has been found to result in more uniform running from day to day because of the effect of fiber fineness upon neps, twist, spinning performance, and yarn strength. For these trials, bales of 3.1 and 5.5 Micronaire reading which had similar and average other fiber properties were chosen. After blending and cleaning, the Micronaire value of the fine bale was found to be 3.4. Although greater extremes in fineness are used, it is believed that the range from 3.4 to 5.5 is adequately representative of over-all mill use. Examining the fiber properties of the various blends from finisher drawing sliver (Table IV), it was found that the blends were similar in all properties except fineness. The measurements of fineness and maturity properties by the Micronaire and Arealometer, respectively, indicate that these properties vary in proportion with the blend.

As was to be expected, neps at carding were affected significantly by the blending of coarse and fine fibers. A plot of neps versus blend percentage is shown in Figure 4; it was found that fiber fineness had a statistically significant effect upon card web neps. The relationship found was linear for the range covered; however, the use of a finer, more immature cotton would probably have changed this to a non-linear relationship. No appreciable difference in product evenness among blends was found.

The effect of blending cottons of different Micronaire fineness upon spinnable limit is shown in Figure 5. From analysis of variance, it was found that the blend percentage had a significant effect upon spinnable limit at the 99% level and that a linear relationship exists. The finer cotton is seen

TABLE IV. Fiber Properties from Finisher Drawing Sliver of Blends Containing Varying Amounts of Coarse (5.5 μg./in.) and Fine 3.4 μg./in.) Cotton

Property	100% Fine	75% Fine 25% Coarse	50% Fine 50% Coarse	25% Fine 75% Coarse	100% Coarse
1. Fiber length (Fibrograph)					
a. Upper half mean, in.	1.10	1.10	1.08	1.07	1.07
b. Mean, in.	0.74	0.76	0.76	0.80	0.83
c. Uniformity ratio, %	67	69	70	75	77
d. Short fiber index, %	18.9	15.4	16.8	12.1	10.3
2. Micronaire reading	3.6	4.0	4.4	4.8	5.5
3. Tensile strength					
a. Pressley (0 in. gauge; 1,000 lb./in.²)	80.3	81.6	80.6	78.9	78.5
b. Pressley	3.44	3.45	3.41	3.27	3.28
c. Stelometer (⅛ in. gauge; g./tex)	16.3	16.3	16.0	15.8	16.0
4. Elongation at break, % (Stelometer, ⅛ in. gauge)	8.2	8.3	8.4	8.4	8.6
5. Arealometer fineness					
a. Surface area, mm.²/mm.²	502	476	452	420	397
b. Shape factor, D	82	73	61	56	43
c. Weight fineness, μg./in.	4.7	5.1	5.1	5.8	5.9

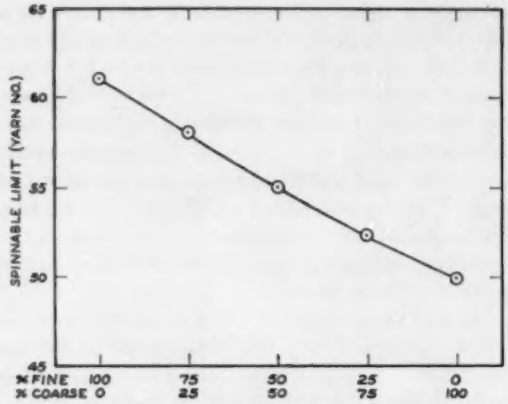

Fig. 5. The effect of varying percentages of fine (3.4 μg./in.) and coarse (5.5 μg./in.) cotton upon spinnable limit.

to be approximately 20% higher in spinnable limit than the coarse cotton.

In spinning yarn for evaluation, a similar twist multiplier (4.1) was used for all blends. The optimum twist for each blend will most likely vary slightly due to fineness, and the results obtained are based on this limitation of using a similar twist multiplier over the range of fineness studied. The effect of fineness upon single strand strength is shown in Figure 6.

For both the 22/1 and 50/1 yarns, an increase of approximately 16% was found in going from 100% coarse to 100% fine. It is also noted that the 50/1 yarn showed a greater initial drop in strength with the addition of coarse staple than did the coarser 22/1. Similar trends were found for skein strength, and the blends showed no appreciable difference in yarn evenness. It is noted that with increasing amounts of coarser fiber the yarn elongation to break decreases even though the fiber elongation properties of both cottons are similar. This is most likely due to greater slippage of the coarser fibers and to the decreasing number of fibers per cross-section, both of which decrease interfiber frictional characteristics of the yarn. Although there were appreciable differences in card web neps among the blends, the yarn appearance grade of the 22/1 was not appreciably improved by the addition of coarser cotton. In the case of the finer 50/1, a significant increase is noted with the addition of coarser staple, indicating that fineness has a greater effect upon yarn appearance in finer counts than in coarser counts.

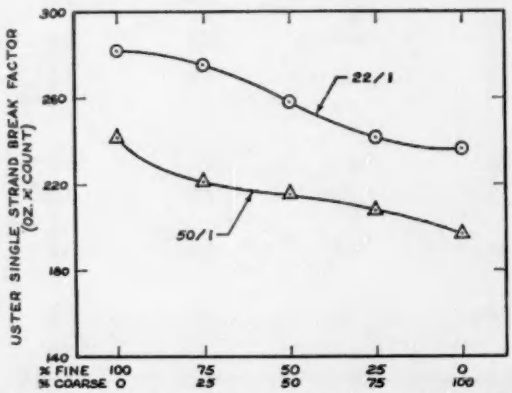

Fig. 6. The effect of varying percentages of fine (3.4 μg./in.) and coarse (5.5 μg./in.) cotton upon yarn strength.

The results of this trial indicate that mixes containing an average fineness of 3.5 to 4.0 μg./in. will give improved yarn quality and spinning performance over coarser mixes. The increased card web neps due to the finer cotton did not affect yarn appearance grade appreciably; however, the effect of these increased neps upon appearance of dyed goods was not investigated and should be considered.

Staple Length

The importance of staple length to yarn quality is well known, but little work has been done in the blending of varying percentages of a short staple with longer staples. Recently [10, 11], the importance of fibers shorter than ½ in. to spinning performance has been shown. In order to investigate the effect of blending varying amounts of a short staple with a longer staple, a bale of ⅞-in. cotton from Texas was chosen. Both the short staple and medium staple ($1\frac{1}{16}$ in., SM) used are similar in other fiber properties. In addition to the difference in staple length, the shorter staple also has a higher percentage of fibers shorter than ½ in., which would have a detrimental effect upon spinning performance and yarn quality. A comparison of fiber properties from finisher drawing sliver of the various blends (Table V) shows the staple length of the blends to become progressively lower as more short staple is added and the short fiber index to become progressively higher.

In Figure 7 it is seen that the addition of shorter staple improved card web neps. The ratio of fiber diameter to fiber length is important with regard to the nepping potential of a fiber, with the shorter length lowering the nepping tendency. Sliver and

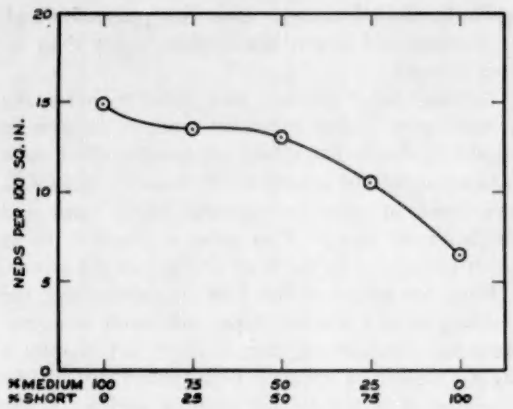

Fig. 7. The effect of blending shorter staple upon card web neps.

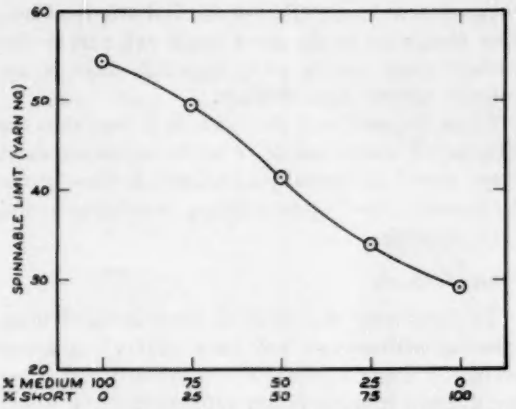

Fig. 8. The effect of blending a short staple ($\frac{7}{8}$ in.) with a medium staple ($1\frac{1}{16}$ in.) upon spinnable limit.

roving unevenness were seen to increase somewhat with the addition of shorter staple. This is to be expected because of the lack of control of the shorter fibers in the drafting zone.

The detrimental effect of blending in shorter staple length upon spinning performance is shown in Figure 8. Although the higher percentage of short fibers ($\frac{1}{2}$ in. and less) has in all probability an effect upon spinning performance, it appears that the difference in the mean length of the fibers would have a greater effect. The relationship is seen to be almost linear, indicating that the blending of shorter staple will lower spinnable limit in proportion to the amount added. Since it is common practice to blend in small amounts of comber noils, vacuum strips, and other waste, their effect upon spinning performance should be realized.

In addition to the large effect staple length variation has upon spinning performance, it is seen to have an equally large effect upon yarn strength (see Figure 9). The blending in of short fibers was also found to cause an increase in yarn unevenness and a decrease in yarn appearance. The blend yarns containing short fibers were found to have lower

TABLE V. Fiber Properties from Finisher Drawing Sliver of Blends Containing Varying Amounts of Medium Staple (1 1/16 in.) and Short Staple (7/8 in.) Cotton

Property	100% Medium	75% Med. 25% Short	50% Med. 50% Short	25% Med. 75% Short	100% Short
1. Fiber length (Fibrograph)					
a. Upper half mean, in.	1.06	1.02	1.00	0.98	0.95
b. Mean, in.	0.79	0.74	0.72	0.71	0.69
c. Uniformity ratio, %	75	72	72	72	72
d. Short fiber index, %	11.3	16.2	17.0	17.7	17.2
2. Micronaire reading	4.4	4.5	4.6	4.6	4.6
3. Tensile strength					
a. Pressley (0 in. gauge; 1,000 lb./in.²)	80.0	80.5	81.0	81.0	82.7
b. Pressley ($\frac{1}{8}$ in. gauge; P.I.)	3.54	3.25	3.21	3.20	3.24
c. Stelometer ($\frac{1}{8}$ in. gauge; g./tex)	17.4	16.9	16.7	16.2	15.7
4. Elongation at break, % (Stelometer, $\frac{1}{8}$ in. gauge)	9.4	9.0	8.3	7.7	7.1

elongations at break. Part of this is due to the lower fiber elongation of the short staple and part to the weaker, more uneven yarn, in which there is apparently greater fiber slippage.

From the results of this trial, it is seen that the blending of shorter staple or waste containing short fibers should be carefully considered in view of the detrimental effect upon spinning performance and yarn properties.

Fiber Strength

To investigate the effect of fiber strength upon spinning performance and yarn quality, an above average strength cotton (95,000 lb./in.^{2}) and a below average strength cotton (70,000 lb./in.^{2}), which were similar in other properties, were chosen. These two cottons were also significantly different in fiber strength at the $\frac{1}{8}$-in. gauge. The strength of fibers from finisher drawing for the various blends (Table VI) was found to decrease in proportion to the amount of weak cotton added.

From the known effect of fiber strength upon yarn strength, one might suspect that stronger fibers would have a large effect upon spinning performance. The effect of blending stronger cotton with a weak cotton is shown in Figure 10; it is seen that there is not a very great effect. In view of this and previous findings, it appears that end breakage at spinning is due more to fiber slippage than to fiber breakage. This in turn would indicate end breakage to be more dependent upon fiber properties such as fineness and length distribution rather than on fiber strength.

Although fiber strength was found to have only a small effect upon spinnable limit, it is seen in Figure 11 that it has a very appreciable effect upon yarn strength. In general a difference of 25%–30% was found to exist between the 100% weak and 100% strong yarns. This effect is found to be in direct proportion to the fiber strength of the blends.

From the results of this trial, it appears that the blending in of a weaker staple will result in a proportionate decrease in yarn strength but in only a slight lowering of spinning performance. With the exception of known strong varieties, such as Acala, the higher strength cottons do not usually sell at a premium. The testing and blending of cotton by strength should result in more uniform yarn strength. In addition, blends could be made to give additional yarn strength without additional cost. It should be realized though, that fiber strength at zero gauge does not predict yarn strength as well as values at the $\frac{1}{8}$-in. gauge.

Conclusions

A series of spinning trials has been run to investigate the effect of blending cottons of dissimilar fiber properties upon spinning performance and yarn quality. The results of these trials allow the following conclusions to be drawn.

TABLE VI. Fiber Properties from Finisher Drawing Silver of Blends Containing Varying Amounts of a Strong Cotton (95,000 lb./in.^{2}) and a Weak Cotton (70,000 lb./in.^{2})

Property	100% Strong	75% Strong 25% Weak	50% Strong 50% Weak	25% Strong 75% Weak	100% Weak
1. Fiber length (Fibrograph)					
a. Upper half mean, in.	1.10	1.10	1.09	1.08	1.05
b. Mean, in.	0.80	0.81	0.80	0.78	0.75
c. Uniformity ratio, %	73	73	73	72	71
d. Short fiber index, %	11	11	13	13	15
2. Micronaire reading	4.3	4.3	4.2	4.1	4.0
3. Tensile strength					
a. Pressley (0 in. gauge; 1,000 lb./in.^{2})	92.5	88.9	84.3	78.0	68.1
b. Pressley ($\frac{1}{8}$ in. gauge; P.I.)	3.84	3.62	3.29	3.13	2.84
c. Stelometer ($\frac{1}{8}$ in. gauge; g./tex)	20.3	19.0	17.9	17.4	16.0
4. Elongation at break, % (Stelometer, $\frac{1}{8}$ in. gauge)	8.2	8.3	8.4	8.7	9.1

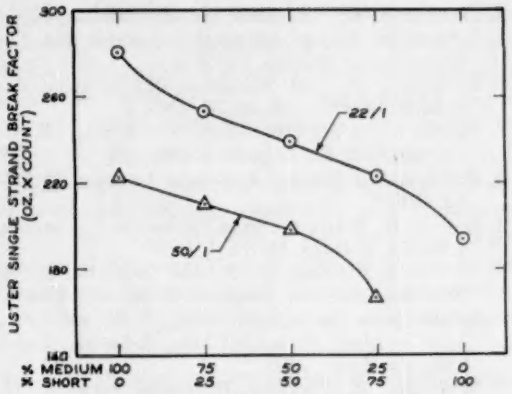

Fig. 9. The effect of blending short staple ($\frac{7}{8}$ in.) with medium staple ($1\frac{1}{32}$ in.) upon yarn strength.

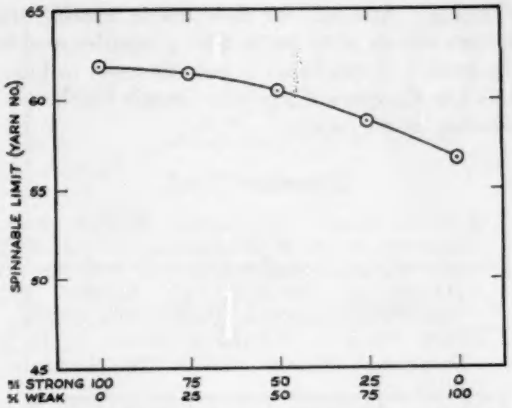

Fig. 10. The effect of blending a strong cotton (95,000 lb./in.²) with a weak cotton (70,000 lb./in.²) upon spinnable limit.

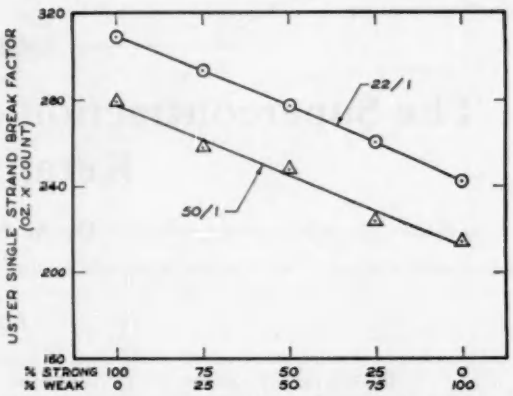

Fig. 11. The effect of blending a strong (95,000 lb./in.²) and a weak (70,000 lb./in.²) cotton upon yarn strength.

1. Differences of two or three grades will not have an appreciable effect upon yarn quality and spinning performance if other fiber properties are normal. Damage by cavitoma results in an excessive amount of short fibers which in turn gives significant losses in spinnable limit and yarn strength. Blends containing up to 25% of a lower grade or cavitomic-damaged cotton can be run without appreciable effect upon spinning performance or yarn quality.

2. Blends containing an average fineness of 3.5 to 4.0 μg./in. (Micronaire) result in optimum spinning performance and yarn quality. Although this fineness range is not optimum in regard to card web neps, this does not appear to have an appreciable effect upon yarn appearance grade. The effect of increased card web neps upon the appearance of dyed fabric was not investigated and should be considered.

3. Of the properties investigated, the blending of shorter staple cotton was found to have the greatest detrimental effect upon spinning performance and yarn quality.

4. The blending of cotton with different fiber strengths does not appear to have a very great effect upon spinnable limit but does have a significant effect upon yarn strength.

5. The results of these blending trials indicate that precalculated blending according to the more important fiber properties can be done to obtain desired yarn characteristics. In many cases, improved yarn quality and spinning performance can be had at no increase in cost of raw material, or, alternatively, similar quality can be had at a lower raw material cost, if fiber properties are measured and the blends predetermined.

Acknowledgments

Appreciation is expressed to the following members of the Textile Research Department, School of Textile Technology: to Clyde Pryor, Robert Putnam, and William Register for processing of samples into yarn; and to Lila Putnam and Dorothy Sumners for the testing and analysis of fibers and yarns. Appreciation is due also to Earl Atkinson, Parker Fertilizer Company, Sylacauga, Alabama; W. C. Bradley Company, Columbus, Georgia; Jim Little, Anderson, Clayton and Company, Memphis, Tennessee; H. A. Poteet, Plains Cotton Growers, Lubbock, Texas; and Mr. Alex Turner, Avondale Mills,

Sylacauga, Alabama, for their aid in locating the various cottons with specific fiber properties used in this study. Appreciation is also expressed to Lummus Gin Company, Columbus, Georgia for the preblending of all cotton.

Literature Cited

1. American Society for Testing Materials, Committee D-13, ASTM Designations (a) 1445-60T; (b) 1447-54T; (c) 1448-59; (d) 1449-58; (e) 1451-59; (f) 180-57T; (g) 1425-60T; (h) 1578-59T; Philadelphia, Pennsylvania (1960).
2. Eddins, Frank S., and Burley, Samuel T., U. S. Dept. Agr. Bulletin A.M.S. 299 (February, 1959).
3. Fiori, L. A., Brown, J. J., and Sands, J. E., TEXTILE RESEARCH JOURNAL **24**, 503–507 (1954).
4. Fiori, L. A., Louis, G. L., and Sands, J. E., TEXTILE RESEARCH JOURNAL **29**, 706–716 (1959).
5. Hunter, J. S., "Response Surface Methodology," American Society for Quality Control and The University of Buffalo, (1958).
6. Leitgeb, D. C. and Wakeham, H., TEXTILE RESEARCH JOURNAL **26**, 67–76 (1956).
7. Mayne, S. C., Jr., Little, J. N., and Berkley, E. E., *Textile Bull.* **84**, 121–129 (1958).
8. Regnery, W., TEXTILE RESEARCH JOURNAL **22**, 49–52 (1952).
9. Ross, J. E., Western Cotton Production Conference, Phoenix, Arizona, March 4, 1958.
10. Tallant, J. D., Fiori, L. A., and Legendre, D. C., TEXTILE RESEARCH JOURNAL **29**, 687–695 (1959).
11. Tallant, J. D., Fiori, L. A., Little, H. W., and Leitz, L. A., Cotton Research Clinic, Asheville, North Carolina, June, 1960.
12. Wakeham, H., TEXTILE RESEARCH JOURNAL **25**, 422–429 (1955).
13. Waters, W. T., Phillips, J., and Fiori, L. A., submitted to Textile Industries.

Manuscript received November 8, 1960.

The Supercontraction of Sound and Weathered Keratin Fibers

O. A. Swanepoel

South African Wool Textile Research Institute, Rhodes University, Grahamstown, South Africa

Abstract

Studies on the supercontraction of sound and weathered wool and mohair fibers have thrown further light on the mechanism of this reaction. It is concluded that the second stage of supercontraction results from the exposure of sterically protected hydrogen bonds. This can occur through disulfide exchange in the highly cross-linked zones of the microfibrils. Some of the cystine cross-links are stabilized by weathering so that disulfide exchange is inhibited, and hence much less contraction occurs.

Introduction

It has been shown that definite chemical changes are associated with the weathering of wool [13]. Particularly noticeable in these changes is the progressive decrease of the cystine content from root to tip. This amino acid has also been considered in connection with the two-stage contraction of keratin fibers [9], and mention has been made of a possible part played therein by disulfide exchange [10]. The present investigation was undertaken to establish in what way supercontraction of keratin fibers is influenced by cystine content and by changes brought about during weathering.

Materials and Methods

Keratin samples. Samples of Merino wool, mohair, and human hair were washed successively in petroleum ether, 0.1% aqueous solution of Lissapol NX (I.C.I.), water, alcohol, and finally in ether, all at room temperature, and then dried in a stream of cold air. All tip/root relationships discussed in this paper refer to the behavior of the tip in relation to that of the root from the same fiber.

Lithium bromide solution. The lithium bromide solution used in this work was 7.82 *M* throughout.

Reduction and blocking. 0.5 *M* thioglycolic acid, made up with an acetate buffer solution of pH 5.2

[19], was used for reduction of the keratin. The reduced sites thereby produced were blocked by reaction with a solution of iodoacetic acid prepared by dissolving 1.0 g. acid in 3 ml. water, adding this to 130 ml. 0.1 *N* $NaHCO_3$, and adjusting the pH to 8.7 by the addition of about 2 ml. 2 *N* NaOH [16].

The reduction was performed by treating 100 mg. of wool with 100 ml. thioglycolic acid solution at 35° C. for varying lengths of time according to the amount of reduction desired. The fibers were then washed in oxygen-free water and immediately treated for 2 hr. with 130 ml. iodoacetic acid solution at 35° C. to block the reduced sites. Both reduction and blocking were carried out in a hydrogen atmosphere to prevent re-oxidation [15] of the reduced sites before blocking had been effected.

The thiol groups in untreated wool were eliminated by carboxymethylation for 4 hr. as described for the blocking of reduced wool.

Supercontraction. The microscope technique described by Haly and Griffith [11] was employed to obtain the kinetic supercontraction curves of the fibers.

Stress–strain measurements. The stress–strain characteristics of the supercontracted fibers, immersed in a 7.8 *M* lithium bromide solution, were measured by applying the beam principle described by Hall [7]. Tension was applied by a liquid loading and unloading system similar to that of Sleichter and Lollar [14], except that, in order to improve the accuracy, mercury was replaced by water. The extensions were measured with a travelling microscope. The length and diameter of the fully supercontracted fiber were taken as the "zero strain" values. The elastic modulus, *G*, was calculated using Treloar's [17] equation

$$f_a = G\left(\alpha - \frac{1}{\alpha^2}\right)$$

where G = elastic modulus, α = (1 + strain), and f_a = force per unit area exerted on the fiber, the area taken being that at zero strain. By plotting f_a against $\left(\alpha - \frac{1}{\alpha^2}\right)$, G can be read from the graph.

Results

Supercontraction studies on wool and mohair fibers were performed at 85° C. Equilibrium contraction for the various segments used was reached in about 90 min., and the kinetic curves obtained for washed but otherwise untreated samples showed two stages of contraction. Whereas these two stages were well defined in the case of unweathered roots, the intermediate stage was not as prominent for the tip sections (see Figures 1 and 2). Moreover, the maximum contraction found for the tips was considerably smaller than that for corresponding roots. Even in cases where weathering of the tips was so slight that there was no change in the ninhydrin index [18] and experienced wool appraisers judged the wool as unweathered, this diminution in the equilibrium contraction value was quite marked.

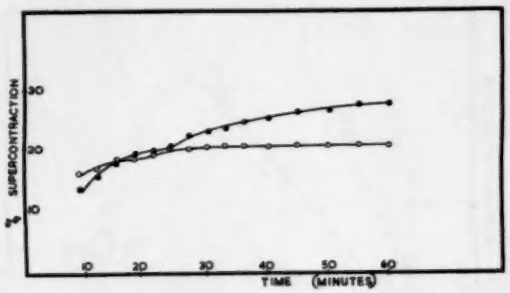

Fig. 1. Supercontraction of Merino wool in 7.8 *M* lithium bromide at 85° C. ● = unweathered root; ○ = weathered tip.

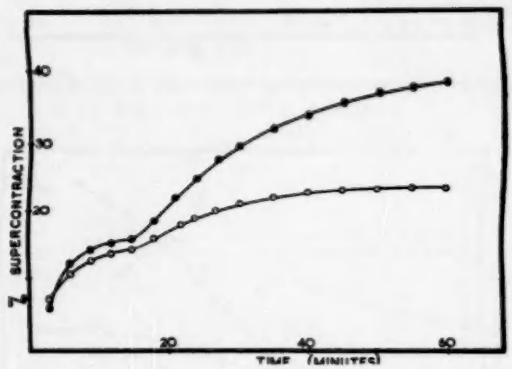

Fig. 2. Supercontraction of mohair in 7.8 *M* lithium bromide at 85° C. ● = unweathered root; ○ = weathered tip.

An investigation of fibers taken from eight different wool samples, all of which were weathered to a slight extent only, revealed that for a given fiber the maximum contraction of the tip generally approached very closely the value obtained for the first-stage contraction of the root (see Table I). From five to eight fibers out of each sample were used for this study, and the values obtained were fairly repro-

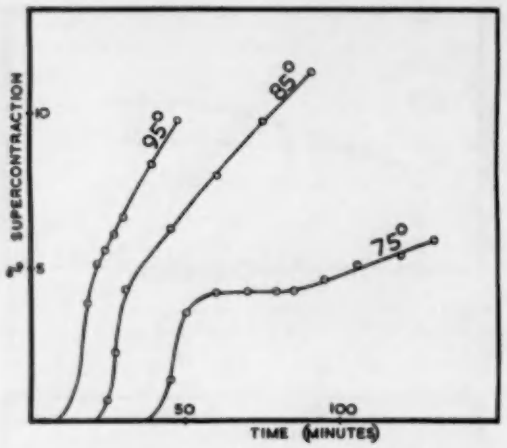

Fig. 3. Supercontraction of human hair in 7.8 *M* lithium bromide at various temperatures.

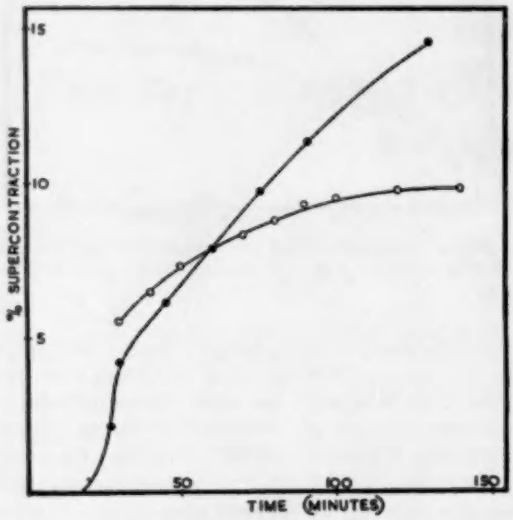

Fig. 4. Supercontraction of human hair in 7.8 *M* lithium bromide at 85° C. ● = unweathered root; ○ = root after exposure to weathering conditions for 2 mo.

ducible throughout. For more heavily weathered wool samples (ninhydrin index greater than 1.4), the maximum supercontraction value was decreased even further.

Human hair was studied under slightly different conditions. When the roots were contracted at 85° C., the intermediate stage could not be seen clearly (see Figure 3), and it was found necessary to reduce the temperature to 75° C. in order to obtain two well-defined contraction stages. Also, the tips

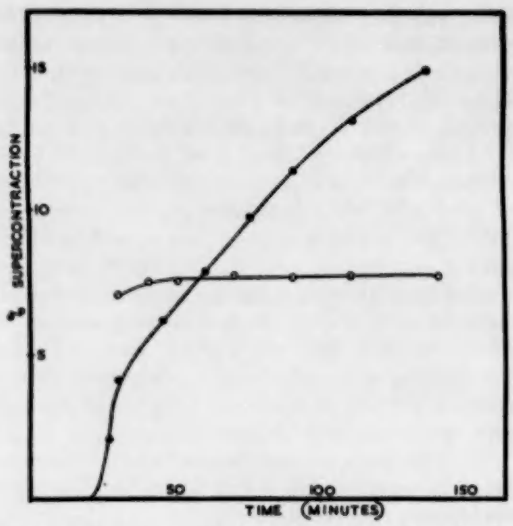

Fig. 5. Supercontraction of human hair in 7.8 *M* lithium bromide at 85° C. ● = normal unweathered root; ○ = unweathered root treated in 1% KCN at 65° C. for 16 hr.

were not used for studying the behavior of weathered fibers; instead, the latter were produced by cementing single root ends, washed as above, at 1-cm. intervals onto a metal bar with polystyrene cement (polystyrene dissolved in chloroform) and exposing them to the atmosphere for two months. This period was found to be adequate since these fibers were devoid of the normal protection afforded by their neighbors and therefore weathered more rapidly. After exposure, the fibers were again scoured before being subjected to supercontraction (results given in Figure 4). The times required for equilibrium contraction of human hair samples ranged from 5 to 7 hr.

TABLE I. Supercontraction Values for Unweathered Roots and Slightly Weathered Tips Obtained from the Same Fiber

Sample no.	% Supercontraction of root at intermediate stage of curve	% Supercontraction of tip at maximum of curve
1	21.0	20.0
2	21.0	20.5
3	20.0	19.3
4	20.0	19.0
5	18.2	18.1
6	17.0	16.5
7	16.0	15.5
8	15.0	15.0

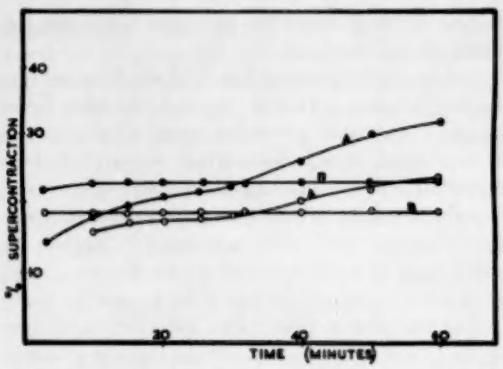

Fig. 6. Supercontraction of wool fibers in 7.8 *M* LiBr at 85° C. A, untreated fibers; B, fibers treated in 1% KCN at 65° C. for 16 hr. ● = unweathered roots; ○ = weathered tips.

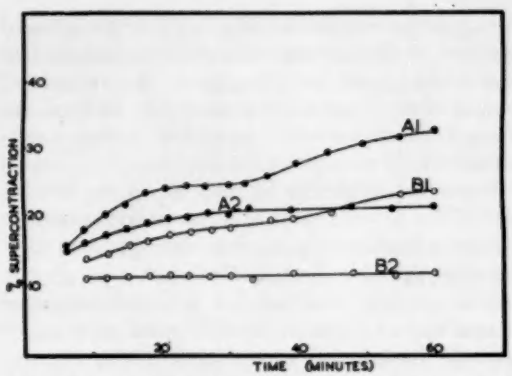

Fig. 7. Supercontraction of Merino wool treated with iodoacetic acid. A1, untreated root; A2, treated root; B1, untreated tip; B2, treated tip.

Heating of wool fiber roots in a 1% KCN solution at 65° C. for 16 hr. resulted in smaller contraction values with total inhibition of the second contraction stage. Similar treatment of the slightly weathered tips likewise produced total inhibition of the already diminished final stage of contraction (see Figures 5 and 6).

As shown in Figure 7, wool fibers treated with a solution of iodoacetic acid at pH 8.7 for 4 hr. also contracted much less than untreated fibers, the contraction taking place in one stage only.

The results of the supercontraction studies on reduced and blocked wool fibers are presented in Figure 8. In curves D, the elongation of the fibers was preceded by contraction which was too rapid for measurements to be made.

The stress–strain measurements on supercontracted fibers showed a decrease of only 1.7% in elastic modulus, *G*, from root to tip in the slightly weathered wool samples.

Discussion

Figures 1 and 2 show that, for weathered wool and mohair tips, two-stage contraction is much less pronounced than in the case of unweathered roots, and the maximum contraction at equilibrium is considerably smaller. This diminution in contraction is marked even for wool tips which have been only very slightly weathered. It would thus appear that the modifications in the wool which are responsible for decreasing its contraction in LiBr must take place in the very earliest stages of the weathering process. Confirmation is provided by the fact that human hair roots, after only two months' exposure to the atmosphere, also show a marked decrease in the maximum supercontraction value.

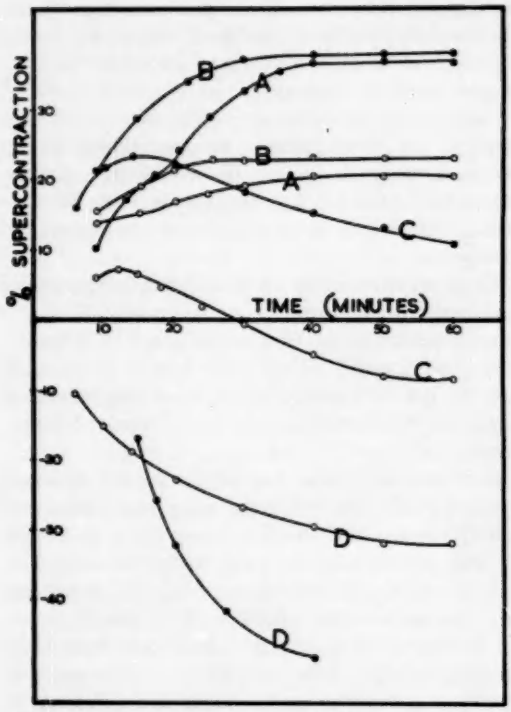

Fig. 8. Supercontraction of wool fibers reduced in 0.5 *M* thioglycolic acid and carboxymethylated. ● = unweathered roots; ○ = weathered tips. A, untreated fibers; B, 30 min. reduction; C, 45 min. reduction; D, 6 hrs. reduction.

Furthermore, the partial suppression of second-stage contraction observed for weathered fibers, coupled with the close correspondence found between

the maximum contraction value of slightly weathered tips and the value after first-stage contraction of unweathered roots, would suggest that weathered keratin is to a large extent unable to undergo the changes which normally take place during supercontraction at the end of the first stage.

Before any effort can be made to explain this behavior of weathered wool, it is necessary to postulate a more precise theory for the mechanism of two-stage contraction of keratin fibers.

It is generally accepted that supercontraction of protein fibers in lithium bromide solutions involves basically the breaking of hydrogen bonds, whereby the peptide chains acquire a greater freedom of movement, and the subsequent twisting of these chains by the high lateral vibrational energy supplied at the elevated temperature. In the first stage of the reaction only readily accessible hydrogen bonds are severed, whereas the breaking of less accessible hydrogen bonds is responsible for the final phase of the supercontraction curve [1, 8]. No explanation is given for the difference in accessibility of the various hydrogen bonds, nor of the molecular changes which take place at the end of the first stage to expose the less accessible hydrogen bonds to the contractant.

These problems can be elucidated by assuming that zones of two kinds occur alternately along the structural units of the fiber, as proposed by Feughelman and Haly [5]. They refer to these zones as X and Y, the X zones contracting during the first stage and the Y zones in the second stage of supercontraction.

Simultaneous contraction of the X and Y zones would account for the single-stage contraction observed when a few disulfide cross-links in keratin are severed either by very mild reduction with thioglycolic acid (see Figure 8, curve B) or by irradiation with ultraviolet light [9]. For this to occur, the hydrogen bonds in both zones would have to be equally accessible to the contractant. Two-stage contraction, on the other hand, indicates a difference in the accessibility of the hydrogen bonds, which must therefore result from the sheltering effect of the disulfide cross-linkages. This is in agreement with the observation of Linderstrøm-Lang, who points out that peptide hydrogens which are thus sheltered are not readily accessible to liquids [12]. On this basis it would appear that the Y zones contain hydrogen bonds which are protected from the contractant by covalent cross-linkages and steric hindrance, whereas in the X zones the hydrogen bonds are free from such interferences.

The protected hydrogen bonds of the Y zones can, however, become accessible through disulfide interchange. That such a reaction could play a part in the final stage of supercontraction has already been suggested, but without elaboration [10]. Conversion of cystine cross-links into thio–ether bonds by treatment of keratin with KCN solution [4] inhibits the second stage of supercontraction (see Figure 6); so, too, does blocking of the free thiol groups by treatment of the protein fibers with iodoacetic acid (see Figure 7). It is apparent therefore that the presence of both cystine cross-linkages and free sulfydryl groups is essential for the second stage of supercontraction to occur.

The possibility that the introduction of stresses in a fiber can lead to a disulfide-sulfydryl interchange was first postulated by Burley [2]. It is feasible that thermal stresses arising from the immersion of the fiber in the heated contracting liquid may be of a sufficient magnitude to bring about an interchange of this nature. This theory is supported by the results summarized in Figure 3, which show that at lower temperatures the fiber is more reluctant to enter the final contraction stage, the rate of the disulfide interchange being proportional to the induced thermal stresses. Moreover, a critical amount of energy is apparently necessary to create stresses of a magnitude which will cause disulfide interchange, as shown by the failure of the fiber to enter second-stage contraction when immersed in lithium bromide at room temperature [11].

A more complete picture of the mechanism of the second stage of supercontraction can now be drawn. As a result of the elevated temperature, the stresses set up in the highly cross-linked Y zones after contraction of the X zones cause disulfide interchange to take place. Disturbances of this nature will cause distortion of the structure of these zones, and diffusion of lithium bromide to the intact hydrogen bonds will be facilitated. Once the breakdown of these hydrogen bonds has commenced, the structure will readily open up to allow more lithium bromide to penetrate to the intact hydrogen bonds. On the breakdown of sufficient hydrogen bonds, the thermal contraction of the zone will start.

The inhibition of the final contraction stage by weathering can be satisfactorily explained on the basis of the above mechanism. Weathering is accompanied by the conversion of some disulfide cross-

linkages into thio-ethers [13], and the probable formation of intermediary oxidation products of cystine in which the disulfide linkage is not broken. This view is supported by comparing the results obtained from stress–strain measurements and from chemical analyses of root and tip portions. The mean molecular weight between cross-links, M_c, is inversely proportional to the elastic modulus, G, according to the equation [17]

$$G = \frac{g\gamma RT}{M_c}$$

where g = constant, γ = density of the saturated fibers, R = gas constant, and T = absolute temperature. Since stress–strain measurements indicate a decrease in G of only 1.7%, the number of cross-links in tip wool can be only slightly lower than in sound root sections; yet cystine analyses show a decrease from 10.5% to 9.5% from root to tip. It therefore seems probable that a considerable amount of cystine has been converted into other compounds also providing cross-links. As thio-ether cross-links and cystine sulfoxides and sulfones cannot enter into an interchange reaction with sulfydryls, the sheltered hydrogen bonds will remain unreactive and hence no second stage of contraction will take place. The conversion of even a small portion of the disulfides will seriously affect the extent of interchange taking place as these unreactive linkages may form barriers between the reactive components.

Wool, reduced for 6 hr. and then blocked, was found to elongate after an initial contraction on immersion in hot LiBr solutions (see Figure 8, curves D). Crewther and Dowling [3] supercontracted wool fibers in solutions of salts, acids, and alkalies and found an elongation of the fiber to values exceeding its initial length in several cases. The explanation given to account for this phenomenon is that partial solution of the protein would decrease the number of points of cohesion between the contractile units of the fiber. This would lessen the stress responsible for the deformation of uncontracted and noncontractile portions of the fiber, which would then tend to return to its original length. Abnormally high swelling of the partially dissolved keratin material accounts for the elongation of the fiber to values exceeding the initial length [3]. It has also been observed that the amount of elongation beyond the fiber's initial length is proportional to the number of disulfide cross-linkages destroyed [15]. Since, therefore, the elongation of reduced and blocked roots in hot LiBr is greater and more rapid than that of similarly treated weathered tips, more cross-links appear to have been broken in the former segments of the fiber than in the latter by the reduction. This suggests once again that the number of stable bonds has been increased from root to tip during the weathering of the fiber, in agreement with the deduction made above.

Fibers subjected to very mild reduction with thioglycolic acid (30 min. treatment at pH 5.2) and subsequent blocking, showed an increase in the maximum supercontraction values of not more than 3% for both root and tip, together with complete disappearance of the intermediate stage (see Figure 8, curves B). Under the reducing conditions used, the number of cross-linkages severed would not be great, though apparently still sufficient to cause direct exposure of the sheltered bonds to the contractant and so give rise to one stage of contraction only.

When the reduction period before carboxymethylation is increased slightly to 45 min., maximum supercontraction is followed by elongation. For the roots a final value is reached corresponding to about 7% over-all contraction, whereas for the tips the eventual elongation results in a negative over-all contraction (see Figure 8, curves C). Once again, elongation could result from the partial solution of parts of the fiber [3]. In the present instance, if it is assumed that the X zones, which are initially more exposed than the Y zones, also dissolve more readily after reduction and carboxymethylation in hot LiBr than the Y zones, then the behavior depicted in curves C can readily be explained. Thus, while the X zones in the sound fiber are causing elongation after the initial contraction, the Y zones which have not been sufficiently damaged to facilitate partial solution, are still contracting, and in doing so, oppose the elongation effect caused by the changes taking place in the X zones. Hence the fiber does not return to or exceed its initial length but shows a residual contraction value. In the case of the tips however, the Y zones are unable to contract due to the greater number of stable (lanthionine, etc.) cross-links formed in these zones by weathering, and the length changes recorded after the initial contraction will be elongations, caused by the partial solution of the X zones only. The equilibrium contraction value for the tips therefore has a negative value.

It will be noticed that the first-stage contraction of the weathered fibers is always lower than that of the sound root sections. This slight suppression is

probably due to previous contraction of the fiber during the period of exposure on the sheep's back. Work in this connection is in progress and will be reported upon at a later stage.

Acknowledgments

The assistance of Drs. D. F. Louw and P. K. Faure in the preparation of the manuscript is gratefully acknowledged.

Literature Cited

1. Brown, A. E. and Beauregard, L. G., "Sulfur in Proteins," Proceedings of a symposium held at Falmouth, Mass., May 1958, p. 65.
2. Burley, R. B., *Proc. Int. Wool Textile Res. Conf., Austr.* **D**, 88 (1955).
3. Crewther, W. G. and Dowling, L. M., TEXTILE RESEARCH JOURNAL **29**, 541 (1959).
4. Cuthbertson, W. R. and Phillips, H., *Biochem J.* **39**, 254 (1942).
5. Feughelman, M. and Haly, A. R., *Kolloid Z.* **168**, 107 (1960).
6. Griffith, J. C. and Alexander, A. E., TEXTILE RESEARCH JOURNAL **27**, 755 (1957).
7. Hall, R. H., *J. Soc. Leather Trades' Chemists* **35**, 195 (1951).
8. Haly, A. R. and Feughelman, M., TEXTILE RESEARCH JOURNAL **27**, 919 (1957).
9. Haly, A. R., Feughelman, M., and Griffith, J. C., *Nature* **180**, 1064 (1957).
10. Haly, A. R. and Feughelman, M., TEXTILE RESEARCH JOURNAL **30**, 365 (1960).
11. Haly, A. R. and Griffith, J. C., TEXTILE RESEARCH JOURNAL **28**, 32 (1958).
12. Linderstrøm-Lang, K., Symposium on Peptide Chemistry held by the Chemical Society of the Royal Institution, London, W. I., 1 (1955).
13. Louw, D. F., TEXTILE RESEARCH JOURNAL **30**, 462 (1960).
14. Sleichter, G. M. and Lollar, R. M., *J. Am. Leather Chemists Assn.* **49**, 414 (1954).
15. Swanepoel, O. A., *Nature*, submitted for publication.
16. Taüber, G., Academic Thesis, Hanover (1957).
17. Treloar, L. R. G., "The Physics of Rubber Elasticity," London, Oxford University Press, 1949.
18. Veldsman, D. P., South African Wool Textile Research Institute Tech. Report No. 11, 1957; Kritzinger, C. C., *S. African Ind. Chemist* **12**, 218 (1958).
19. Zahn, H. and Traumann, K., *Melliand Textilber.* **35**, 1069 (1954).

Manuscript received November 14, 1960.

Relaxation Shrinkage of Wool Fabrics: Its Release with Regain and Time

K. Baird

C.S.I.R.O. Wool Research Laboratories, Division of Textile Physics, Ryde, N.S.W., Australia

Abstract

Relaxation shrinkage occurs in wool fabrics when strains set into the fabric are released, usually by the effects of moisture. In this paper, the dependence of relaxation shrinkage on the amount of moisture added and on the time are examined. It is shown that, for fabrics at various stages of finishing, shrinkage is approximately a linear function of the amount of moisture added, up to the point of fiber saturation. It also appears that shrinkage takes place rapidly, being almost complete within thirty minutes of spraying with distilled water at room temperature.

Introduction

The relaxation shrinkage which all-wool woven fabrics exhibit has been investigated by a number of workers during the past thirty years. The first published work dealing specifically with this subject seems to be that of Cryer [3], who examined the effectiveness of Hoffman pressing, damp wrappers, and immersion in cold and hot water as means

of producing relaxation shrinkage. Two articles in the Wool Science Review [1] gave a general account of the problems of shrinkage in garment production and its prevention. The work of von Bergen and Clutz [7] showed clearly the presence of at least two types of shrinkage, a true relaxation of strain, and a reversible change of dimensions with regain. Van Overbeke et al. [6] examined methods of promoting relaxation shrinkage and concluded that soaking in water was the only one which gave reliable results. The work of Davidson [4] entailed a comprehensive study of the relaxation shrinkage brought about by steam pressing and soaking in water. The effects of such variables as fabric structure, water temperature, time and number of treatments, and pH of soaking liquor were all considered, and further work along these lines has recently been done by Cednäs [2].

The mechanism causing the reversible change of dimensions with regain has also been investigated by Cednäs [2] in more detail. This phenomenon has been termed "hygral expansion" in these laboratories and will be referred to as such in this paper. There is an analogy with thermal expansion in other substances, where heating and cooling cause expansion and contraction. Some fabrics, in particular all those woven from wool, exhibit a reversible change of dimensions with regain, expansion and contraction of the length in both warp and weft directions occurring with an increase and decrease of regain, respectively. This is quite reproducible and a separate phenomenon altogether from shrinkage. The weave structure of the fabric and the setting treatment it has received are of approximately equal importance in determining the magnitude of the effect.

The reason why relaxation shrinkage occurs is now well established; by the application of tension or pressure at some stages in the finishing routine—particularly when combined with drying—the fabric may be either cohesively or temporarily set [1] to a length or width different from that which it assumes in the fully relaxed state. Subsequent applications of steam or water can then partially or wholly release the set, with a consequent change of dimensions.

Partly for this reason, and partly to raise the fabric regain to a more desirable level, it is common mill practice to steam or spray water on the fabric, following those processes which tend to stretch it or to dry it out. Frequently the fabric is allowed to lie in a tensionless state for some hours after such steaming or spraying, so that the moisture content can become equilibrated throughout the piece, and so that maximum relaxation will occur.

Technical data on this practice seem to be seriously lacking, however. It is not generally known what is the optimum increase in regain which should be brought about to promote the greatest relaxation, while still leaving the fabric with an acceptable appearance and finish. Also, the rate at which relaxation of strains takes place after spraying with water is largely a matter of conjecture.

The work described in this paper helps to bridge these gaps by showing how the shrinkage induced varies with the amount of moisture added and its dependence upon time.

Experimental

General

Five worsted fabrics of 100% wool were used, the details of which are shown in Table I. The fabrics were withdrawn at different stages of finishing, the main processes for each being shown in the Table. The samples were taken straight from the last machine listed for each. Half a yard was discarded from the end of the length, and the next 1½ yards, full width, were loaded into a plastic bag to prevent any changes of regain before the laboratory tests began. The fabrics were obtained from three different mills, under their normal production conditions.

Variation of Relaxation Shrinkage with Added Moisture

From each of the 1½-yard lengths, 14 samples, 30 cm. square, were cut in a regular pattern and marked with eight small spots, forming a square of side 25 cm., allowing three length measurements to be made in both warp and weft directions. Each sample was then sprayed once at room temperature with distilled water, to which 0.1% non-ionic detergent was added to ensure rapid penetration and even distribution of the moisture. The samples of any one fabric were all at approximately the same regain at the beginning of the laboratory tests. For Fabrics B and C this was the same as their regain in the mill, while Fabrics A, D, and E had regains about 3.5% lower at the mill than those at which the tests began.

[1] For definitions of cohesive and temporary set, see Woods [9].

TABLE I. Details of Fabric Samples Used

Sample	Weave	Weight, oz./linear yard	Width, in.	Warp yarns			Weft yarns			Threads/in. finished		Finishing processes included
				Quality	Count Wstd.	Count Tex.	Quality	Count Wstd.	Count Tex.	Warp	Weft	
A	Plain tropical worsted	8½	58	64's	2/48	2/18.4	64's	2/48	2/18.4	59	55	Scour, Tenter.
B	Barathea 5-thread sateen	13	58	64's	2/44	2/20	60's	1/27	1/33	80	76	Scour, Mill, Dye, Tenter, Crop.
C	Venetian 5-thread warp-face sateen	15	58	60's	2/36	2/24.5	60's	2/36	2/24.5	90	60	Scour, Tenter, Crop, Dry blow, Electric press.
D	2/2 Twill navy serge	15	58	64's	2/36	2/24.5	64's	2/36	2/24.5	73	69	Scour, Dry, Tenter, Crop, Dry blow, Rotary press.
E	Venetian 5-thread warp-face sateen	14	58	64's	2/40	2/22	58's	1/19	1/64	92	64	Scour, Tenter, Crop, Rotary press.

The amount of moisture added by spraying was controlled so that the final regains of the samples ranged from the initial value up to saturation. Two samples of each fabric were subjected to a normal relaxation shrinkage test, i.e., immersion for 30 min. in water at 50° C.

For each fabric, the fourteen samples were divided as follows: after randomizing they were split into two sets of seven, each set receiving approximately the same treatment; with the first group, the shrinkage was measured 1 hr. after spraying; with the second, 18 hr. after spraying.

Variation of Relaxation Shrinkage with Time

One strip, 25 × 8 cm., was cut from each fabric and marked with a pair of spots 23 cm. apart. After measuring at the original regain, the strip was sprayed with distilled water and the length observed by means of a travelling microscope at intervals up to 18 hr. after spraying. The sample was lying horizontally and free of any external restraint. It was then possible to determine the dependence of shrinkage upon the time elapsed after spraying.

Effect of Hygral Expansion

It is necessary to eliminate the effects of hygral expansion (i.e., reversible change of dimensions with regain) in this work, to obtain the correct measurements of relaxation shrinkage.

In the first series this was achieved simply by drying each sample to its original regain before taking the final measurement. As well as the required shrinkage, an expansion occurred when the regain was increased by spraying, but an equal contraction took place on returning the sample to the original regain.

For the second series it was necessary to examine the hygral expansion vs. time relationship as well as the apparent (total) change of dimensions with time so that the true relaxation shrinkage curve could be obtained. The sequence of observations necessary was as follows.

After the complete curve of fabric dimensions vs. time after spraying (with the sample regain held at the "sprayed" value) was obtained, the contraction was measured when the sample was dried to its initial regain. This gave the magnitude of total hygral expansion for that sample. It was then relaxed in warm water (50° C.) for 1 hr., to remove any remaining relaxation shrinkage, and dried to its initial regain. It was then measured and sprayed again, the same amount of moisture being added as before. The dimensions vs. time curve was again observed, this time only hygral expansion being present. Since its magnitude here was found to be the same as previously, it was assumed that the behavior was similar on both occasions. Finally, the first length vs. time curve was subtracted from the hygral expansion curve to yield the length contraction caused by relaxation shrinkage as a function of time.

Throughout this work, the regain of each sample was determined by oven drying at 105° C. at the completion of all tests performed on the sample.

Discussion of Results

Figure 1 shows the results of the first series, i.e., the dependence of relaxation shrinkage upon the amount of moisture added, for both warp and weft direction of all five fabrics. On four of them, the warp shrinkage was greater than the weft; this agrees with the results of previous workers (see, e.g., Table IV, Table VI, Davidson [4]), and also with other work in this laboratory, where it has been shown that approximately 80% of all fabrics examined exhibited the same characteristic. Since Fabric A was tentered only, it is to be expected that the weft shrinkage would be greater than the warp shrinkage owing to the greater strain which is normally imposed across the width of the fabric during drying. Although the samples of each fabric were divided into two sets, measurements of shrinkage 1 hr. after spraying and 18 hr. after spraying showed no statistically significant difference. The results have therefore all been plotted as a single set of observations.

The points marked "Wet" refer to the samples of each fabric which were soaked at 50° C. Such treatment left the samples with only a very small residual shrinkage which could occur on further immersion in water. It is important that approximately the same shrinkage was brought about by spraying to about 30% regain (in which case there was no surface moisture present after a few minutes) as by soaking in water. This should be equally true of steaming although difficulties may be encountered in raising the fabric regain sufficiently by this means.

In mill practice of course the amount of moisture which may be added to the fabric is limited by the deterioration which occurs in the finish due to relaxation at a high moisture content, unless it is acceptable to refinish the piece.

The results of the relaxation shrinkage vs. time investigation are shown in Figure 2 for either warp or weft direction for each of the five fabrics. The middle curve in each case represents the actual dimensional change which takes place when a fabric is sprayed and then held at that regain. As already mentioned, this curve is always a combination of two effects, the relationship between the two determining

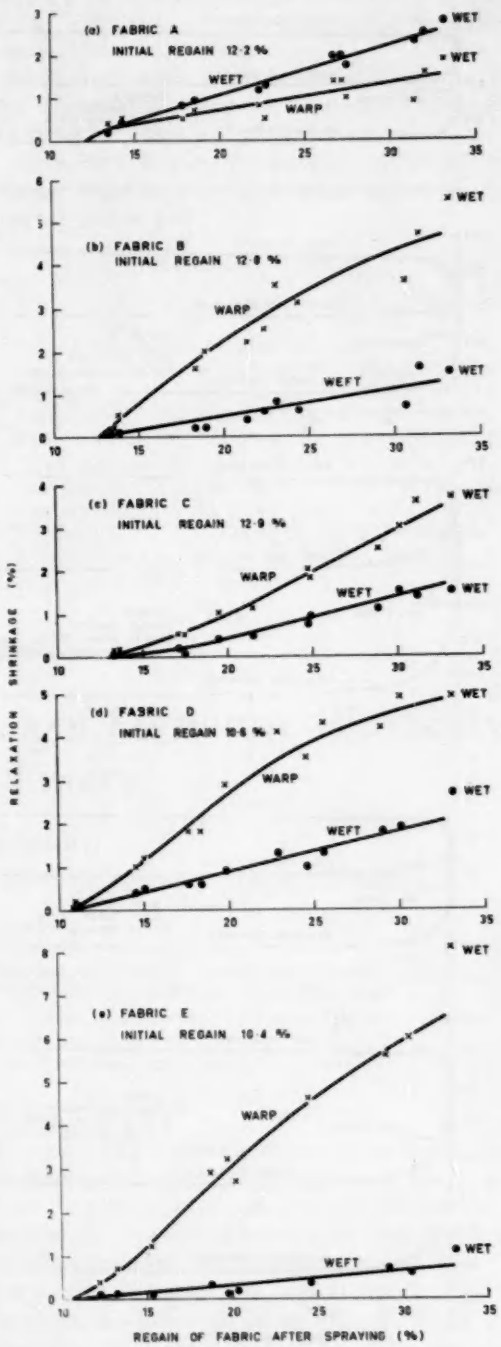

Fig. 1. Relaxation of 5 worsted fabrics, both warp and weft directions, as a function of the regain to which the samples were taken by spraying. (× = warp measurements; • = weft measurements)

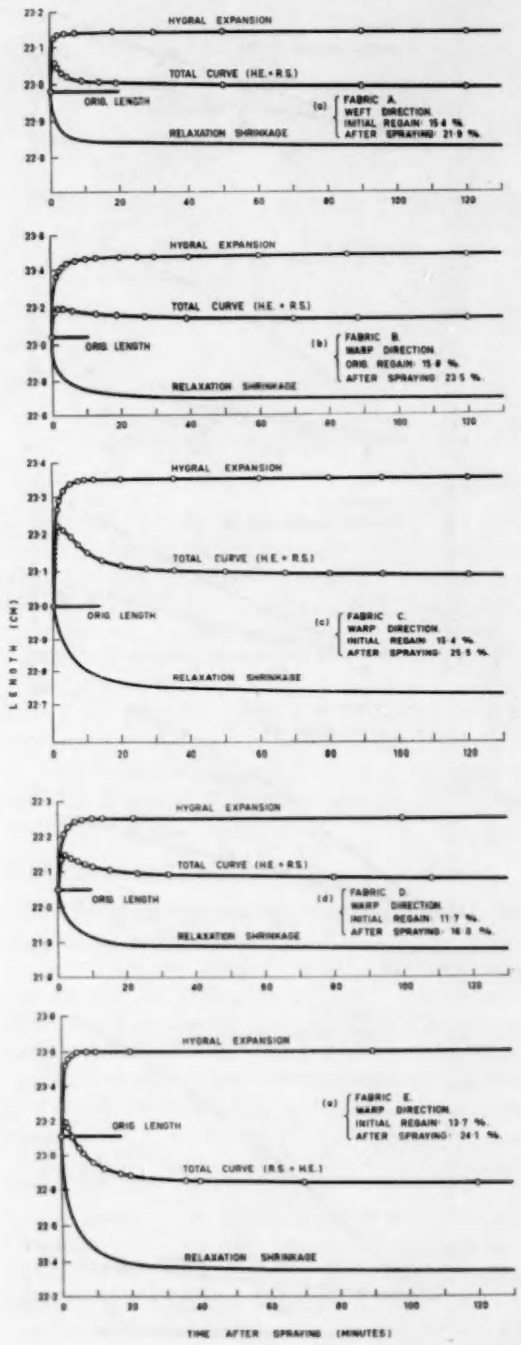
HYGRAL EXPANSION
TOTAL CURVE (H.E.+R.S.)
ORIG. LENGTH
RELAXATION SHRINKAGE
(a) FABRIC A. WEFT DIRECTION. INITIAL REGAIN: 15.4 %. AFTER SPRAYING: 21.9 %.
(b) FABRIC B. WARP DIRECTION. ORIG. REGAIN: 15.8 %. AFTER SPRAYING: 23.5 %.
(c) FABRIC C. WARP DIRECTION. INITIAL REGAIN: 15.4 %. AFTER SPRAYING: 25.5 %.
(d) FABRIC D. WARP DIRECTION. INITIAL REGAIN: 11.7 %. AFTER SPRAYING: 16.8 %.
(e) FABRIC E. WARP DIRECTION. INITIAL REGAIN: 13.7 %. AFTER SPRAYING: 24.1 %.
TOTAL CURVE (R.S.+H.E.)
LENGTH (CM)
TIME AFTER SPRAYING (MINUTES)

whether there is an increase or a decrease in the sample length.

The upper curve for each sample is the hygral expansion curve. When the sample regain is decreased, the length decreases to the same extent as the increase shown. The lowest of each set of three curves represents relaxation shrinkage only, and Figure 3 shows these curves as percentage length changes for all five samples.

Since the regain increment was different for each sample, a comparison between the curves of Figure 3 and those of Figure 1 can only be made by considering the latter over the appropriate regain increment. Good agreement is found between the two, although the shrinkages of Figure 3 are somewhat lower than the others. This occurred because the two series of measurements were not made simultaneously; a delay between the first and second series allowed some shrinkage to occur with the fabrics stored at their original regain.

Observations on the fabrics over longer periods than those shown revealed only a very slow increase in shrinkage in every case. The greatest change was 0.02% per hour, up to 4 hr. after spraying, and the average over a longer period was less than 0.008% per hour (up to 24 hr.). After 24 hr. there was virtually no further change in any sample. It may be noted that the shrinkage takes place more rapidly in Sample A than in any other; this is because of its light weight compared with the other fabrics, the moisture being able to diffuse into the structure much more quickly.

The curves of Figure 2 indicate the importance of distinguishing clearly between apparent and true shrinkage behavior, particularly with fabrics in the finishing process, where changes of regain are frequently encountered. These results also reveal the rapidity with which fabric dimensions stabilize after a change of regain. There seems to be no essential difference between the conditions which were employed in the laboratory and those which obtain in the normal method of spraying fabric during finishing. It therefore appears that where lengths of fabric are sprayed to remove relaxation shrinkage, the

Fig. 2. Complete dimensional change of fabric samples as a result of spraying, shown as a function of time. The hygral expansion and relaxation shrinkage curves occur simultaneously, giving the middle curve as the observed behavior in each case. Figures (b) and (e) have the ordinate scale doubled for convenience.

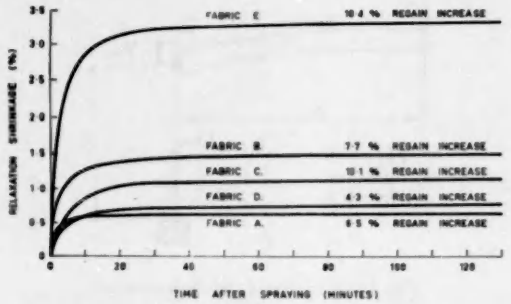
FABRIC E 10.4 % REGAIN INCREASE
FABRIC B 7.7 % REGAIN INCREASE
FABRIC C 10.1 % REGAIN INCREASE
FABRIC D 4.3 % REGAIN INCREASE
FABRIC A 6.5 % REGAIN INCREASE
RELAXATION SHRINKAGE (%)
TIME AFTER SPRAYING (MINUTES)

Fig. 3. Relaxation shrinkage (% of original length) shown as a function of time. These are the (reprocessed) curves of relaxation shrinkage from Figure 2.

effect should be very nearly complete within ½ hr., while any change of dimensions after 1½ hours is negligible.

Conclusions

It appears that the relaxation shrinkage which can occur in any particular fabric is approximately a linear function of the amount of moisture added to the cloth. The regain must be raised nearly to that of fiber saturation to render any residual shrinkage small.

In all work where changes of regain occur, it is most important to distinguish between the effects of relaxation shrinkage and of hygral expansion.

When fabric is sprayed with water to remove relaxation shrinkage, the effect should be very nearly complete within ½ hr.

Literature Cited

1. Anon. *Wool Science Review,* No. 4, 25 (1949); No. 5, 3 (1950).
2. Cednäs, M., *J. Textile Inst.,* in press.
3. Cryer, N., *J. Textile Inst.* **26**, 331 (1935).
4. Davidson, A. N., *J. Textile Inst.* **45**, T323 (1954).
5. Moncrieff, R. W., *Wool Record* **94**, 1577 (1958).
6. Van Overbeke, M., Mazingue, G., and Outreman, P., *Bull. inst. textile France* No. 38, 7 (1953).
7. von Bergen, W., and Clutz, C. S., TEXTILE RESEARCH JOURNAL **20**, 580 (1950).
8. Whewell, C. S., *Can. Textile J.* **75**, 37 (1958).
9. Woods, H. J., *J. Textile Inst.* **26**, T93 (1935).

Manuscript received November 14, 1960.

Measurement of the Modulus of Dynamic Elasticity of Staple Fibers

H. G. Weyland

Central Research Institute of A. K. U. and Affiliated Companies, Arnhem, Holland

Abstract

A description is given of an apparatus with the aid of which the modulus of dynamic elasticity of fibers can be determined at about 1000 cycles/sec. as a function of the strain. In principle the dynamic elasticity constant of the fiber is determined by measuring the resonance frequency of a cantilever spring which is loaded with the fiber.

The results of measurements on various types of natural, regenerated, and synthetic fibers are given.

Introduction

From the literature many data are known on the elastic properties of yarns and fibers. One of these properties, the modulus of dynamic elasticity, whose magnitude is determined by the type and orientation of the chain molecules, may be useful in the classification of these materials. Much work has been done in this field by H. de Vries [3]. His measuring method, based on that of Ballou and Silverman [2], consists in determining the modulus of dynamic elasticity as a function of the strain from the velocity of sound. In view of the magnitude of the velocity of sound this method is only suitable, however, for measurements on filament yarns. As it may be of importance to include fibers in this investigation as well, a method was developed with the aid of which the modulus of dynamic elasticity of staple fiber can be measured

at about 1000 cycles/sec. in a simple way as a function of the strain.

The object of this article is to describe this measuring method and to mention a number of results of measurements on various types of natural, regenerated, and synthetic fibers.

The Modulus of Dynamic Elasticity

By the modulus of elasticity of a yarn or fiber we understand the ratio between a very slight change in stress and the resulting change in strain in the longitudinal direction of the thread. So this is a differential modulus of elasticity. This definition is represented by the formula

$$E = \frac{d\sigma}{d\epsilon}$$

where E = modulus of elasticity, $d\sigma$ = change in stress, $d\epsilon$ = change in strain.

For most polymers this quantity is dependent on the state of deformation and the deformation speed. It is therefore necessary to define the circumstances under which the measurement is made.

In this connection we speak of the modulus of dynamic elasticity, $E_{dyn.}$, when this modulus is measured at small periodic variations of the strain, as occur with longitudinal vibrations in a thread, e.g. sound vibrations. Now the formula for the speed of propagation of sound, v, in a thread, without attenuation is

$$v = \sqrt{\frac{E_{dyn.}}{\rho}}, \text{ where } \rho = \text{density.}$$

As the internal damping of fibers is slight, this formula makes it possible to calculate the value of $E_{dyn.}$ from the velocity of sound v at a known value of ρ.

Principle of the Measurement

In principle the method described in this article consists in determining the dynamic spring constant, K, of the fiber by measuring the resonance frequency of a cantilever spring which is loaded with the fiber.

Figure 1 gives a scheme of the arrangement. One end of the fiber is fixed to the end R of the spring, the other in the clamp C. With the aid of clamp C the fiber, which has a clamping length l_0, is stretched to a length $l = l_0 + \Delta l$.

The spring is so rigid that y_m, the displacement of R, with respect to the extension (Δl) may be neglected. By driving the system (spring + fiber) electromagnetically at R with the frequency ω, the fiber is subjected to a small periodic variation in length (dl).

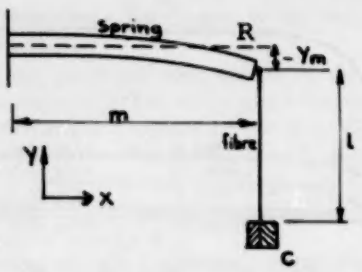

Fig. 1. Principle of the measurement.

From the definitions of

$$E_{dyn.} = \frac{d\sigma}{d\epsilon} \tag{1}$$

and Poisson's ratio

$$\mu = -\frac{1}{2A} \cdot \frac{dA}{dl}$$

where A = the cross-sectional area, follows

$$E_{dyn.} = \frac{k\rho l_0}{T}\left(1 + \frac{\Delta l}{l_0}\right)^{2\mu+1} + 2\mu\sigma$$

where ρ = density of the fiber; T = mass/unit length at $\Delta l = 0$; $k = \frac{dF}{dl}$; F = force; $\sigma = \frac{F}{A}$, stress in the fiber.

For yarns and fibers the following formula may be considered a close approximation

$$E_{dyn.} = \frac{k\rho l_0}{T}\left(1 + \frac{\Delta l}{l_0}\right)^2 \tag{2}$$

because for these matrials $E_{dyn.} \gg \sigma$ and $\mu \approx 0.5$. If we neglect the damping of the system and the mass of the fiber, the following differential equation holds for the system spring plus fiber

$$\rho_s \cdot A_s \frac{\partial^2 y}{\partial t^2} + E_s \cdot I_s \frac{\partial^4 y}{\partial x^4} = 0 \tag{3}$$

where t = time, ρ_s = density of the spring, A_s = cross-sectional area of the spring, E_s = modulus of elasticity of the spring, and I_s = moment of inertia of the cross-section, A_s. Equation 3 must satisfy the following boundary conditions (see Figure 1)

$$x = 0 \begin{cases} y = 0 \\ \dfrac{\partial y}{\partial x} = 0 \end{cases}$$

$$x = m \begin{cases} \dfrac{\partial^2 y}{\partial x^2} = 0 \\ \dfrac{\partial^3 y}{\partial x^3} = \dfrac{k y_m}{E_s I_s} \end{cases}$$

$$t = 0 \quad y = 0$$

Let y be $\tau(t) \cdot \xi(x)$ and let us substitute this in Equation 3; it follows with the boundary conditions mentioned

$$\frac{k}{K} = \frac{(qm)^3\{1+\cosh(qm)\cos(qm)\}}{3\{\sinh(qm)\cdot\cos(qm) - \cosh(qm)\sin(qm)\}} \quad (4)$$

where

$$q^4 = \omega^2 \frac{\rho_s A_s}{E_s I_s} \quad (5)$$

ω = resonance frequency,

$K = \dfrac{3E_s I_s}{m^3}$ (elasticity constant of the spring).

It follows from Equations 4 and 5 that for ω many solutions are possible, viz. the fundamental tone and the harmonics. As the system is driven at a fixed frequency (the fundamental tone) the other solutions are of no importance to us.

It follows from Equation 4 that for the unloaded spring ($k = 0$) the value $qm = 1.875$. This value, together with Equation 5, gives the resonance frequency of the unloaded spring (ω_0)

$$\omega_0^2 = \frac{E_s I_s}{\rho_s A_s} \cdot \left(\frac{1.875}{m}\right)^4 \quad (6)$$

Elimination of $\dfrac{E_s I_s}{\rho_s A_s}$ and qm from Equations 4, 5, and 6 gives

$$k = Kf\left(\frac{\omega}{\omega_0}\right) \quad (7)$$

The values of this function can be determined numerically. If we also eliminate k from Equations 2 and 7, this gives

$$E_{\text{dyn.}} = \frac{\rho l_0}{T}\left(1 + \frac{\Delta l}{l_0}\right)^2 \cdot Kf\left(\frac{\omega}{\omega_0}\right) \quad (8)$$

It is seen that with the aid of Equation 8 $E_{\text{dyn.}}$ can be calculated from a measurement of ω, if the values of ρ, T, l_0, Δl, K, and ω_0 are known.

Description of the Apparatus

The calculation of $E_{\text{dyn.}}$ with the aid of Equation 8 from a measurement of the resonance frequency ω is rather complicated. It was therefore tried to construct the apparatus in such a way that this calculation would be simpler. The principal factors concerned are $\left(1 + \dfrac{\Delta l}{l_0}\right)^2$ and $f\left(\dfrac{\omega}{\omega_0}\right)$.

When the fiber is clamped in as shown in Figure 2, the factor $\left(1 + \dfrac{\Delta l}{l_0}\right)^2$ can be replaced by a constant with good approximation, as will appear from the following.

In Figure 2 the fiber is fixed in the clamps C_1 and C_2 via the hooklet H at the end of the spring V and is at an angle φ with the horizontal axis. By displacing the clamps horizontally in the direction of the arrow, the fiber obtains the desired extension. If the thread is fixed in this way, the elasticity constant k used in the Formulae 4 and 7 should be replaced by $2k\cos^2\varphi$. Equation 8 will now be

$$E_{\text{dyn.}} = \frac{\rho}{T}\left\{\frac{l_0\left(1 + \dfrac{\Delta l}{l_0}\right)^2}{2\cos^2\varphi}\right\} Kf\left(\frac{\omega}{\omega_0}\right)$$

For a suitable initial value of φ (51.0°) and $0 < \dfrac{\Delta l}{l_0} < 0.2$, the factor $\dfrac{l_0\left(1 + \dfrac{\Delta l}{l_0}\right)^2}{2\cos^2\varphi}$ is constant to an accuracy of about 1%.

The function $f\left(\dfrac{\omega}{\omega_0}\right)$ can be simply incorporated in the reading scale for ω, when an RC generator is chosen with a Wien bridge as the network which

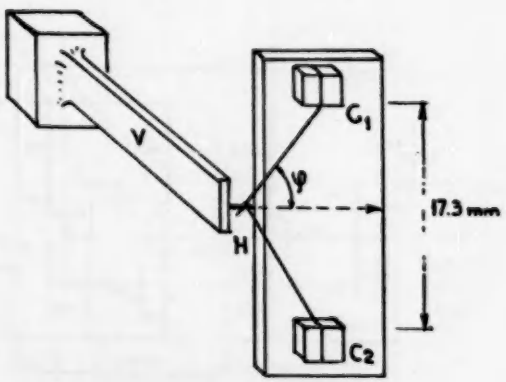

Fig. 2. Clamping of the thread.

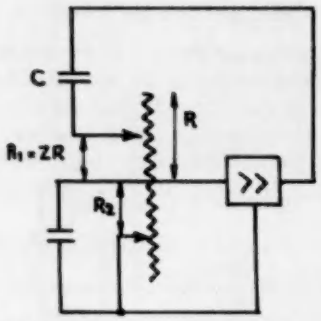

Fig. 3. Principle of the generator.

determines the frequency. The fact is that for this type of generator the following formula holds (Figure 3).

$$\omega^2 = \frac{1}{C^2 R_1 R_2}$$

If R_1 is a linear potentiometer, R_1 can be written: $R_1 = zR$.

If R_2 is adjusted in such a way that at $z = 1$ ($R_1 = R$), the frequency $\omega = \omega_0$, it follows that $\left(\frac{\omega}{\omega_0}\right)^2 = \frac{1}{z}$.

So a reading scale on the shaft of potentiometer R_1 can be calibrated directly in $\left(\frac{\omega}{\omega_0}\right)$, or, according to Equation 7, in $\frac{k}{K}$.

The frequency ω_0 can be adjusted with the aid of R_2, without this changing the scale value on R_1. So this makes it possible to exchange springs with different resonance frequencies (ω_0) and to calibrate this scale.

With close approximation it may be put that the maximum amplitude of the end of the spring is reached at the resonance frequency ω. So a simple amplitude indicator is sufficient to adjust the resonance frequency. For this purpose a capacitive system was provided in the soft-iron core of the coil which electromagnetically drives the spring. Figure 4 gives the complete electronic circuit.

As the displacement of the end of the spring with respect to the extension of the fiber by stretching should be negligible, the variation of ω is small (20–100 cycles/sec.). The adjusted frequency ω of the generator may therefore drift only slightly. By choosing the correct resistances and capacities of the Wien bridge it is possible to make the network independent of the temperature. The influence of the instability of the tubes on the frequency was eliminated as far as possible by a considerable feedback and voltage stabilization. Moreover, the amount of power absorbed was kept as low as possible by the application of transistors. As a result of these measures the frequency drift $\frac{\Delta\omega}{\omega}$ over some hours was very small ($<10^{-4}$). In spite of these measures the accuracy of the measurement of $\frac{k}{K}$ is such that two springs are necessary to cover the whole range of current fibers.

The foregoing shows that the determination of the modulus of dynamic elasticity as a function of

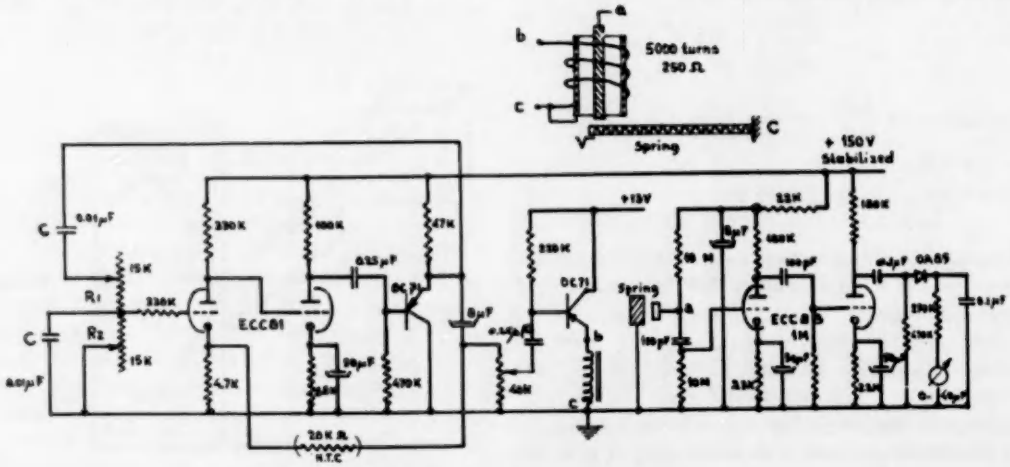

Fig. 4. Complete electronic circuit of the apparatus.

the strain makes it necessary to measure the following quantities: the denier (T) at the beginning of the measurement; $f\left(\frac{\omega}{\omega_0}\right) = a$ at the desired strain values. The denier (T) can be determined with the aid of a vibroscope [5].

$E_{dyn.}$ is now calculated from these measurements according to

$$E_{dyn.} = b\frac{\rho}{T}a \qquad (9)$$

where b = a constant dependent on the type of spring, ρ = density, T = denier (mass/unit length), and $a = f\left(\frac{\omega}{\omega_0}\right)$ scale reading on resonance.

For most types of fibers sufficiently accurate values of ρ are known. (See *inter alia* Table II.) Figure 5 gives a photograph of the apparatus.

Accuracy of the Measurements

In the first instance it will be ascertained how far the approximations applied cause a systematic measuring error. For this purpose we will consider the most extreme case, viz. an Enkalon fiber (nylon-6). This fiber has a low modulus of dynamic elasticity and a high tensile strength. In Formula 9, from which $E_{dyn.}$ is calculated, the following approximations have been applied:

1. The factor $\frac{l_0\left(1+\frac{\Delta l}{l_0}\right)^2}{2\cos^2\varphi}$ has been assumed to be constant.
2. σ has been neglected with respect to $E_{dyn.}$.
3. μ has been assumed to be 0.5.

Figure 6 gives the error (δ) resulting from the approximations 1 and 2 as a function of $\frac{\Delta l}{l_0}$ at Poisson's ratios $\mu = 0.4$ and $\mu = 0.5$. It is seen that for $\frac{\Delta l}{l_0} < 0.2$ the maximum error can be $\pm$ 2%. It appears from the literature (*inter alia* [1]) that the value of Poisson's ratio μ of fibers is between 0.5 and 0.4, so that the error made by using the approximation formula may be assumed to be < 2%.

The random errors to be expected are of approximately the same order of magnitude. It is difficult to estimate their value, because they are determined by the vibroscope [5] with which the denier (T) is determined, the degree of crimp of the fiber, and the adjustment errors of the generator.

Fig. 5. Photograph of the apparatus.

Tests showed that in most cases the standard deviation of the reproducibility is within 1%.

Calibration of the Apparatus

In addition to the geometric constant of the apparatus $\frac{l_0\left(1+\frac{\Delta l}{l_0}\right)^2}{2\cos^2\varphi}$, the determination of $E_{dyn.}$ according to the measuring method described in this article requires the use of the elasticity constant K of the spring. This constant can be determined statically by loading the end of the spring

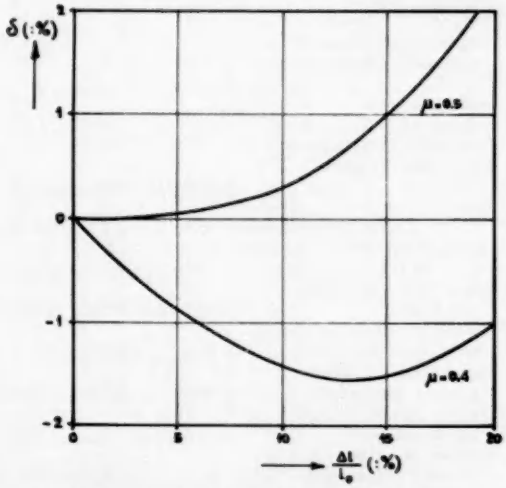

Fig. 6. Magnitude of the measuring error by the approximation: $E_{dyn.} = \frac{b\rho}{T}a$.

TABLE I

Res. freq.	Dimensions			Elasticity constant K × 10^6 dyne/cm.		
ω_0, cycles/sec.	l, cm.	b, cm.	h, cm.	Statically	Dynamically	Calibration
959.8	2.49	0.59	0.077	8.5	7.7	8.6
938.7	1.72	0.59	0.035	2.46	2.3	2.16

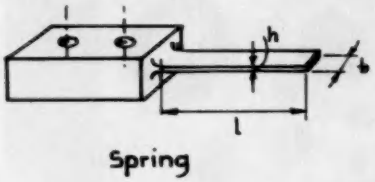

Spring

TABLE II. Dynamic Elastic Constants of Various Fibers at 20° C. and 65% RH

Type of fiber	E_0, 10^{10} dyne/cm.^{2}	C, 10^{10} dyne/cm.^{2}	ρ nominal density, g./cm.^{3}
a. Natural fibers			
Wool, protein	6.5	8	1.32
Cotton, native cellulose	16	2	1.54
Rameh., native cellulose	66	—	1.54
b. Regenerated fibers			
Fibrenka (A.K.U.), cellulose	16.5	4.7	1.49
Colvadur (Glanzst. Courtaulds), cellulose	16.5	4.8	1.49
Topel (Courtaulds, Ala.), cellulose	15.5	4.5	1.49
Vicara (Virg. Carolina Chem. Comp.), protein	3.4	1.7	1.25
Ardil (I.C.I.), protein	4.5	—	1.30
Acetate rayon staple (Brit. Celanese), cellulose acetate	5.9	2.0	1.32
c. Synthetic fibers			
Enkalon (A.K.U.), nylon-6	3.1	0.65	1.14
Perlon (V.G.F.), nylon-6	3.0	0.6	1.14
Rilsan (Soc. Organico), nylon-11	4.0	0.6	1.14
Terlenka 1 (A.K.U.), polyester	13.5	2.0	1.38
2 (A.K.U.), polyester	8.1	2.4	1.38
Dacron* 61 (DuPont), polyester	11.0	2.0	1.38
64 (DuPont), polyester	8.6	2.4	1.38
Orlon* (DuPont), polyacrylonitril	8.3	3.0	1.16
Acrilan (Chemstrand Corp.), polyacrylonitril	12.6	3.0	1.17
Dynel (Union Carbide Chem.), modacrylic	6.8	2.1	1.30
Darvan (Goodrich), polyethylenedinitril	5.3	2.1	1.18
Kuralon (Kurashiki Rayon Comp.), polyvinylalcohol	11	3.2	1.3
Rovyl (Rhodiaceta), polyvinylchloride	3.8	3.8	1.40

* DuPont trademark.

with a known weight and measuring the deflection. It is also possible to calculate the elasticity constant from the resonance frequency (ω_0) and the dimensions of the spring. The values obtained according to these methods are rather inaccurate, however, because the dimensions cannot be determined with sufficient accuracy and the formulae used are not correct, owing to the presence of the hooklet at the end of the spring. The elasticity constant K can also be determined from the geometric dimensions of the apparatus and the modulus of elasticity, measured with the aid of the velocity of sound. Naturally this is only possible when filament yarns are concerned. In this case the calibration of the apparatus is based on an existing measuring method. Accordingly the value of K obtained by this method was used for the further measurements.

Table I gives the elasticity constants determined by the above-mentioned methods.

Measurements on Various Fibers

In Reference 3 an elaborate analysis is given of the course of $E_{dyn.}$ as a function of the strain of different types of yarn. This analysis leads to the examination of the reciprocal value of $E_{dyn.}$ as a function of $ln\left(1 + \frac{\Delta l}{l_0}\right)$. It appears that from the course of this function some quantities are found which are characteristic of the material, viz. E_0, i.e., the modulus of dynamic elasticity at $\Delta l = 0$ and the slope of the straight part $1/C$ of the curve.

Figure 7 gives $1/E$ as a function of $ln\left(1 + \frac{\Delta l}{l_0}\right)$ for a rayon and an Enkalon thread (nylon-6). The value of E_0 is highly dependent on the previous history of the yarn, and in general C was found to be a material constant.

In the case of highly crimped fibers, the determination of E_0 with the aid of the apparatus described in this article gives rise to some difficulties, because in this case there is a difference between the strain adjusted with the apparatus and the real elongation, which results in a horizontal shifting of the curve. E_0 must then be estimated from the course of this curve.

Table II gives the values of E_0, C, and ρ for a great number of fibers.

The values of C for rayon staple correspond with those for rayon filament yarn. E_0 lies in the same area as well. The same applies to the synthetic fibers and filament yarns. Cotton, though it con-

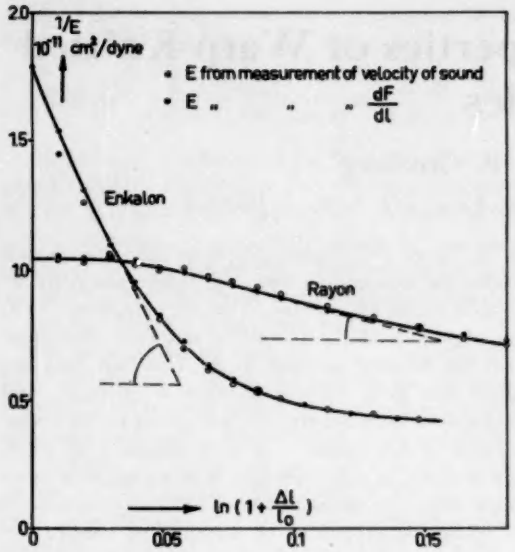

Fig. 7. $1/E$ as a function of $ln\left(1+\frac{\Delta l}{l_0}\right)$ for a rayon and an Enkalon thread (nylon-6).

sists of cellulose as well, has a C-value which is less than half the value for rayon (owing to the helical structure ?). Wool has a higher C-value, comparable with that of other protein fibers (silk) [4]. For further data on the values E_0 and C for various types of filament yarns reference is made to [4].

Acknowledgment

The author wishes to thank Dr. H. de Vries for his helpful advice and suggestions. Acknowledgment is made to the Algemene Kunstzijde Unie N. V. for permission to publish this work.

Literature Cited

1. American Institute of Physics, "American Institute of Physics Handbook," New York, McGraw-Hill, 1957, pp. 3–80.
2. Ballou, J. W. and Silverman, S., TEXTILE RESEARCH **14**, 282–292 (1944).
3. de Vries, H., "On the Elastic and Optical Properties of Cellulose Fibers," Thesis, Delft Technical University, 1953.
4. de Vries, H., *Rayon Rev.* **10**, 53–59 (1956).
5. Gonsalves, V. E., TEXTILE RESEARCH JOURNAL **17**, 369–375 (1947).

Manuscript received November 28, 1960.

Correction

The following corrections should be made in "Cotton Quality Study VI. Wrinkle Resistance and Recovery from Deformation," by Henry Tovey, which appeared in the March 1961 issue:

Page 196, 2nd column, 8th line from bottom should read:

they would not prevent the relative motion of the structural

Page 199, 1st column, 7th line from top should read:

swollen fibers, and side chain formation and *intra*molecular

Page 207, 1st column, 20th line from top should read:

tertiary nitrogen atom, but the presence of primary or second-

Page 209, 1st column, 17th line from bottom should read:

as carboxymethylation [167, 168, 379, 586],

The Load–Extension Properties of Warp Knitted Fabrics

D. L. Cook and P. Grosberg

Department of Textile Industries, The University, Leeds 2, England

Introduction

The purpose of this investigation was to find what determines the load–extension properties of warp knit fabrics. In particular, to what extent are they determined by the yarn properties and to what extent by the structural properties of the fabric? This paper is concerned solely with the warp-wise extension of these fabrics.

It is fairly evident that a large part of the extensibility of these fabrics is a result of the deformation of the loop, and as a result the first section of this paper is concerned with finding a suitable expression for predicting the load–extension properties of a loop.

The Load-Extension Properties of the Loop

The relaxed warp knitted structure can be considered [2] to consist of a set of pin-jointed elasticas joined to each other as in Figure 1, the bending moment in the underlap being small, so that the loop can be approximated to by a simple elastica. It will be assumed initially that the resistance to deformation during initial extension of the cloth will be governed by the resistance of the "loop" shown in Figure 1. This loop differs from the geometrical models constructed by Pierce [7], Munden [4], and Leaf [3] for weft knitted structures, but it has been shown [2] that for the different geometry of warp knitting this rather simple loop model is considerably more accurate. Although obviously no pin joint exists in the actual structure, it is considered —as a result of observation—that the effect of friction at the cross-over point does produce an effect which can be represented on a model by means of a pin joint. The main justification for this model is the statistical analysis of the geometrical properties of warp knitted fabrics given in Reference 2. If the bending moment in the underlap is assumed to be negligible, then the loop—when under zero load—becomes one of Euler's elastic curves [1] and its shape can be obtained from an elastica produced as in Figure 2A. Figure 2B shows the same elastica under the action of a load. It is necessary, therefore, to obtain an expression for the extension $b - b_0$ for a given load P. It will be assumed throughout that the bending moment in the underlap does not affect the loop, initially because it is small, and under load because friction will prevent the transmission of this moment. This transmission of bending moment, as can be seen by observation, only takes place when the fabric relaxes under zero tension.

While the properties of the original elastica are well known, the determination of the properties of the elastica under load is a rather more intractable problem. However, as a result of a semi-quantitative analysis, a simple expression for P against $(b - b_0)/b_0$ has been obtained which was found to give good agreement with experimental values obtained with various materials.

Semi-Quantitative Analysis

As a result of observation of elasticas under load it was seen that except under low loads the upper half of the elasticas tend to become two straight lines. As a result we can assume that the bending moment in this region must be small. If the half angle at the upper part of the elastica is θ (see Figure 2B) then taking moments about O we have

$$P/2x = Qy$$

therefore

$$\tan\theta = 2Q/P \quad \text{and} \quad P = 2Q/\tan\theta$$

In addition, we have that the radius of curvature of the loop at the point of application of the load P is given by:

$$r = EAk^2/\text{Bending Moment}$$

where E is the Young's modulus of the material of the beam and Ak^2 the moment of area of the cross-section of the beam. For yarns, the bending modulus differs from the Young's modulus, and strictly speaking E is the bending modulus.

Since the bending moment $= bQ$, where b is the height of the loop,

$$P = Q\frac{2}{\tan\theta} = \frac{EAk^2}{br}\frac{2}{\tan\theta} = \frac{2EAk^2}{br\tan\theta} \qquad (1)$$

As the load increases and the loop becomes elongated, r and $\tan\theta$ both decrease; it is therefore necessary to find how r and $\tan\theta$ alter as the loop becomes elongated. To do this it would be necessary to know the loop geometry. This cannot be done without an exact analysis, and consequently the following approximation has been made.

The loop can be approximated to a segment of a circle of radius r and two tangents as shown in Figure 2B. The total length of the approximate loop must be equal to the length of the unextended loop of height b_0. It has been shown [2] that this length equals 2.5534 b_0. The dimensions of this approximate loop can be found from the geometrical relationships

$$\pi r + 2r\theta + 2r/\tan\theta = 2.5534\, b_0 \qquad (2)$$

$$r + r/\sin\theta = b \qquad (3)$$

from which it is possible to calculate θ and r/b_0 for various values of b/b_0. The approximate loop so obtained for $b/b_0 = 1$ is compared with the true unstretched loop as obtained from Euler's equation in Figure 3, where it is seen that even for this extension —where the approximation is at its worst—the approximate loop, marked A, is reasonably similar to the true loop shape B. For all the other loops it is easy to show that θ, as found by this method, is too small and r too large, so that the value of $r\tan\theta$ as found by the approximate formula might be expected to be a close approximation.

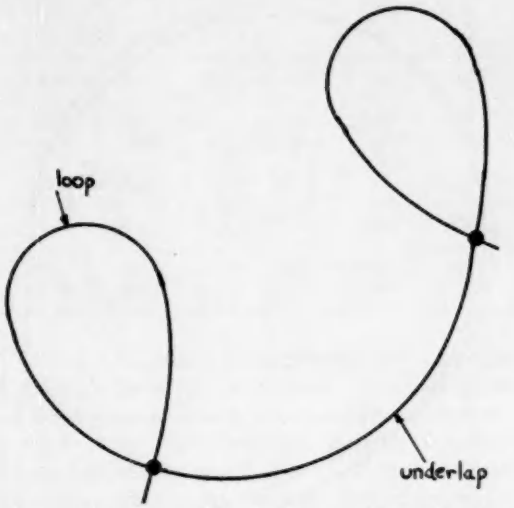

Fig. 1. The relaxed warp knitted structure considered as a set of pin-jointed elasticas.

To aid calculation we can write

$$P = \frac{2EAk^2}{b_0^2} f(\theta) \qquad (4)$$

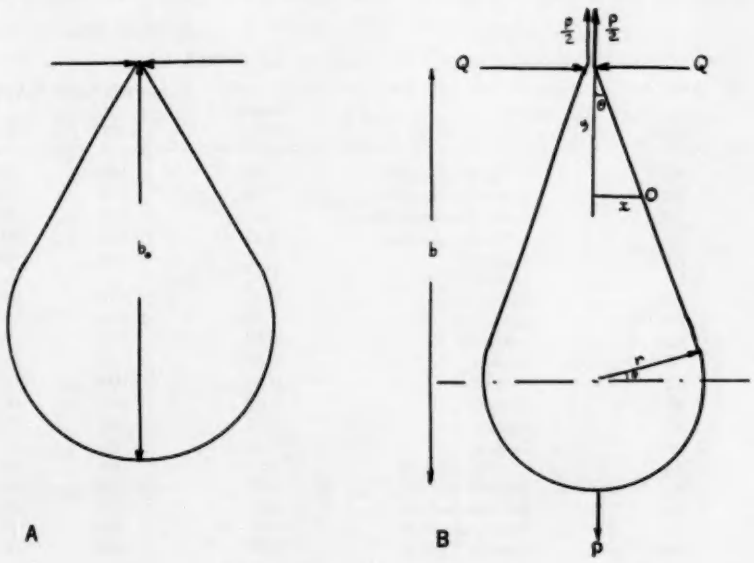

Fig. 2. A, the unextended loop; B, the loop under load.

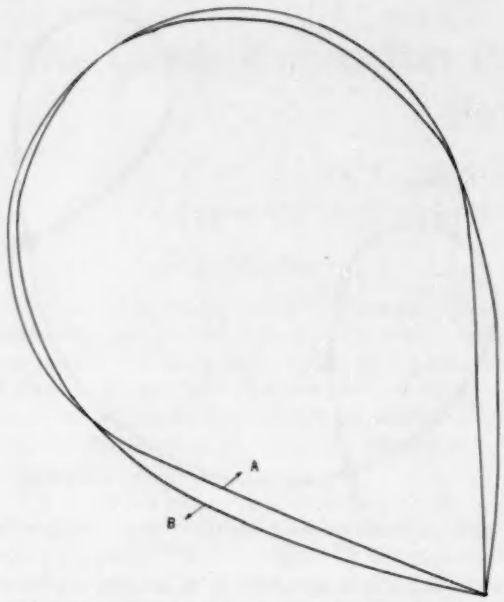

Fig. 3. A, approximate loop; B, the true elastica.

where

$$f(\theta) = \frac{(\pi + 2\theta + 2\cot\theta)^2 \cos\theta}{6.52(\sin\theta + 1)}$$

θ is found in terms of b/b_0 from Equations 2 and 3 and hence $f(\theta)$ can be plotted in terms of $(b - b_0)/b_0$ as a percentage. These values have been calculated and are plotted in Figure 4. The equation obtained by this means is found to fit the experimental load–extension curve of elasticas formed from steel and nylon quite accurately at high loads. However, it cannot apply at low loads since the assumption as to the linearity of the upper part of the elastica cannot apply under these conditions. In fact, since when $b = b_0$, $f(\theta)$ is not zero, it would imply that a fixed but small load had to be applied to form the original unstretched elastica. To obviate this difficulty it is proposed to subtract this small load from each reading, i.e.,

$$P = \frac{2EAk^2[f(\theta) - f(\theta_0)]}{b_0^2}$$

$$= \frac{2EAk^2[F(\theta)]}{b_0^2} \qquad (5)$$

This semi-quantitative equation is found to fit the load–extension properties of the elastica fairly accurately. The following procedure was used to test the equation.

Experimental Verification

A strip of feeler steel and a nylon bass string of very accurate cross-section had eyes attached to their ends so that by passing a rod through the two ends the pin-jointed elastica was obtained. The rod was then clamped horizontally and the loop loaded by hanging weights from a hook suspended from a brass roller of $\frac{3}{8}$-in. diameter resting on the strip at the bottom of the loop. Elongation of the loop was measured by means of a travelling microscope

TABLE I

Cloth	Structure	Run-in ratio	Length of stitch, 0.001 in.		Spacing	
			Front	Back	Courses	Wales
E1	3-Needle sharkskin	1.66	166	100	19.5	24.7
E2	3-Needle sharkskin	1.58	158	100	18.9	22.0
E3	3-Needle sharkskin	1.52	152	100	18.8	21.1
E4	3-Needle sharkskin	1.47	147	100	18.7	20.6
L1	Locknit	1.23	118	96	14.4	24.7
L2	Locknit	1.30	—	—	—	—
L3	Locknit	1.4	149	106	20.4	26.3
L4	Locknit	1.54	154	100	18.8	27.8
L5	Locknit	1.70	163	96	18.0	27.8
S1	Sateen	0.60	99	166	16.1	27.2
S2	Sateen	0.58	100	171	16.4	27.8
S3	Sateen	0.62	100	162	15.6	27.8
S5	Sateen	0.63	100	158	14.8	28.1
S6	Sateen	0.61	100	163	15.4	28.4
R1	Reverse locknit	0.72	100	138	17.5	25.5
R3	Reverse locknit	0.79	100	127	16.9	24.0
R4	Reverse locknit	0.82	100	122	15.3	25.2
R5	Reverse locknit	0.85	100	117	15.0	24.8
R6A	Reverse locknit	0.89	100	112	14.5	23.4

TABLE II

	Cloth number								
	E1	E2	E3	E4	L1	L2	L3	L4	L5
Load at 10%, g.	170	150	170	180	160	140	140	140	150
Extension of 2,750 g., %	35.8	38.5	39.7	41.0	48.0	42.0	42.4	39.0	39.6

	Cloth number									
	S1	S2	S3	S5	S6	R1	R3	R4	R5	R6A
Load at 10%, g.	240	200	210	200	210	160	160	140	160	160
Extension of 2,750 g., %	49.2	51	54.5	61.1	57.0	48.0	41.5	52.1	50	50.9

focused on the lowest point of the loop. b_0 and Ak^2 were determined by direct measurement of the loop and the strip and rod respectively. E was assumed to be 30×10^6 for the steel, while the value of E for the nylon was approximated to by determining the Young's modulus in tension. This was taken directly from the bass strings' initial load–extension curve—as found using a Denison tester. From these results it is possible to calculate values of $Pb_0^2/2EAk^2$ for various values $(b - b_0)/b_0$. These are shown together with the values of $F(\theta)$ plotted as a solid line on Figure 5, the open circles being values for the nylon bass string, the solid for the steel feeler strip. As can be seen, the fit so obtained is good. It is therefore proposed to examine how closely load–extension properties of warp knitted cloth can be predicted from the load–extension properties of the model loop as predicted by Equation 4.

The Load–Elongation of Warp Knitted Fabrics at Low Extensions

Nineteen fabrics were constructed from the same yarn in four basic structures but with varying run-in ratios. The details of all these fabrics are given in Table I. All lengths are expressed in thousandths of an inch. These fabrics were relaxed in cold water and dried without tension in a standard atmosphere. To decrease the edge effects it is desirable to have a long narrow strip of fabric. The length of the strip is limited, however, by the test machine and the width by the accuracy with which one can cut narrow sections and also determine rather small loads. To ameliorate this difficulty, 2-in.-wide strips, 10 in. long, were cut from each fabric. These strips were then folded over to give a ½-in.-wide strip which was then mounted in the grips of a Scott Inclined Plane tester. This method of test is due to Munden [5].

The results so obtained are summarized in Table II, which gives the load needed to extend the fabric 10% and the extension under a load of 2750 g. (This is very close to the maximum extension of these fabrics.)

Agreement with Theory

The measured load is in very close agreement with the calculated load needed to extend the loop by 10%. To calculate these values the following assumptions have been made: (i) Ak^2 was taken as

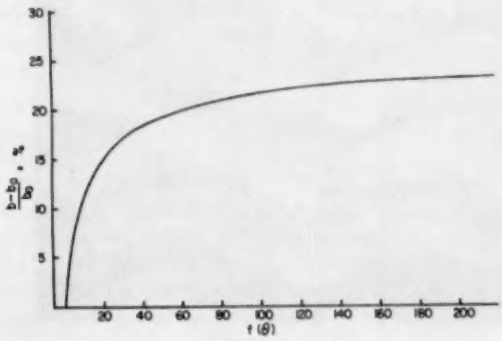

Fig. 4.

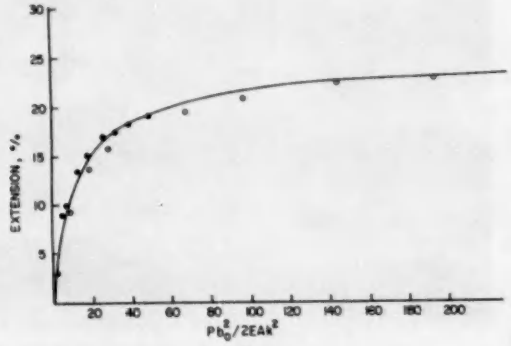

Fig. 5.

TABLE III

Fabric type:	Sateen	Locknit	Reverse locknit	Shark-skin
Calculated force	170	140	180	210
Experimental force	170	140	160	220

being Ak^2 for each filament in the yarn times the number of filaments in the yarn. As the yarn is a filament yarn of low twist, this should be exact [7]. (ii) E was approximated to by determining directly the Young's modulus in tension by extending some of the yarn from which the cloth had been made. (iii) b_0 was assumed to be equal to a course spacing, c, plus the diameter of the yarn, an approximation which has been found to be fairly accurate [2].

The calculated and measured values for the force needed to extend the fabric 10% are shown averaged in Table III.

These results show that the initial extension of the warp knitted fabric can be predicted fairly accurately from Equation 4. Examination of the actual and calculated load–elongation curves for these various materials shows agreement up to an extension of about 15%. At larger extensions, however, the two diverge, the divergence becoming increasingly large. The maximum extension of a loop is only 27.5%, but all the fabrics extend by a much larger amount than this—some over 60%. The calculated extension at 2,750 g. for all the fabrics varies very little, being between 22% and 23%. The fabrics therefore extend under high loads by considerably more than can be explained in terms of loop extension.

Deviations at High Extension

Three factors contribute towards this discrepancy:

(a) The length of yarn in the loop does not remain constant during extension. The loop is not an elastica but part of a stitch which consists of a loop plus an underlap or straight cross-link between one loop and the next. During extension of the fabric, some of the yarn from the cross-links moves into the loop.

(b) Frictional restraints due to contact with neighboring loops result in more force being necessary to extend the loop than would be necessary for an isolated loop.

(c) Elastic deformation of the yarn: if all the load were to pull on the two sides of the loop, this would result in a maximum stress of 0.3 g./denier. As the elastic deformation for the nylon under these conditions is of the order of 1%, the effect of elastic deformation will be neglected.

An attempt will now be made to estimate the relative size of these factors.

The Load–Elongation of Warp Knitted Fabrics at High Extensions

Experimental

The amount of yarn which moves from the cross-link into the loop was found by taking photomicrographs of the fabric at various stages of extension. Tracings were then taken of 10 front loops from enlargements made from the photomicrographs. A typical photomicrograph is shown in Figure 6. The central axis of the yarn was then drawn by eye on each tracing, thus producing a single closed loop.

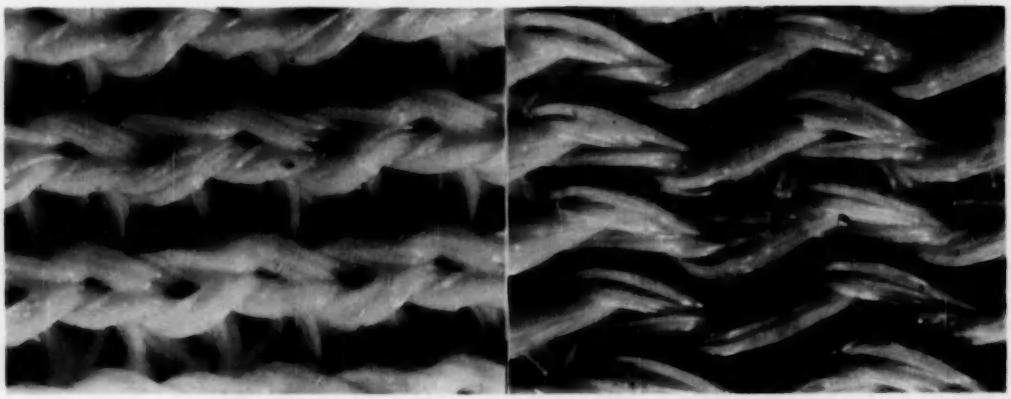

Fig. 6. Right, unstretched cloth; left, cloth stretched 40%.

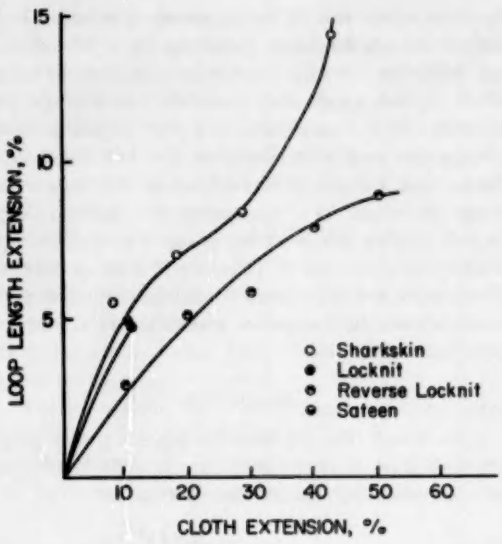

Fig. 7.

The length of this axis was measured by means of an opisometer (the start and finish of the measurement being taken at the cross-over point). By this means the values for the percentage change in length of yarn in the loop were obtained. These are shown plotted on Figure 7. For some of the fabrics this method was unsatisfactory since the loop developed a "tail" on extension, which consisted of two practically parallel yarns. This made it impossible to find any exact cross-over point from which the loop length could be accurately measured.

Agreement with Theory

The method adopted for estimating to what extent these two factors are responsible for the deviations found at high loads is as follows. Figure 8 shows the complete cycle of the load–extension curve of the fabric drawn in solid lines. If it is assumed that at any extension the force needed to extend the cloth is $L(x)$ and the frictional force is $F(x)$, then the upper curve is a curve of $L(x) + F(x)$ against x, and the lower one is a curve of $L(x) - F(x)$ against x.

Hence by taking the mean between the two curves the dashed line is obtained, which should be the curve of $L(x)$ against x. From the point A onwards this can no longer be done and the graph from here on (shown dotted) is extrapolated by eye. The shape of this part of the curve must be treated with reservation.

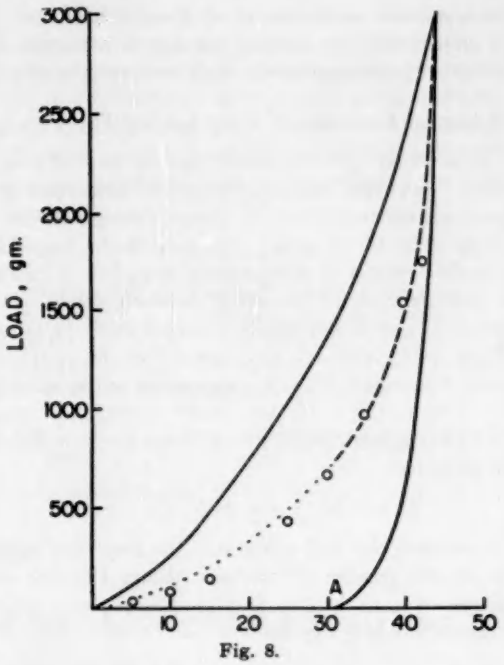

Fig. 8.

If the percentage elongation of the cloth is x, and the loop length is increased by a percentage y, then the extension of the enlarged loop is given by

$$\frac{b - b_0}{b_0} = 1 - \frac{100 + x}{100 + y}$$

For any value of x it is therefore possible to find $(b - b_0)/b_0$. This can be inserted in Equation 5 to obtain the theoretical load. However, b_0 no longer has the same value which it had initially, viz. course spacing, c, plus yarn diameter, d. By definition, b_0 is now

$$b_0 = (c + d)\frac{100 + y}{100}$$

By this means the points shown on Figure 8 have been calculated. As can be seen, the upper four points agree with the dashed line. The lower four points follow the general trend indicated by the dotted line.

As has been pointed out, the technique used cannot be used on all the fabrics, but the agreement shown where it can be used shows that the two factors already considered are the most probable causes of the deviations in the behavior of the cloth under these conditions.

In addition, an attempt has been made to estimate

the maximum extension of all these fabrics, and it is shown that by making the above assumptions, reasonably close agreement with practice is achieved.

Maximum Extension of Warp Knitted Fabrics

It is found by examination that the loop at maximum [1] extension has compressed the loop from the previous course (where it passes through it) to a single diameter of yarn. The axis of the loop will therefore consist of two tangents to a circle of radius d and the part of the circle between them. The length of such a loop can be obtained using Equation 2 and noting that r is the diameter of the yarn and $r \sin \theta$ in Figure 2B is the maximum course spacing c'.

As θ is a small angle, $\theta \approx d/c'$ and the loop length is given by

$$2c' + d(\pi + 2d/c')$$

In addition, the link connecting the loops can never be shorter than c. It has been shown [2] that the length of yarn in one unit of the structure when unstretched is given by

$$2.55c + 1.29\sqrt{c^2 + w^2} + \text{a diameter correction}$$

This diameter correction represents the length needed to connect the loop and cross-link and also correct for any other three-dimensional deviations. If it is assumed that this does not alter on stretching, the value of c' can be obtained from the relationship

$$2c' + d\left(\pi + 2\frac{d}{c}\right) + c' = 2.55c + 1.29\sqrt{c^2 + w^2}$$

Hence

$$\frac{c'}{c} = 0.85 + 0.43\sqrt{1 + \left(\frac{w}{c}\right)^2} - \frac{1}{3}\frac{d}{c}(\pi + 2d/c)$$

For the fabrics used in this study d/c varied from 0.14 to 0.18 so that to a maximum error of 2%

$$\frac{c'}{c} = 0.69 + 0.43\sqrt{1 + \left(\frac{w}{c}\right)^2} \qquad (6)$$

Figure 9 shows the maximum elongation of the structures plotted against the ratio of the courses: wales/in. The solid line is Equation 6. It is seen that one curve fits all the types of structure. It is difficult to obtain large variations of c/w for any one structure, but for sateens and reverse locknits, where such a range was available, the average extension for the structure and the variation with c/w agrees well with Equation 6. For sharkskins the average value is reasonably close but there is no range of values of c/w among the fabrics. The locknit fabrics, while showing one or two discrepancies, show the same trend as the other fabrics. The graph would appear to substantiate the conclusions that the maximum elongation is a function of c/w only.

Conclusions

It is found that the initial load–elongation properties of warp knitted fabrics can be calculated from an expression which can be written as:

$$\text{Load/unit width} = \frac{2EAk^2}{(c + d)^2 w} F(\theta) \qquad (7)$$

where $F(\theta)$ is a function of the strain only and is given on the attached graph, Figure 5. Its value has been obtained from a semi-quantitative analysis which has been found to be accurate.

As Pierce [6] has shown that the initial exten-

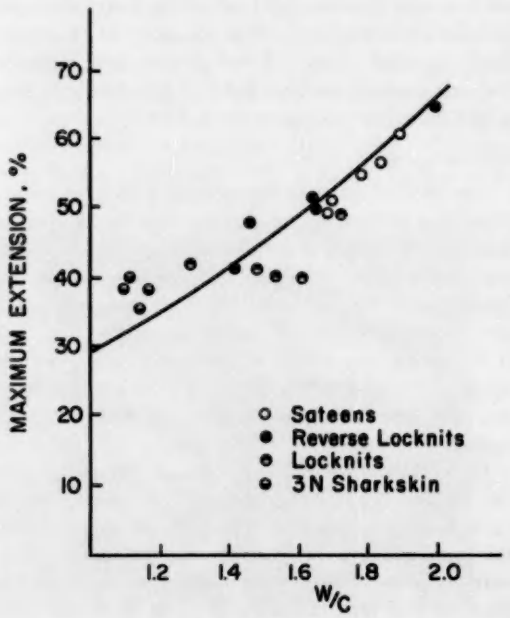

Fig. 9.

[1] It should be noted that the maximum referred to here is not the true maximum as this will be the elongation at break which takes place at a higher order of magnitude of load. It represents the beginning of the very flat load–elongation curve due to yarn extensibility.

sion modulus is correlated with his measure of drape and handle, it is interesting to note that while Equation 7 shows that the initial extension modulus depends on the courses per inch, the wales per inch, and the yarn stiffness, it is independent of the guide bar movement which produced the cloth—except for stable fabrics similar to Queen's Cord, which have not been considered. The so-called semi-stable fabrics do not differ from the rest.

This equation applies fairly accurately up to 15% extension; beyond this the structure begins to break down, the loop, robbing the underlap, and the maximum extension found being nearly twice that predicted by the equation given.

Where possible, the processes of breakdown have been followed on photomicrographs, which showed that the process of "robbing" begins very early on and continues up to a maximum. If the loop extension is corrected for this robbing, the curve is found to fit the given equations once more.

It is shown that the maximum extension of the cloth is a function of w/c (and to a much smaller extent d/c) and that it can be predicted reasonably well from purely geometric considerations. The maximum extension is also independent of the cloth structure.

Literature Cited

1. Euler, L., "Elastic Curves," *Isis* **20**, 1 (1933).
2. Grosberg, P., *J. Textile Inst.* **51**, T39 (1960).
3. Leaf, G. A. V., *J. Textile Inst.* **51**, T49 (1960).
4. Munden, D. L., *J. Textile Inst.* **50**, T448 (1959).
5. Munden, D. L., private communication.
6. Pierce, F. T., *J. Textile Inst.* **21**, T377 (1930).
7. Pierce, F. T., TEXTILE RESEARCH JOURNAL **17**, 123 (1947).

Manuscript received November 18, 1960.

Softness of Cotton Yarns as Affected by Fiber and Yarn Properties

Edith Honold and James N. Grant

Southern Regional Research Laboratory,[1] New Orleans, Louisiana

Abstract

Yarn softness is evaluated quantitatively as the percent increase in yarn width under a definite lateral force. Single-yarn softness decreases with twist and increases with yarn number and fiber maturity. With the above parameters constant, softness has no relation to fiber linear density. An equation is developed for estimating single-yarn softness from yarn diameter and twist and from fiber maturity. The softness of 2-ply yarns as related to the component single yarns is discussed. For modified cottons, increased fiber friction apparently contributes to the decrease in yarn softness.

An equation is developed to estimate the single-yarn diameter from yarn number and twist multiplier. The possibility that the diameter of the 2-ply yarn is related mathematically to the ply yarn twist multiplier and to the softness of the original unplied single yarn is discussed.

Introduction

Frequent allusions are made in the literature to yarn softness in relation to other yarn and fabric properties. Sometimes the statement is direct; e.g., when twist is low, the yarn is soft with loftiness and enhanced covering power in the fabric while, conversely, a high twist renders the yarn hard, wiry, and of reduced covering power [9]. In other instances, the reference is indirect in that a property which is related to yarn softness is cited as influencing other yarn and fabric properties; e.g., the flexibility of a fabric is influenced partially by the twist in the yarn [7], and contraction in a fabric during weaving has been attributed, in part, to yarn flexibility [8]. The extent to which a yarn flattens

[1] One of the laboratories of the Southern Utilization Research and Development Division, Agricultural Research Service, U. S. Department of Agriculture.

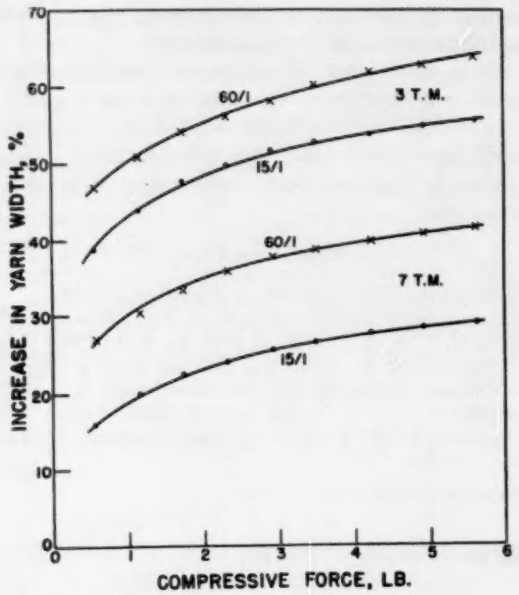

Fig. 1. Effect of compressive force on yarn deformation for yarns of different number and twist.

when incorporated into a fabric is indicative of the yarn softness. This flattening affects the void volume distribution between interyarn and interfiber spaces [6] which, in turn, influences air permeability [2], is important in the question of cover [10], and may influence fabric abrasion resistance [3].

A method was presented [11] for the quantitative evaluation of yarn softness from the deformation of yarn cross section under lateral pressure. The deformability was measured in terms of the percent increase in yarn width when the yarn was pressed laterally between two parallel plane surfaces. The softness values of the 31/2 (2×19 tex) cotton yarns in that report were dependent upon the twist in the original single yarns and in the plied yarns.

The softness value for any plied yarn is the resultant of the component single-yarns' softness and of their geometric arrangement and mobility with respect to each other. In order to study the relation of yarn softness to fiber characteristics and arrangement, the softness values were determined on single yarns. The results form the primary basis for this report.

Samples

The basic group contained 67 natural-cotton Z-twist single yarns with yarn numbers (cotton system) ranging from 9.6 to 70.2 (60 to 8.4 tex) and with twist multipliers of 3–7. These yarns had been spun in the course of various research projects at this laboratory from cottons of different characteristics, with fiber linear densities ranging from 2.8 to 4.9 μg/in., except for one of 8 μg/in., and with maturities ranging from 47% to 96%. A limited number of additional samples were compared with this basic group or with individuals therefrom: yarns spun at a commercial mill; single yarns carefully untwisted from plied yarns; yarns after various treatments, such as mercerization, acetylation, or resin addition.

Procedure

In a report by Skau et al. [11], a detailed description was given of the apparatus and the method of measuring yarn softness. Briefly, the apparatus consists of three major parts: a device for compressing the yarn laterally between two small parallel plane surfaces; a means of determining the compressive force applied; and an optical system for measuring the yarn widths.

The original width is measured with the yarn under sufficient longitudinal load to straighten with minimum stretching [4]. The increased yarn width is measured with the yarn laterally compressed by a force of 3.5 lb. At least 50 pairs of width measurements were made at indefinite intervals along a sample or along several specimens of the sample, and the average of the percent increases under the selected lateral force is the softness value reported.

Results and Discussion

Yarn width increased as the lateral compressive force was increased; it increased linearly with the logarithm of the force (Figure 1). A measure of softness at a selected pressure rather than at a selected compressive force would have certain advantages. A similar curve could be established for each yarn, but the pressure at any chosen force could only be estimated approximately since the area of contact cannot be measured directly and must be estimated by assuming some geometric, regular change in yarn cross section. The area is dependent on both the compressibility of the yarn and the original yarn diameter. Therefore, in agreement with the previous report [11], yarn softness is defined as "the percent increase in yarn width when a 4-mm. length of the yarn is pressed laterally be-

tween two parallel surfaces under an applied force of 3.51 lb." The softness values, thus determined, represent different pressures on different yarns; this fact should be borne in mind when the graphs are considered.

Single Yarns

Softness. The influence on softness of twist, yarn number, or fiber characteristics had been inferred in the choice of samples from the assortment of single yarns. Figure 2 does not include all available data but rather is illustrative of the relationships discussed.

The softness decreased with increasing twist for a given cotton spun to a given yarn number (Figure 2A). When the yarn twist is negligible, the fibers tend to lie parallel to the yarn axis and can move outward freely if the yarn is compressed laterally. This behavior was demonstrated in a continuous-filament nylon yarn of 7 turns per inch when, under lateral pressure, the 13 filaments lay side by side. As the yarn twist is increased and the fibers wind around the yarn axis, the peripheral fibers, having the longest path, exert pressure toward the yarn axis if their entanglement limits slippage. The inward pressure packs all the fibers more tightly and reduces their freedom to slip under a laterally applied compressive force. The greater the twist, the more restricted is the motion of the fibers against external pressure and, as a result, the smaller is the distortion from circularity of the yarn cross section.

The softness increased as the yarn number increased for a given cotton spun with the same twist multiplier (Figure 2B). For the twist-multiplier and yarn-number ranges given, the calculated angle between the "average" fiber and the yarn axes is essentially constant for the same twist multiplier thus making the twist variation insignificant. The change in softness with yarn number is related primarily to the cross-sectional dimensions of the yarn or rather to that portion of the yarn perimeter presented to the lateral compressive force. The contact along the yarn length is constant, but the widthwise contact varies with yarn number; therefore the pressure per unit area of contact increases as the yarn becomes smaller, i.e., as the yarn number increases.

The data showed no definite relationship between yarn softness and fiber linear density when other parameters were constant (Figure 2C), but softness increased as fiber maturity increased when twist and yarn number were constant (Figure 2D). Fiber shape affects yarn softness in that the rounder (more mature) fibers probably have greater mobility with respect to each other so that there is a greater measurable increase in yarn width with lateral pressure. This is logical, since circular cylinders would be expected to slide or roll by each other more readily than elliptical or flattened cylinders.

Parenthetically, the four graphs would be altered if pressure, instead of force, were constant. In Curve A, the spread between extremes would be increased approximately 10 percent-units; in Curve B, the

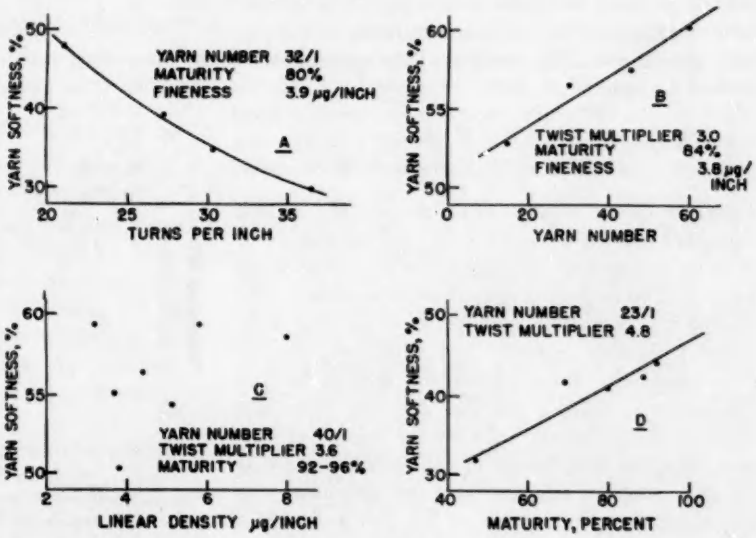

Fig. 2. Effects of certain yarn or fiber properties on yarn softness: A, yarn twist; B, yarn number; C, fiber linear density; D, fiber maturity.

spread would be decreased by about 5 percent-units. Deformation curves for different forces (similar to Figure 1) for the yarns of Figures 2C and 2D were not determined, but from similar curves for other yarns, a slight increase in spread might be expected.

An attempt was made to consolidate twist and yarn number effects by introducing the concept of work, i.e., the more work expended in twisting the yarn, the harder should be the yarn and the smaller should be the softness value. In the rotation of rigid bodies, the work expended is equal to the product of the component of the forces perpendicular to the axis times the perpendicular distance of the component from the axis times the angular displacement (θ) of the body in the direction of the moment. Though a yarn is by no means a rigid body, with certain assumptions an expression may be evolved which is analogous to work and which will be designated "twisting factor" (TF).

A given length of untwisted yarn is assumed to be fixed at one end and to be twisted by rotation of the free end. The applied torque is assumed to be equivalent to a constant mean force acting at a distance from the yarn axis which halves the cross-sectional area of the finished yarn, i.e., at 0.707 yarn radius, r. The twisting force then turns a unit length of the "average" fiber along a helix of "average" radius, 0.707 r, for a number of turns or for an angular displacement of θ. The work expended is equivalent to the constant force times 0.707 r times θ. The number of turns, θ, per unit length of fiber was calculated in terms of cotton-system yarn number, yn, twist multiplier, TM, and yarn diameter in cm., d, from simple geometric relations. The equation thus derived becomes

$$TM \propto \frac{d \times TM \times \sqrt{yn}}{\sqrt{(d^2 \times TM^2 \times yn) + 1.30776}} \qquad (1)$$

Turns/in. can be substituted for the product of twist multiplier and the square root of yarn number. The twisting factors were calculated thus for the 67 single yarns and were plotted against softness values. An inverse proportionality and trends in softness associated with fiber maturity and with yarn number were suggested. From all available data of the type illustrated in Figures 2B and 2D, two correction factors were estimated: 0.24 for the change in softness value per unit change in yarn number and 0.33 for the change in softness value per unit change in maturity. A yarn number of 35 (17 tex) and a maturity value of 85% were selected arbitrarily as "standard," and all softness values were corrected to this standard. The plot of twisting factors, TF vs. "standardized" softness values resulted in the linear relationship of Figure 3, for which the calculated regression line is expressed by the equation

$$\text{Softness ("Standardized")} = 97.47 - 131.29TF \qquad (2)$$

The correlation coefficient is -0.89 with a standard error for softness of 3 percent-units.

In a comparison of similar yarns from this laboratory and from a commercial mill, the softness values of the mill yarns were slightly lower than their SRRL counterparts. Since the yarn numbers of the paired samples varied somewhat, all softness values were "standardized" for comparison with theoretical values as calculated from Equations 1 and 2. The standardized values were within statistically acceptable limits except for the three commercial warp yarns, each of which was 4 percent-units lower than its theoretical value and still lower than its SRRL companion.

Single yarns reclaimed from ply yarns had softness values slightly higher than the values calculated from the equations, but the significance of the differences is statistically doubtful. Two single yarns were untwisted from two 30/2 yarns; one had a twist multiplier of 3 in both the single and plied yarns, and the other, one of 7. The measured softness of these two singles differed from the softness values of the singles before plying by less than 1 percent-unit.

Diameter. Various methods have been proposed for measuring yarn diameters. In some techniques, the yarn cross section is distorted from circularity

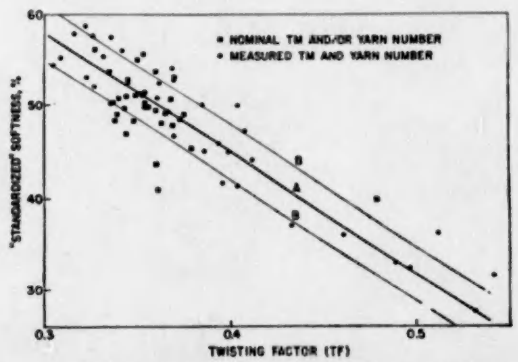

Fig. 3. Softness is inversely proportional to twisting factor (TF). A, regression line; B, standard error for softness.

in varying degrees and the measured width is larger or smaller than the original diameter depending upon which axis of the deformed yarn is measured. In the thickness gauge method, for example, the smaller axis of the deformed yarn is measured; the method is less desirable than the microscopic technique [1]. The extent to which the measured yarn width deviates from the true yarn diameter is a function of the yarn softness and of the magnitude of the pressure applied.

From the unpressured diameters of the basic group, an equation was developed to express yarn diameter in terms of yarn number and twist multiplier. A twist factor has a logical place in the equation since it is generally accepted that increased twist decreases the yarn diameter.

In a series of yarns with yarn number constant and twist varying, a linear relationship was found to exist between yarn diameters and the reciprocals of twist multipliers. The yarn diameter at infinite twist ($1/TM = 0$) corresponded to a yarn volume approximately 20% more than the cellulose volume as calculated from yarn number. Assuming that, for different yarn numbers, the volume enclosed by cotton fibers thus tightly packed is 120% of the cellulose volume, the intercepts for various yarn numbers from 10/1 to 70/1 were calculated using the first member of Equation 3 below. These values plus the experimentally determined data yielded a family of lines the slopes of which varied regularly with yarn number: slope $= 0.195\ yn^{-.58}$. Therefore, yarn diameter in centimeters ($d_{cm.}$) may be calculated from the equation

$$d_{cm.} = \frac{0.076}{\sqrt{yn}} + \frac{0.195}{TM(yn^{.58})} \qquad (3)$$

when yn is yarn number and TM is twist multiplier.

The theoretical diameters were calculated for the 67 single yarns using either experimentally determined or nominal values for yarn numbers and twist multipliers. The theoretical–experimental differences in diameter ranged from -0.0024 to $+0.0025$ cm. A statistical analysis of the differences indicated that, for these single yarns, the equation is applicable with a standard error of ± 0.0009 cm. (± 0.00035 in.).

The equation may be specific for the conditions under which these yarn diameters were measured, i.e., with each yarn under a designated longitudinal load which ranged from 2 to 3 g. and under room conditions with relative humidity in the 50%–60% range. Conceivably, variation of either condition might alter the relationship, but limited data indicated that the differences would be small.

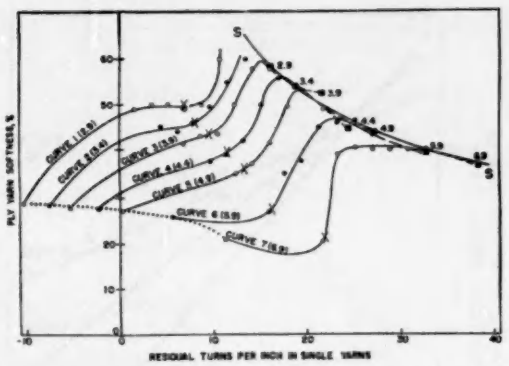

Fig. 4. Ply yarn softness varies with twist changes in component single yarns. Each curve represents yarns twisted from two single yarns of original twist multiplier as designated. The squares represent the single yarns before plying. The dotted line connects all ply yarns of 7.9 twist multiplier. The crosses indicate balanced yarns.

Measured diameters were within limits of estimate of Equation 3 for four additional singles measured subsequently, for eleven singles carefully untwisted from 2- or 3-ply yarns, and for eight filling or warp yarns spun at a commercial mill.

Ply Yarns

Softness. The 98 yarns (31/2) of the previous report [11] were used to illustrate relationships between ply yarns and their original singles. The softness values at the various twist multipliers (Figure 2) [11] were replotted in Figure 4 against residual-twist-in-single-yarn. The data for the single yarns form a smooth curve (SS) and the softness values of the low-twist ply yarns tend to follow this curve. As estimated from Curves 3 through 6, the maximum softness value occurred in each series for that ply yarn in which approximately 30% of the twist had been removed from the single yarns. As more twist was inserted into the ply yarn, the softness values decreased rapidly from the peak to that of the balanced yarn (B) where approximately 50% of the twist had been removed from the single yarns.

The measured softness of the ply yarn is the resultant of the twist remaining in the singles and the twist inserted into the ply yarn. In the original single yarns, the fibers are lying reasonably parallel to the angle of twist. When countertwisted into

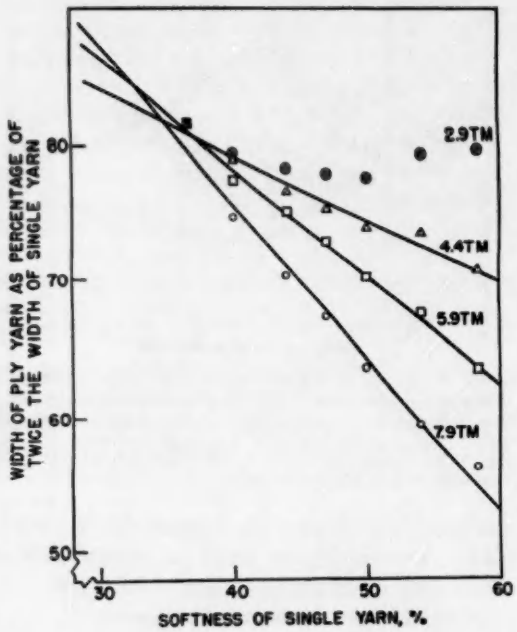

Fig. 5. Width of ply yarns, of given ply twist multiplier, decreases with increasing softness of original singles.

the ply yarn, the fibers are forced to twist in the reverse direction and within a confined space, i.e., against the force holding the singles adjacent to each other. The counterforce is negligible when the plying twist is small, and the softness of the untwisted component single yarns controls the measured softness until a maximum value is reached. At increased ply twist, the fibers undoubtedly become entangled as their direction of twist is reversed, thus further limiting fiber mobility; as a result, the softness value is lowered.

Diameter. A pair of single yarns placed side by side obviously should be twice as wide as the individual single yarn. However, when twisted together, the compressive twisting force should decrease the 2-ply yarn diameter, particularly if the single yarn is soft and yielding. The extent of compression was calculated for each of the 31/2 yarns by expressing each ply-yarn diameter as the percentage of twice the width of its original single yarn. Generally, the percentages decreased as the ply twist increased and as the softness of the original single yarns increased.

These calculated percentages of compression were plotted against softness values of the original single yarns for each group of yarns having a common ply twist multiplier. The result for the 4.4, 5.9, and 7.9 *TM* yarns was a series of lines as illustrated in Figure 5. For the 1.9 through 3.4 *TM* groups, the linear relationships were not as well defined (e.g., 2.9 *TM* group in Figure 5), while the line for the 1.4 *TM* group was horizontal (not shown). The slopes of these lines changed with sufficient regularity to permit the development of an equation which expressed ply-yarn diameter in terms of ply twist multiplier and single yarn softness. The diameters of 92 yarns, as calculated by the equation, were within $\pm 3\frac{1}{2}\%$ of the experimental smoothed diameters. The few exceptions were in the two series plied from the singles of lowest twist and occurred in that section of each series between the balanced yarn and the yarn in which all twist had been removed from the component single yarns; even in these, the experimental diameters were only 4% to $6\frac{1}{2}\%$ higher than the calculated values. The equation is not generalized sufficiently to apply to all 2-ply yarns (Z/S); however, the equation does show that the ply yarn diameter is related mathematically to the ply twist and to the softness of the original single yarn for this particular group of yarns.

Modified Cotton Yarns

Softness. For a limited number of yarns, softness changed with various treatments or processings. Single yarns of modified cotton were compared with either their natural-cotton counterparts or with the natural-cotton yarns before treatment. Duplicate softness values of several pairs are given in Table I.

Yarn softness was decreased by sizing, colloidal silica (SiO_2) impregnation, Soxhlet extraction with ethanol, resin (dimethylol ethyleneurea) treatment, or acetylation (26% and 36%) when the cotton had been acetylated as rovings. Interfiber friction evidently affects yarn softness since each of the above treatments alters the fiber surfaces. Sizing tends to bind the fibers together thereby decreasing their mobility. Brown [5] has shown that fiber friction increases with percent takeup of colloidal silica. The hot ethanol removed the greater portion of the natural waxes from the fiber surfaces as reflected in the average loss in dry weight of about $1\frac{3}{4}\%$.

Factors other than change of fiber surface must be involved in the yarn-softness reduction since yarns from cotton acetylated as rovings had lowered

softness values while those from cotton acetylated as raw stock showed no significant change. Similarly, the processing involved in resin treatment, but without the resin, lowered the softness more than when resin was added, while the combination of resin and the softener Polymul,[2] which is considered a lubricant, increased the yarn softness value to nearer that of the untreated yarn. The softness values of some modified yarns remained within the range of their controls; these were yarns mercerized and stretched, blends of natural and cut fibers, and yarns spun from cotton which had been heated to about 365° F. (185° C.) for 15 sec.

Diameter. Of the modified cotton yarns, the diameters of the mercerized, restretched yarns and of the colloidal-silica treated yarns were less than their controls. The average diameters of the acetylated, alcohol-extracted, and resin-treated groups were higher than their corresponding controls. However, a considerably larger number of samples would have to be measured before the differences had any real statistical significance.

TABLE I. Comparison of Softness Values* of Modified Cotton Yarns and their Controls

Modification	Control	Treated	Percent difference
Sized	45.4	33.1	−27
	50.1	39.4	−21
Impregnation with colloidal silica	44.0	28.7	−35
	43.5	28.5	−34
Extracted with hot ethanol†	42.7	25.1	−41
	37.4	28.8	−23
Resin (DMEU) treated‡	42.2	32.9	−22
	58.6	52.7	−10
Partially acetylated (26%) as roving	46.6	36.4	−22
	47.4	36.1	−24
Fully acetylated (36%) as roving	46.6	39.1	−16
	47.4	40.3	−15
Partially acetylated (25%) as raw stock	42.3	38.3	− 9
	40.2	41.0	+ 2
Resin procedure without resin	45.1	33.2	−26
Resin plus softener (Polymul)	45.1	40.3	−11
Mercerized and restretched	47.9	49.0	+ 2
	51.8	53.0	+ 2
Blend of natural and cut fibers	48.1	46.1	− 4
	31.6	29.7	− 6
Heated as fibers (365° F. for 15 sec.)	48.1	49.0	+ 2
	31.6	32.2	+ 2

* Softness values as measured without correcting to "standard."
† Extremes of 7 pairs.
‡ Extremes of 6 pairs.

Summary

The softness of a yarn, or its ability to deform under lateral pressure, affects certain physical properties of the yarn and of the fabric into which it is incorporated. Softness may be evaluated quantitatively as the percent increase in yarn width when the yarn is under a definite lateral force.

The softness values of the Z-twist single yarns of a wide range in twist, yarn number, and fiber characteristics were dependent on the type of cotton and on certain spinning factors. An equation was developed to estimate single yarn softness from yarn number, twist multiplier, diameter, and fiber maturity. In 2-ply yarns, the yarn softness was influenced by the softness of the component single yarns when the ply twist was low. After increasing to a maximum, the softness value decreased sharply as more twist was inserted into the ply yarn. Various treatments, such as resin addition, reduced the yarn-softness values for a limited number of single yarns of variously modified cottons. A change in the surface characteristics of the fibers was a contributing factor to the reduction in softness.

An equation was developed to estimate the unpressured diameters of single yarns from yarn number and twist multiplier. For the group of 2-ply yarns studied, the ply-yarn diameter related mathematically to the ply twist multiplier and to the softness of the original unplied single yarn. The difference between the diameters of the untreated and treated yarns was of doubtful significance in a majority of the paired samples.

Acknowledgments

The authors wish to express their appreciation to J. J. Brown, Jack Simpson, J. E. Sands, and W. G. Sloan for samples of yarns from other investigations and for data on the properties of those yarns and their fibers; to E. L. Skau for his guidance during the initial period of this investigation; and to George I. Pittman for preparation of graphs.

[2] Use of a company and/or product named by the Department does not imply approval or recommendation of the product to the exclusion of others which may also be suitable.

Literature Cited

1. American Society Testing Materials, Philadelphia, Pa. ASTM Designation D204-57T.
2. Backer, Stanley, TEXTILE RESEARCH JOURNAL **21**, 703–714 (1951).
3. Backer, S., and Tanenhaus, S. J., TEXTILE RESEARCH JOURNAL **21**, 635–654 (1951).
4. Ball, H. J., *Bull. Lowell Textile Inst.* Ser. 45, No. 2 (Nov. 1941).
5. Brown, H. M., Langston, J. H., and Rainey, W. T., Jr., TEXTILE RESEARCH JOURNAL **25**, 462–471 (1955).
6. Hoffman, R. M., TEXTILE RESEARCH JOURNAL **22**, 170–178 (1952).
7. Hoffman, R. M., and Beste, L. F., TEXTILE RESEARCH JOURNAL **21**, 66–77 (1951).
8. Kennamer, H. G., Mayne, S. C., Jr., and Berkley, E. E., TEXTILE RESEARCH JOURNAL **26**, 812–820 (1956).
9. Landau, A. K., *Textile World* **86**, 2510–2511 (1936).
10. Peirce, F. T., *J. Textile Inst.* **28**, T45–96 (1937).
11. Skau, E. L., Honold, E., and Boudreau, W. A., TEXTILE RESEARCH JOURNAL **28**, 206–212 (1958).

Manuscript received November 28, 1960.

The Molecular Structure and Mechanical Properties of Polyethylene Terephthalate Fibers

I. M. Ward

Imperial Chemical Industries Limited, Fibres Division, Hookstone Road, Harrogate, Yorkshire, England

Abstract

In this paper, the application of several techniques of molecular structure determination to polyethylene terephthalate (henceforth abbreviated to PET) polymer and fibers will be described. These investigations have been directed partly towards obtaining an understanding of the dynamic mechanical properties of PET and related polymers and partly to the characterization of PET fibers with respect to crystallinity and orientation.

In considering the dynamic mechanical properties of PET and their relationship to the molecular structure two main points have been investigated: first whether the dynamic mechanical transitions can be related to specific motions of the molecular chains and second whether the influence of crystallinity and orientation can be simply understood.

Introduction

PET is a particularly interesting polymer from the viewpoint of molecular structure because the structure can be varied very widely. The essential features can be summarized as follows. When the molten polymer is rapidly quenched to room temperature it solidifies in a state of disorder, the so-called amorphous state, giving an X-ray pattern with a characteristic "amorphous" halo but no evidence of three-dimensional order.

If this amorphous material is subsequently heated to temperatures above about 100° C., crystallization occurs and an unoriented, partially crystalline sample is formed, the degree of crystallinity depending on the temperature and time of this heat treatment. Stretching the unoriented polymer produces samples of varying crystallinity and molecular orientation, the exact values of these quantities depending on the amount of stretch and the temperature of the stretching process.

Such polymer structures are very complicated systems to characterize. X-ray techniques are clearly available to identify the so-called crystalline fraction, the regions possessing three-dimensional order. To describe the remaining material, however, with its varying degrees of order, very different techniques are necessary. In this paper we shall principally be concerned with two spectroscopic techniques which have been widely applied to the analysis of polymers, infrared spectroscopy and nuclear magnetic resonance.

The first complete study of the infrared spectrum of PET was that of Miller and Willis [8], who assigned the principle absorptions to the corresponding

molecular vibrations. These authors and others (notably Cobbs and Burton [2, 9]) noted that many of the absorption bands of this polymer are affected by heat treatment, i.e., crystallization. It is now generally accepted that these changes are due to configurational changes affecting the glycol residue [5].

This interpretation of the infrared changes has considerable implications. In particular it suggests that many of the effects formerly attributed to the onset of crystallinity are more correctly ascribed to configurational changes within a chain molecule, i.e., they are more closely related to the orientation of individual chain molecules than to the production of three-dimensional order. This view has led to a reconsideration of the relative importance of crystallinity and orientation on the elastic modulus of PET fibers, and in determining the drawing behavior of these fibers. It also bears directly on the interpretation of the dynamic mechanical transitions.

PET shows two dynamic mechanical transitions, one at $-40°$ C., the γ-transition, and one at $+80°$ C., the β-transition or glass transition. Both these transitions are associated with a dielectric loss process. On the basis of the dielectric loss measurements of Reddish [11] it was proposed that each of these transitions could be attributed to specific molecular motions; the γ-transition to motion of end groups and the β-transition to motion of the carbonyl groups (i.e., a configurational change involving rotations about the carbonyl phenylene bond). The *trans–gauche* configurational change can also give rise to a loss maximum due to change in relative positions of the —C—O— bonds. It therefore appeared that this gave a third possible molecular motion which could be associated with the γ or the β-transition.

A possible way to resolve some of these problems is to apply the technique of nuclear magnetic resonance. This has been done and the results will be discussed here, in as much as they throw light either on the molecular interpretation of the transition or on the influence of crystallinity and orientation on the elastic modulus of PET fibers.

General Interpretation of the Dynamic Mechanical Transitions of PET and Related Polymers

Dynamic Mechanical Measurements on Methylene Terephthalate Polymers

The most convenient way of studying the so-called transitions of PET is by making dynamic mechanical measurements. A fairly simple and accurate way of doing this is to measure the behavior in cantilever of rod-shaped specimens driven at resonance [12]. From the resonance curve and frequency, the work loss and modulus can be determined. The apparatus is developed to enable measurements to be taken over the temperature range from $-180°$ C. to $+200°$ C.

This technique, however, yields rather limited information because only unoriented samples are examined. Thus the modulus measured is a mixture of the elastic moduli of the sample. For comparisons of polymers with different chemical composition it will be assumed that it is adequate to ensure that all the samples are unoriented and heat crystallized to approximately the same crystallinity; the effects of crystallinity and orientation will be considered at a later stage.

A typical set of results for PET is shown in Figure 1. It can be seen that there are two transitions, one at about $-40°$ C., which is customarily called the γ-transition, and the other at about $+110°$ C., the β-transition. The β-transition is the so-called glass–rubber transition, and in this temperature range PET samples undergo a large change in modulus, softening to a rubber-like solid from a rigid glass-like solid.

Measurements have been made on PET and the related series of polymers in which larger numbers of methylene groups are included in the glycol residue [3]. In addition polyisophthalic anhydride and polymethylene have been examined. The polymers were all annealed for about an hour at a temperature at least 50° C. above their glass transitions to put the specimens into a stable state with a high degree of crystallinity and no preferred direction of orientation.

The results are shown in Figure 2, where the temperatures of the various loss maxima and the melting points are plotted as a function of the number of methylene groups in the glycol residue. Looking at these results, the most obvious features are as follows. All the polymethylene terephthalate polymers show a similar pattern of two main loss peaks together with the rising loss towards the melting point. With increasing numbers of methylene groups the two main loss peaks move by equal amounts to lower temperatures.

It is particularly interesting to compare these results with those for polymethylene and poly(isophthalic anhydride). Polymethylene shows a single loss peak at $-120°$ C., which is at approximately

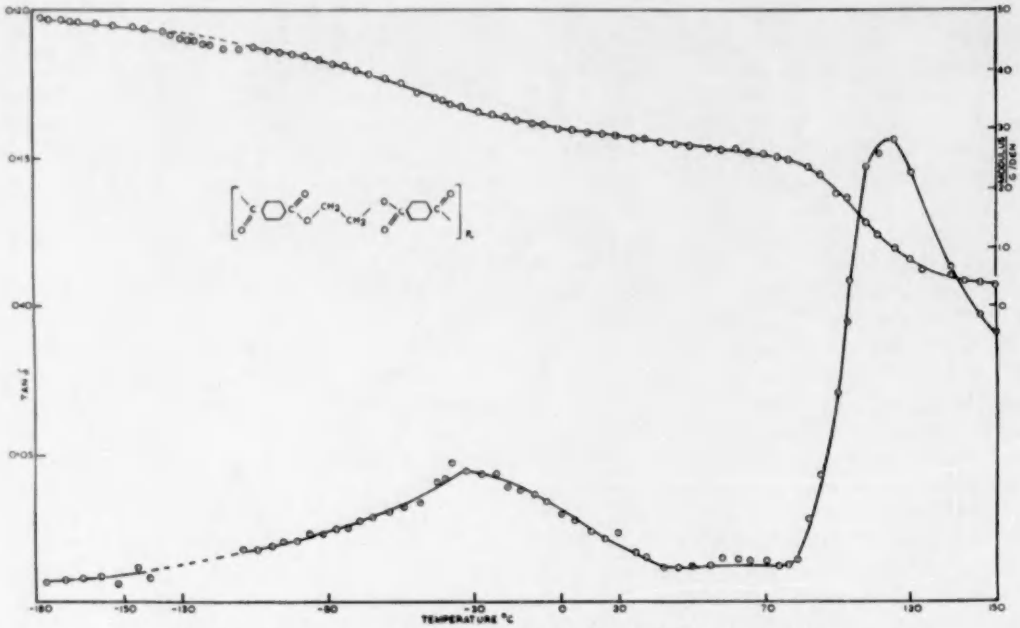

Fig. 1. Dynamic loss and modulus of PET from $-180°$ C. to $+150°$ C.

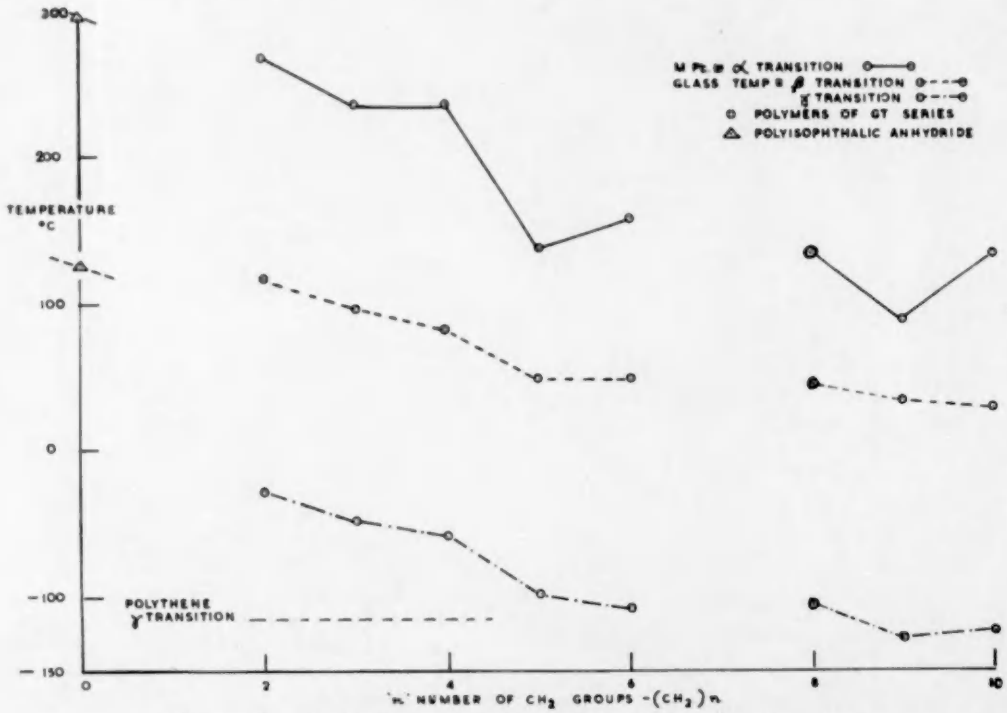

Fig. 2. Plot of transition temperatures against number of $-CH_2$ groups.

the same temperature as the γ-transition peak of poly(decamethylene terephthalate). Poly(isophthalic anhydride), on the other hand, shows almost no lower loss peak and shows a high temperature loss peak of about 130° C. Straightforward inference from these two facts would be that the γ-transition in PET and the other polyesters is similar to the γ-transition of polymethylene, i.e., that it arises from the hindered rotations of methylene groups in the amorphous regions of the polymer, and that the β-transition is associated with this motion and also motion of the paraphenylene linkages.

Evidence will be presented from other sources, principally nuclear magnetic resonance and infrared spectroscopy, which show that this plausible explanation is incorrect. However, it is mentioned in passing because it is certainly the interpretation of these transitions which immediately suggests itself if one considers the dynamic mechanical measurements only.

Infrared Measurements on PET and Related Compounds

As mentioned above, the β-transition temperature range is the temperature range at which crystallization can occur in these polymers. It is therefore relevant to any molecular interpretation of this transition to study the changes in the infrared spectrum which are associated with crystallization.

The infrared spectra of amorphous and heat-crystallized PET are shown in Figure 3. It can be seen that many of the absorptions are affected by crystallization. The assignments of these absorptions have been made partly by comparison with the spectra of simple monomeric substances and partly by deuteration techniques [5]. Figure 3 also shows the spectrum of poly(tetradeuteroethylene terephthalate) in which the hydrogens of the methylene groups have been replaced by deuterium. Deuteration shows very clearly that the majority of the absorption bands affected by crystallinity can be assigned to vibrations of the glycol residue. It was therefore suggested that a simple explanation of these infrared results is that in the amorphous regions there are two possible configurations of this part of the molecule. This is illustrated in Figures 4a and 4b. The *trans* configuration of this group is given in Figure 4a. This is the fully extended configuration and is the only configuration in the crystalline material. Figure 4b shows the *gauche* configuration of this group, which it is proposed also exists

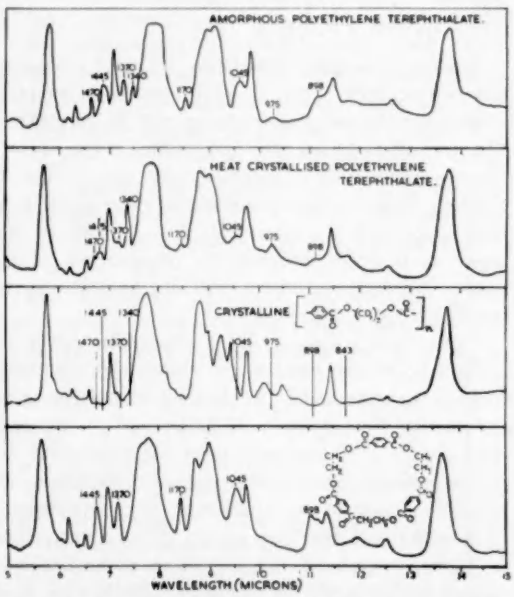

Fig. 3. Infrared spectra of amorphous and heat crystallized polyethylene terephthalate, polytetradeuteroethylene terephthalate and cyclic trimer.

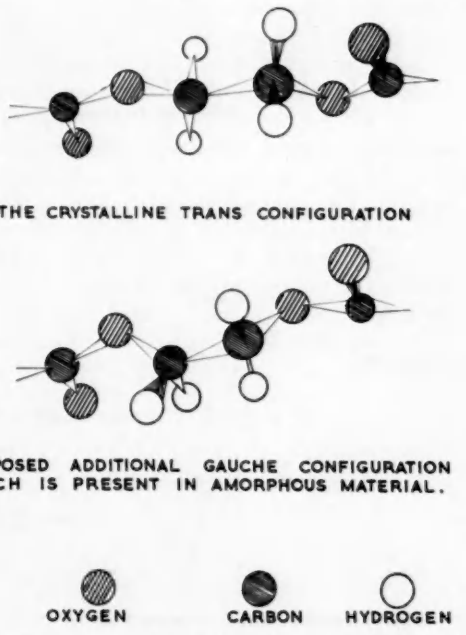

Fig. 4. *Trans* and *gauche* configurations of glycol residue.

as well as the *trans* configuration, in amorphous material. This provides a simple explanation of the infrared data since one set of bands (those that increase in intensity on crystallization) can be assigned to the *trans* vibrations and the other set (those which decrease on crystallization) to the *gauche* vibrations. Since crystallization sets in above the β-transition it is reasonable to infer that the β-transition is associated with at least the configurational change of the glycol residue.

Some support has been obtained for this interpretation of the infrared spectrum of PET, from the spectrum of the cyclic trimer of ethylene terephthalate. In this molecule three paraphenylene linkages are joined by three glycol linkages. Figure 3 also shows the spectrum of the cyclic trimer. It can be seen that the trimer shows the absorptions assigned to the *gauche* configurations only, the corresponding *trans* absorptions being absent. Molecular models of the cyclic trimer suggest that it is very likely that the glycol linkages are in the *gauche* configuration, but that the molecule could have two possible structures. In one the carbonyl groups in the paraphenylene linkages are *cis* with respect to the benzene ring and the methylene groups *gauche,* the benzene rings in this case being in the plane of the molecule. In the other configuration of the molecule, the paraphenylene groups are *trans,* the methylene groups are again *gauche,* but the benzene rings in this case are perpendicular to the plane of the molecule, so that the whole molecule is approximately triangular.

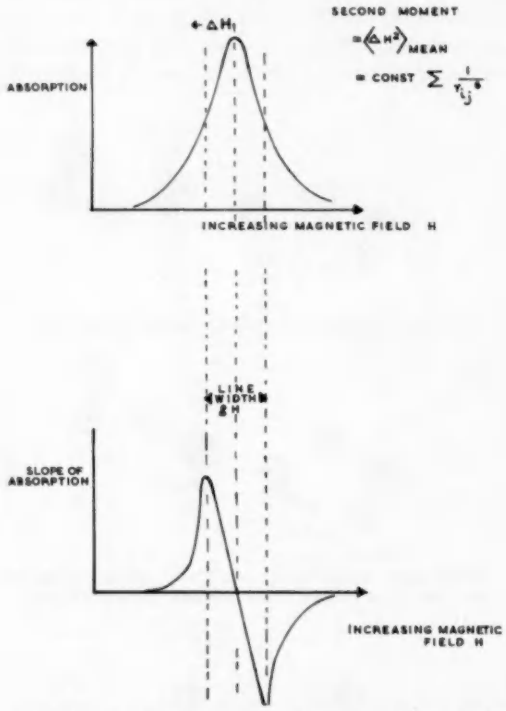

Fig. 5. Typical n.m.r. absorption curve for a rigid polymeric system.

Measurements of the refractive indices of the crystals by optical means have been compared with the theoretical calculation of refractive indices for the two suggested forms by using bond polarizabilities. The results are shown in Table I. This calculation shows that the planar form is the correct one and this has been confirmed by additional X-ray measurements. Thus it must be concluded that in the trimer molecule the carbonyl groups are in the *cis* position with respect to the benzene ring. This suggests that the configurational changes associated with the β-transition are greater than those proposed on the basis of the infrared data alone and involve the phenylene/carbonyl bond in addition to the glycol residue.

Nuclear Magnetic Resonance Measurements on PET and Related Polyesters

Nuclear magnetic resonance (n.m.r.) measurements have been made on PET and the other polyesters over the temperature range 90° K. to 300° K. The second moments and line widths of the absorptions were measured together with spin-lattice relaxation times. Full accounts of this work have been published elsewhere [1, 6, 17] and in this paper it is only necessary to quote some of the results for second-moment and line-width measurements.

Figure 5 is a typical n.m.r. absorption curve for a rigid polymeric system and shows the absorption of the magnetic nuclei (in the case of polyesters the protons in the polymer) as a function of the magnetic field. In measurements of the absorption line one is usually concerned with two quantities; the second moment of the absorption line, (its moment of inertia) and the line width. The n.m.r. signal is normally obtained, for experimental reasons, as a plot of the derivative of the absorption against magnetic field. A convenient measure of the line width of the absorption is therefore the distance between

TABLE I. Measured Refractive Indices for Single Crystal of Cyclic Trimer Compared with Values Calculated from Bond Polarizabilities for Planar and Triangular Molecules

Direction	Perpendicular to plane of molecule	In plane of molecule
Triangular molecule	1.71	1.51 and 1.51
Planar molecule	1.44	1.69 and 1.65
Observed	1.45	1.68 and 1.67

the points of maximum slope which are the maximum and minimum of the derivative curve.

It was shown by Van Vleck that the second moment is proportional to the summation of $1/r^6$ where r is the distance between any pair of protons. For a crystalline solid this quantity can therefore be computed from the crystal structure.

When the structure is not rigid, however, and in the cases of interest here this is due to the onset of molecular motions in the solid state, the second moment is reduced by an amount depending on the extent of the molecular motion. The changes in the second moment and line width of the n.m.r. absorption line occur when the frequency of the motion is equal to the line width of the absorption in the cycles. For polyethylene terephthalate and related polymers, the line widths are about 5 gauss, and this corresponds to a frequency of about 100 kc./sec. in the apparatus which has been used. Thus appreciable narrowing of the n.m.r. signal will be caused by molecular motions of appreciable amplitude at frequencies greater than about 100 kc./sec.

It is most convenient to consider the n.m.r. results in two sections, first the results obtained in the temperature range from − 180° C. to room temperature, and second those obtained at temperatures above room temperature.

Table II shows the results obtained for second moments of polyethylene terephthalate and the other polyesters at fixed temperatures from − 180° C. to room temperature. In addition the calculated values for the second moments of the polymers based on the structure of the crystalline regions determined by X-ray measurements are given, and the last column shows the estimated temperature of the γ-transition at 10^5 c./sec., calculated from dynamic mechanical measurements.

There are two points to make about these results. First, the measured second moments at the lowest temperatures are greater than those calculated from the structure of the crystalline regions. It has been suggested that this arises from the tangling of the molecules in the noncrystalline regions. This could give rise to some very short intermolecular distances, and since the second moment depends on the inverse sixth power of the interproton distances, it could be very appreciably increased. This is a minor point as far as the interpretation of the transitions is concerned, although it is of considerable interest in view of some features of the stretching or drawing processes in these polymers, which will be discussed below.

Second, it can be seen from these results that the second moments change very gradually in this temperature range, and it should perhaps be emphasized that the derivative signal does not show a structure anywhere in this temperature range in any of the polyesters. This brings out immediately the difference between these polyesters and polymethylene. In the polyesters, the low temperature loss process is restricted to very small molecular motions, motions which are inadequate in extent to give rise to any appreciable line narrowing. In polyethylene, on the other hand, the apparently similar γ-transition is associated with the large scale segmental motions in the amorphous region of the polymer, and a clear structure is observed on the n.m.r. signal.

The n.m.r. results obtained at higher temperatures, i.e., above room temperature, however, are much more interesting because in several cases the deriva-

TABLE II. Measured and Calculated Second Moment Values from 90° K. to 293° K.

	Measured values				Estimated temp. of lower loss peak at 105 c. (° K.)
	90° K.	195° K.	293° K.	Calculated	
Polyethylene terephthalate	13.0	13.4	12.4	10.1 ± 0.8	293
Polytetramethylene terephthalate	19.3	—	15.5	—	242–279
Polypentamethylene terephthalate	22.3	18.7	14.3	—	141–214
Polyhexamethylene terephthalate	23.1	—	15.3	16.2 ± 1.4	179–203
Polynonamethylene terephthalate	21.5	17.0	10.5	—	165–180
Polydecamethylene terephthalate	22.5	16.5	15.0	18.0 ± 1.5	162–179

tive signal shows a composite structure. This composite structure appears in all cases above the β-transition.

To compare the motions of the different parts of the molecule two deuterated polymers have also been examined. These are poly(tetradeuteroethylene terephthalate), where the n.m.r. signals only arise from the benzene ring protons, and polyethylene deuteroterephthalate, where the methylene group protons are observed. All the samples in this first comparison were unoriented and heat crystallized to give a stable crystallinity up to 200° C.

The more important results are shown in Figure 6. At room temperature all three polymers show a single broad signal. At about 110° C. PET shows a composite signal, and as the temperature is raised the narrow component increases at the expense of the broad component. A very narrow signal is observed with both the deuterated derivatives, but only the deuterated glycol derivative shows a clearly resolved composite signal. These results suggest that the narrow component of the PET signals arises partly from methylene group protons which are undergoing considerable reorientation at frequencies greater than 10^5 c./sec. and partly from benzene ring protons which are undergoing similar reorientation. The broad component, on the other hand, from this simple comparison appears to arise primarily from protons attached to benzene rings which remain rigid even above the β-transition. X-ray data obtained at temperatures up to the melting point revealed no major change in the crystal structure. This confirms, as one would expect, that the benzene rings which remain rigid at least include those in the crystalline regions.

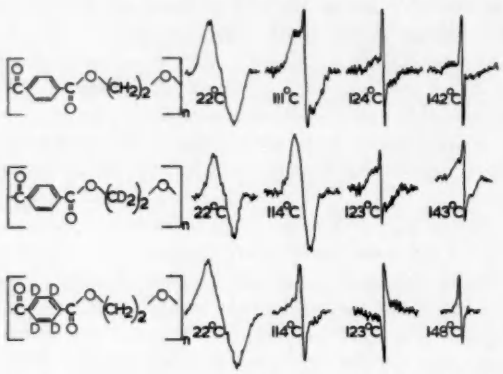

Fig. 6. Derivative spectra of polyethylene terephthalate and deuterated derivatives.

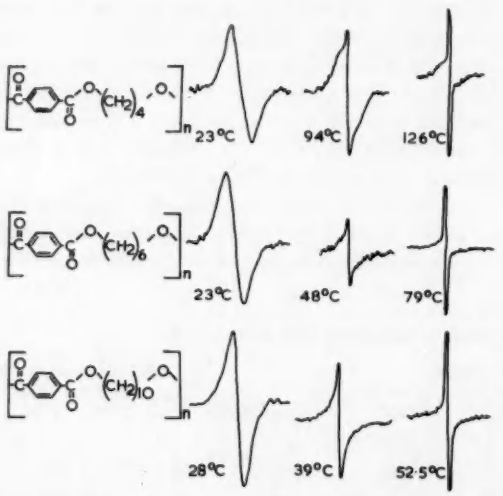

Fig. 7. Derivative spectra of polytetramethylene terephthalate, polyhexamethylene terephthalate, and polydecamethylene terephthalate.

Detailed second-moment measurements on the broad components of the PET absorptions suggest that the broad component can arise not only from protons attached to rigid benzene rings but also contains contributions of the methylene group protons which are either rigid or undergoing hindered rotation.

Figure 7 shows the appearance of a narrow component in some of the other polyesters, and this

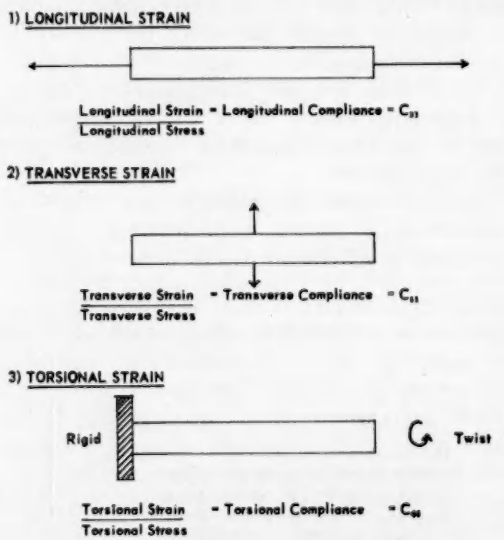
1) LONGITUDINAL STRAIN
Longitudinal Strain / Longitudinal Stress = Longitudinal Compliance = C11
2) TRANSVERSE STRAIN
Transverse Strain / Transverse Stress = Transverse Compliance = C22
3) TORSIONAL STRAIN
Rigid
Twist
Torsional Strain / Torsional Stress = Torsional Compliance = C66

Fig. 8. Three simple types of deformation.

shows that the extension of the glycol residue from 2 to 10 methylene groups, which as discussed above decreases the β-transition temperature, is accompanied by a corresponding decrease in the temperature at which the narrow component appears in the n.m.r. spectra.

It appears from these results, then, that the β-transition is a composite process at a molecular level, first involving rotations of the methylene groups and then, as the temperature is raised, rotations of the benzene rings, eventually including most of the molecules in the noncrystalline regions. This conclusion is consistent with the inferences which have already been made from X-ray data and infrared data.

Influence of Crystallinity and Orientation on Dynamic Mechanical Properties

Mechanical Behavior below the Glass Transition

The discussion of the effects of crystallinity and orientation will be dealt with in two stages. First the effects of crystallinity and orientation on the room temperature dynamic modulus will be considered, and second the effects related to the glass transition.

This division has been made because it is considered that the n.m.r. results, by showing that the amorphous regions of PET are rigid at room temperature, justify ignoring crystallinity effects on the room temperature modulus to a first approximation and considering the effects of orientation as one would for a crystalline solid.

The elastic behavior of an anisotropic solid can be described by a tensor. If the strain is represented by e and the stress by s then a generalized Hooke's Law can be written as $e = C_{ij}s$ where C_{ij} are the compliance constants, i and j having values 1, 2, and 3. An oriented fiber possesses cylindrical symmetry so that only five independent coefficients exist and, providing the Z axis is chosen for the symmetry axis (i.e., the fiber axis), the compliance coefficients C_{ij} can be written:

$$C_{ij} = \begin{vmatrix} C_{11} & C_{12} & C_{13} & 0 & 0 & 0 \\ C_{12} & C_{11} & C_{13} & 0 & 0 & 0 \\ C_{13} & C_{13} & C_{33} & 0 & 0 & 0 \\ 0 & 0 & 0 & C_{44} & 0 & 0 \\ 0 & 0 & 0 & 0 & C_{44} & 0 \\ 0 & 0 & 0 & 0 & 0 & \frac{1}{2}(C_{11} - C_{12}) \end{vmatrix}$$

In a fiber there are in principle three simple types of deformation which can be obtained. These are shown in Figure 8, and experiments based on these three types of deformation will provide values for C_{11}, C_{33}, and C_{44}.

If simultaneous measurements are made of the longitudinal stress and the longitudinal strain in an oriented fiber, the longitudinal compliance can be determined, i.e., the value of C_{33} in the tensor.

If on the other hand, a fiber of lower orientation is measured, a similar experiment will clearly give a very different result, since even if the structure of the molecular units is unaltered by the orientation process (which is most unlikely), in the unoriented fiber one will clearly find a mixture of the compliances of the oriented fiber.

Thus the effect of orientation will be twofold; first orientation of the chain molecules and second a change in the basic molecular structure, e.g., the introduction of regions of crystallinity and entanglement.

With this in mind, the results obtained by dynamic mechanical measurements on PET fibers of different crystallinity and orientation will be considered [14]. These are shown in Figure 9.

The results show clearly the importance of both crystallinity and orientation. It can be seen that the β-transition, in particular, is markedly affected both in position and character. The longitudinal compliance which is being measured here is reduced by both crystallinity and orientation, and this is true at all temperatures.

In the case of a single crystal of a crystalline solid, such as quartz, the compliances (C_{ij} of the above tensor) can be found by applying suitable strains and simultaneously measuring the stresses induced. If this material is made polycrystalline by fusing a mass of small crystals (fused quartz in this example) an isotropic solid is obtained whose compliances can be expressed by two constants which are similar to the Lamé constants. These constants can be expressed as linear sums of the original compliances, providing that certain simplifying assumptions are made about continuity of stress or strain, and that it is assumed that the compliances of the crystals are not themselves affected by the orientation process.

The longitudinal compliance of an unoriented fiber has been calculated by assuming that this can be considered to be a random aggregate of elements each of which has the elastic compliances of the oriented fiber. It was assumed that the stresses are contin-

uous and the strains discontinuous. The unoriented fiber is considered as consisting of an aggregate of elemental cubes in equilibrium. The symmetry axis of each cube is defined by the polar angles θ and ϕ with the Z axis of the sample. The strains e_{xx}, e_{yy}, etc., are then calculated in terms of the stresses on the cube faces s_{xx}, s_{yy}, etc., and clearly involve the angles θ, ϕ, and the components of the compliance. By summation over all possible values of θ and ϕ, the over-all strains of the sample can be calculated, and this calculation will yield the new compliance tensor. For the component of this compliance tensor corresponding to the longitudinal compliance measured by Thompson and Woods this gives

$$\bar{C}_{11} = \frac{1}{2}C_{11} + \frac{4}{15}C_{13} + \frac{1}{5}C_{33} + \frac{2}{15}C_{44}$$

In a recent publication on the elasticity of anisotropic materials Hearman [18] quotes a similar calculation by Reuss. As discussed above, straightforward deformation experiments yield values for C_{11}, C_{33}, and C_{44}. If it is assumed that to a first approximation Poisson's ratio is 0.5, it can be shown that $C_{13} = -\frac{1}{2}C_{33}$ and thus

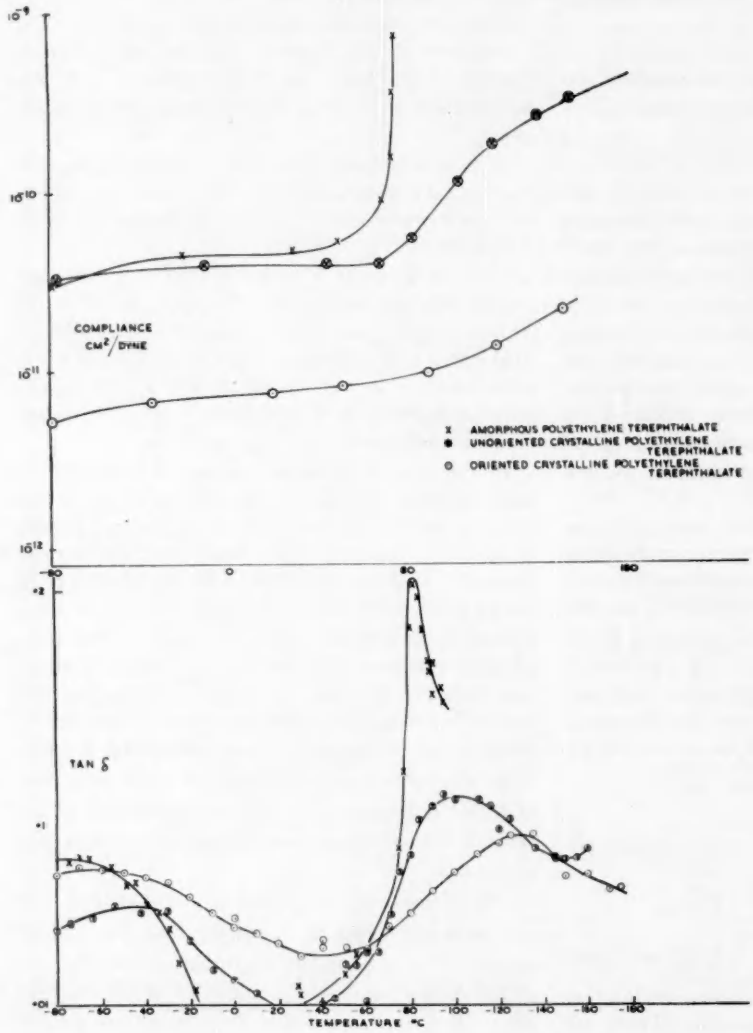

Fig. 9. Dynamic mechanical data for PET fibers of different crystallinity and orientation.

TABLE III. Comparison of Compliances for Polyethylene Terephthalate

Longitudinal compliance [14] (oriented fiber)	$C_{33} = 0.8 \times 10^{-11}$ cm.²/dyne
Transverse compliance [7] (oriented film)	$C_{11} = 10 \times 10^{-11}$ cm.²/dyne
Torsional compliance [7] (oriented fiber)	$C_{44} = 15 \times 10^{-11}$ cm.²/dyne

Calculated longitudinal compliance for a random assembly of crystalline units (assuming fiber is incompressible)

$$\bar{C}_{33} = \bar{C}_{11} = \tfrac{1}{2}C_{11} + 1/15C_{33} + 2/15C_{44}$$

Thus calculated $\bar{C}_{33} = 7 \times 10^{-11}$ cm.²/dyne

Measured $\bar{C}_{33}$ (unoriented crystalline fiber) $= 3.5 \times 10^{-11}$ cm.²/dyne.

$$\bar{C}_{11} = \frac{1}{2}C_{11} + \frac{1}{15}C_{33} + \frac{2}{15}C_{44}$$

Results have been obtained for polyethylene terephthalate which enable us to estimate the major compliances for an oriented sample at room temperature. These are shown in Table III together with the theoretical value for the longitudinal compliance of an unoriented crystalline polymer and the experimental value for a sample of unoriented crystalline yarn.

These results suggest that a major part of the difference between the room temperature longitudinal compliance of an unoriented and an oriented sample can be attributed to orientation effects alone.

Mechanical Behavior and n.m.r. Results above the Glass Transition

Above the glass transition, however, the nuclear magnetic resonance data show that a very different situation prevails and the amorphous regions then achieve considerable flexibility. It would therefore be expected that the n.m.r. measurements (which show this flexibility in detail) would reflect the changes in modulus shown by the mechanical measurements. The n.m.r. results for samples of different crystallinity and orientation will now be discussed. Four samples have been compared in detail, two samples of polymer chip, heat-crystallized at 160° C.

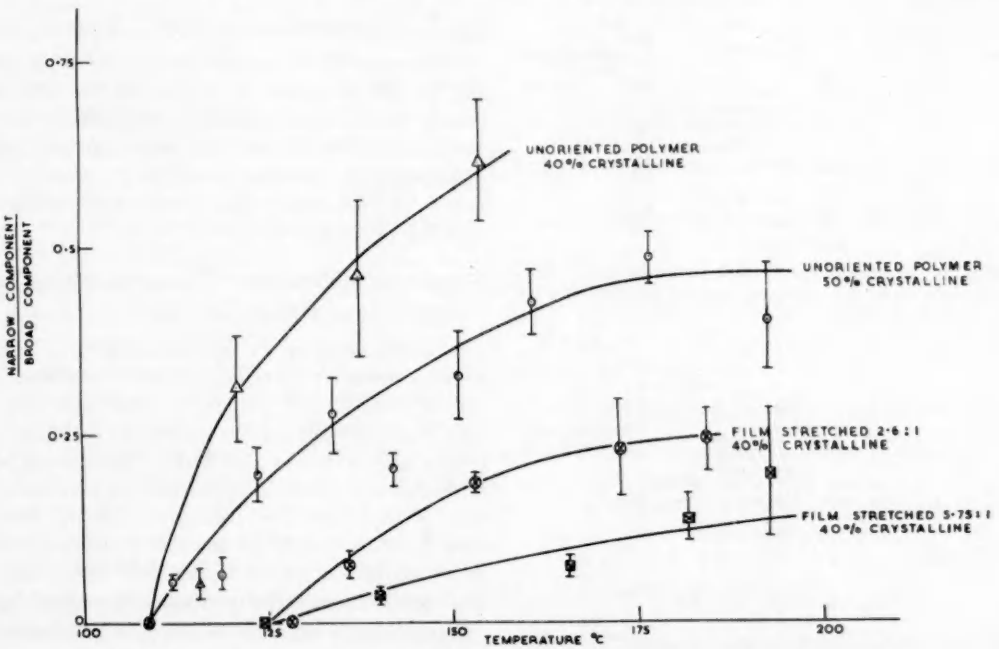

Fig. 10. Comparison of ratio of narrow to broad component for samples of varying crystallinity and orientation.

and 200° C. to give unoriented samples of 40% and 50% crystallinity, and two oriented samples, one very highly oriented, the other only partially oriented, which were subsequently heat-crystallized to about 40% crystallinity.

The most significant n.m.r. results are given in Figure 10, which shows the ratios of the intensities of the narrow and broad components of the n.m.r. signals in the different samples.

It can be seen that the proportion of the narrow component decreases, first with increasing crystallinity and second with increasing orientation.

The decrease of the narrow component with increasing crystallinity is an expected result, as it would not be expected that large scale reorientation and possibly diffusion of the molecules could occur in other than the noncrystalline regions. The decrease in the narrow component with increasing orientation is also capable of a fairly straightforward explanation. In a highly oriented crystalline sample it seems likely that most of the noncrystalline material will be highly oriented to the extent that the molecules will always have their chain orientation parallel to the direction of stretching. Such orientation would prevent reorientation of the molecules about axes other than the molecular axis, i.e., it would be expected that the molecular motions would be confined to hindered rotations about the chain axis. These hindered rotations would reduce the second moment by a factor of about four but would not be sufficient to give the very narrow line which has been observed. Confirmation has been obtained for this point by measuring the anisotropy of the broad component in oriented samples with sheets of film and varying the direction of the magnetic field with respect to the axis of orientation [19].

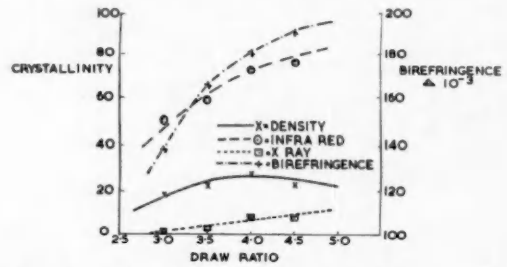

Fig. 11a. Crystallinity and other parameters as a function of draw ratio for oriented samples of PET. Yarn drawn over heated pin.

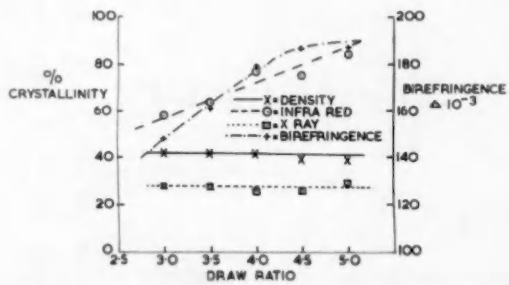

Fig. 11b. Crystallinity and other parameters as a function of draw ratio for oriented samples of PET. Yarn drawn over heated pin followed by heated plate.

These n.m.r. results can be compared with the results showing the influence of crystallinity and orientation on the dynamic mechanical properties above the β-transition. As one would expect, the increase in the high temperature modulus of unoriented samples with increasing crystallinity is directly related to the decrease in mobility of the polymer as shown by the n.m.r. data. It also appears that the increase in modulus due to orientation (although this again may be partly a pure orientation effect, as at room temperature) is also due to considerable restriction of the molecular mobility itself due to orientation and crystallization.

Characterization of PET Fibers

Discussion of the characterization of PET fibers will be divided into three parts. In the first part, results on the measurements of crystallinity will be discussed, in the second part molecular orientation measurements, and finally the implications of the results of both these types of measurement for the drawing of PET filaments.

Comparison of Crystallinity Measurements by X-ray, Infrared, and Density Techniques

A comparison of X-ray, infrared, and density measurements on fibers of different crystallinity and orientation has been made. A detailed account of this work has been given elsewhere [4], and the results will be summarized here. The starting point in this sort of comparison has been to take the view that by definition the crystallinity of the fiber is directly related to the presence of three-dimensional order as determined by X-ray diffraction. Clearly this view is open to the question of the exact degree of three-dimensional order required, i.e., the minimum number of adjacent unit cells required to give a discrete X-ray reflection. Attempts are being made

to investigate this point separately, but here it will be assumed that the X-ray measure of crystallinity is the ratio of the total integrated intensity of the X-ray diffraction maxima, typical of three-dimensional order, to the intensity of the diffuse halo due to the noncrystalline material. This measure of crystallinity, then, has been compared with that obtained from density and infrared measurements.

It has been discussed in detail above how in the infrared spectrum of PET one set of absorptions characterizes the material in the *gauche* configuration.

In some previous investigations [2] the intensity of a convenient absorption (that at 898 cm.$^{-1}$) has been used to determine the so-called amorphous content. All these various treatments of amorphous unoriented polymer will reduce the intensity of this absorption. The decrease in the intensity of this band can therefore be used as a measure of the decrease of amorphous content. It is convenient, for purposes of easy comparison, to convert this to a measure of the crystallinity of the sample, and this will be called the infrared measure of crystallinity. The density measure of crystallinity is another somewhat arbitrary measure of crystallinity and is obtained from the measured over-all density using the density of the crystalline material calculated from the X-ray crystal structure and assuming that the density of the noncrystalline material remains constant even when the polymer is oriented.

For this comparison a series of PET fibers was manufactured by applying varying stretching and heat-crystallizing treatments to the original melt-spun filaments of zero crystallinity and very low molecular orientation.

The results are summarized in Figure 11. There are two points which can be made immediately. First, the infrared measure of crystallinity is very much higher than the X-ray measure and, in fact, correlates closely with the increase in molecular orientation as determined by the birefringence. This is an expected result, since the drawing process will tend to produce fully extended *trans* configurations without necessarily producing crystallinity.

Second, there is the comparison between crystallinities measured by density and X-rays. Here again, there is no definite correlation, but this result could not be predicted and it suggests that it is incorrect to assume that the noncrystalline material in oriented fibers possesses a constant density equal to that of amorphous unoriented polymer. Taking the X-ray measure of crystallinity as the correct one, and the density of the crystalline regions as that calculated from the crystal structure, the density of the noncrystalline material can be calculated. The results suggest that the density of the noncrystalline material builds up to a value of 1.355 g./cm.^{3} and then remains remarkably constant. This suggests that the forces applied during the drawing processes can compress the polymer to a fixed extent, quite apart from the increase in density due to crystallization.

Molecular Orientation Measurements

The complete characterization of partially crystalline fibers requires that we estimate the orientation of the crystalline and noncrystalline regions separately, as well as obtaining their relative proportions, i.e., the crystallinity.

In the case of PET the molecular orientation has been measured using two methods [10], the optical birefringence of the polymer and the optical dichroism of dichroic dyestuffs incorporated in the polymer at the melt-spinning stage. From these measurements two orientation factors can be obtained.

1. Orientation factor for visible dichroism of dye molecules

$$\phi_D = \frac{D_\parallel - D_\perp}{D_\parallel + 2D_\perp} = \frac{a_1 - a_2}{a_1 + 2a_2}\left(1 - \tfrac{3}{2}\,\overline{\sin^2\alpha}\right)$$

where a_1 = absorption of polarized light along principal axis of dye molecule;
a_2 = absorption perpendicular to principal axis;
α = angle between principal axis of dye molecule and fiber axis.

2. Orientation factor derived from refractive indices (birefringence)

$$\phi_o = \text{birefringence } \Delta_n = k(\sigma_1 - \sigma_2)\left(1 - \tfrac{3}{2}\,\overline{\sin^2\alpha'}\right)$$

where σ_1 = principal polarizability of the molecular chain;
σ_2 = polarizability in a plane perpendicular to principal polarizability σ_1;
α' = angle between principal polarizability and the fiber axis.

It can be seen that there is a formal correspondence between the expressions for the orientation factors based on dichroism and birefringence, and in fact

both orientation factors are comparable in that they reflect the orientation of the polymer chains in a similar manner. The angles α and α' are in both cases the angle between an axis perpendicular to the plane of the polymer molecules and the fiber axis.

In an amorphous sample, orientation factors derived from dichroism and birefringence would always be equivalent. The onset of crystallinity during the drawing process, however, leads to a more complicated situation, since on account of their large size the dye molecules would be expected to be present only in the noncrystalline regions. This expectation is confirmed by the comparison of the orientation factors for dichroism and birefringence shown in Figure 12. These results were obtained by taking a series of yarns drawn to a series of draw ratios as with the yarns used for the crystallinity measurements described previously.

It can be seen the graph consists of two nearly straight portions with an abrupt change of slope. X-ray measurements show that this is due to the comparatively sudden onset of crystallization at a draw ratio of about three. Above this draw ratio the dichroism relates only to the orientation of the noncrystalline regions. These regions are thus shown to be less well oriented than the crystalline regions. This is perhaps an expected result, since the noncrystalline regions will contain all entanglements and non-ordered molecules.

The general picture which emerges from these results, then, is that at low draw ratios a yarn of high orientation and little or no crystallinity is produced. This was confirmed by measurement of shrinkage in boiling water, shown in Figure 13. It can be seen that at low draw ratios, where there is low crystallinity, the yarns shrink back to their original length, or even less than that. Figure 13 also shows the close connection between changes in dichroism and shrinkage, and indicates that it is reasonable to assume that both the dichroism and the shrinkage primarily reflect the disorientation of the noncrystalline regions of the fiber.

The Drawing of PET Filaments

The essential feature of the drawing process in PET is the sigmoid shape of the stress–strain curves [13]. Typical drawing curves exhibiting this are shown in Figure 14a. The final rise in modulus shown by these curves implies that reinforcement occurs, and it is of some interest to consider how this arises at a molecular level. The theory of Treloar [15] shows that the sigmoidal stress–strain curve can be produced by a network of long-chain molecules. There are three possible mechanisms for forming the locking points of such a network: first, entanglements; second, chemical cross-links; and third, the formation of crystalline regions.

It would appear from the low crystallinities of fibers drawn to low draw ratios that the principal

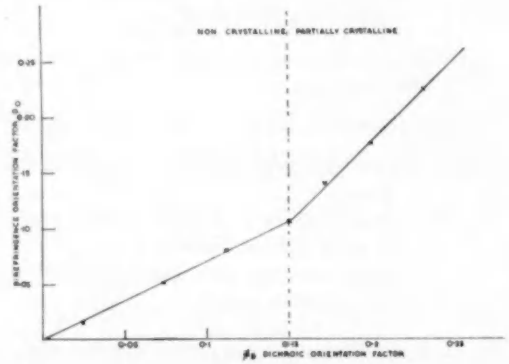

Fig. 12. Comparison of orientation factors for dichroism and birefringence.

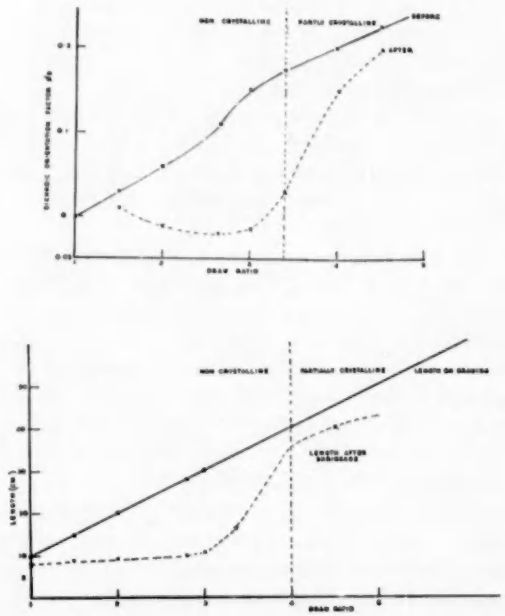

Fig. 13. Shrinkage results for PET fibers of different draw ratio.

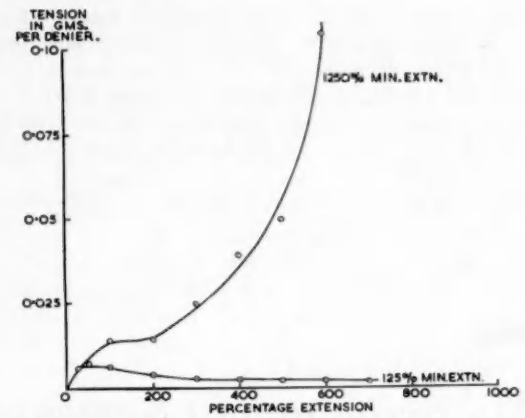

Fig. 14a. Drawing of amorphous PET at 97° C.

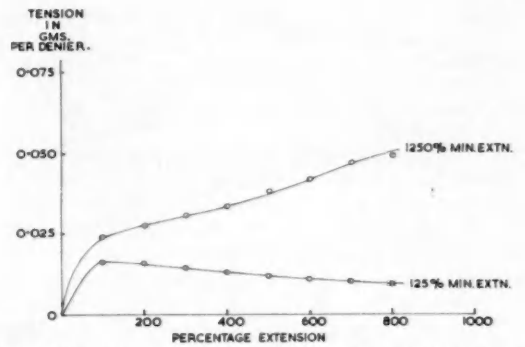

Fig. 14b. Drawing of poly(ethylene methyl terephthalate) at 61° C.

cause of reinforcement in polyesters is not the formation of crystalline regions, but the presence of entanglements, since chemical cross-links do not occur. Independent evidence for the existence of such entanglements has come from the n.m.r. measurements, where the large second moments at low temperatures indicate the close approach of some of the hydrogen atoms.

It had previously been considered that the reinforcement occurring in the drawing process arises from stress-induced crystallization. Although the onset of crystallization may well increase the reinforcement, and this is certainly true at high draw ratios, it is clear that it is not essential to it. This point has been confirmed by the production of oriented fibers of poly(ethylene methyl terephthalate), which is a noncrystalline polymer (Figure 14b). Here the X-ray measurements show that the fibers are noncrystalline, although considerable molecular orientation is produced and the density increases on drawing from 1.17 to 1.2 g./cm.[3]

Conclusion

In this paper the application of several techniques of molecular-structure determination to PET polymer and fibers has been considered. Three main points have been discussed: the general interpretation of the dynamic mechanical transitions; the characterization of PET fibers for crystallinity and orientation; and the influence of crystallinity and orientation on mechanical properties and in determining the drawing behavior of PET filaments. The principal conclusions may be summarized as follows.

First, the n.m.r. and infrared work suggests that all the large scale molecular motions set in above the β-transition, and that at room temperature the amorphous regions of polyethylene terephthalate are effectively rigid. This explains the comparatively high room temperature modulus and the comparatively small effect of crystallinity on the room temperature modulus. Orientation, however, as we would expect for a crystalline solid, is very important in determining the room temperature modulus. Above the glass transition, the mechanical properties are affected appreciably by both crystallinity and orientation. As one would expect from the n.m.r. data, crystallinity is now very important and the n.m.r. results show that the changes we find in the mechanical properties are directly reflected in the changes in the extent of molecular mobility.

Finally it has been shown that the characterization of polyethylene terephthalate fibers requires an adequate understanding of the role of the noncrystalline regions. Crystallinity, as such, appears to play a less important part than the orientation and composition of the noncrystalline material in determining much of the behavior of this polymer.

Literature Cited

1. Bateman, J., Richards, R. E., Farrow, G., and Ward, I. M., *Polymer* **1**, 63 (1960).
2. Cobbs, W. H. and Burton, R. L., *J. Polymer Sci.* **10**, 275 (1953).
3. Farrow, G., McIntosh, J., and Ward, I. M., *Makromol. Chem.* **36**, 147 (1960).
4. Farrow, G. and Ward, I. M., *Polymer* **1**, 330 (1960).
5. Grime, D. and Ward, I. M., *Trans. Faraday Soc.* **54**, 595 (1958).
6. Land, R., Richards, R. E., and Ward, I. M., *Trans. Faraday Soc.* **55**, 225 (1959).
7. Marsden, P. J. and Foster, E. L., unpublished work.

8. Miller, R. G. J. and Willis, H. A., *Trans. Faraday Soc.* **49**, 433 (1953).
9. Miller, R. G. J. and Willis, H. A., *J. Polymer Sci.* **19**, 485 (1956).
10. Patterson, D. and Ward, I. M., *Trans. Faraday Soc.* **53**, 1516 (1957).
11. Reddish, W., *Trans. Faraday Soc.* **46**, 459 (1950).
12. Robinson, D. W., *J. Sci. Instr.* **32**, 2 (1955).
13. Thompson, A. B., *J. Polymer Sci.* **34**, 741 (1959).
14. Thompson, A. B. and Woods, D. W., *Trans. Faraday Soc.* **52**, 1383 (1956).
15. Treloar, L. R. G., "The Physics of Rubber Elasticity," 2nd Ed., London, Oxford University Press, 1958, Chapter 4.
16. Van Vleck, J. H., *Phys. Rev.* **74**, 1168 (1948).
17. Ward, I. M., *Trans. Faraday Soc.* **56**, 648 (1960).
18. Hearman, R. F. S., *Advances in Physics* **5**, 323 (1956).
19. Farrow, G. and Ward, I. M., *Brit. J. Appl. Phys.* **11**, 543 (1960).

Manuscript received November 28, 1960.

Dimensional Changes in Multicomponent Systems of Fabrics: A Theoretical Study

Joel Lindberg

Swedish Institute for Textile Research, Gothenburg, Sweden

Abstract

In a system of two fabrics attached to each other, dimensional changes may give rise to compression and extension stresses in the plane of the fabrics. High stresses may lead to buckling of the compressed fabric, which may impair the appearance of the system. The paper discusses three different types of dimensional change occurring in practice, namely changes due to external stresses, changes due to setting operations, and changes due to releasing frozen-in internal stresses or producing internal stresses by swelling.

Each of these dimensional changes is defined. Equations are derived which, for a smooth system, give the relation between the initial difference in dimension between the fabrics, dimensional changes taking place after the fabrics are attached to each other, and certain mechanical properties of the fabrics. Three fundamental cloth parameters are shown to govern the results, namely formability, settability, and dimensional stability.

Introduction

Only rarely is a fabric used strictly as a fabric; most frequently it is a component of a garment. Generally a garment is constructed of several parts, which are joined together by seams. In a normal seam there are always two components, namely sewing thread and fabric. Two fabric parts which are joined may be cut from the same piece but in different directions. However they may also be taken from different fabrics, e.g., when an outer fabric is joined to an interlining. Therefore there will be at least three components—sewing thread and two fabric components. The fabric components may be similar or different. Only the interaction between the fabric components is considered here, but the analysis could easily be extended to include the interaction between sewing thread and fabric.

The behavior of a two-component system will be different from that of either component. Dimensional changes occurring in the components will interact with each other and produce internal stresses in the system, which could cause deformation of the components and affect the appearance of the system, for instance by producing seam puckering.

It is characteristic for a multiple component system that there are one or more layers of fabric between two points of attachment (Figure 1). This is true for one stitch but also holds over any area. A collar is made up of at least two layers (Figure 2).

Dimensional changes can produce tension along the seams, but also across the collar, over the length and the width. A two-component system can therefore have a very variable geometry, depending on the direction in which one studies the interaction between the two components.

Dimensional changes in the system could be produced or occur in different ways. For example, internal "frozen-in" tension could be relaxed at higher humidity or temperature, fibers could swell causing contraction or expansion, external forces could be applied during sewing, or when a pucker is pressed down. It is evident that interaction between the components in a multicomponent system is very important in sewing and pressing. A more general treatment of garment manufacturing problems is published elsewhere [5].

Forces and Deformations in a Simple Two-Component System

Assume that two fabric parts are joined together as in Figure 3. The two parts, denoted by c and e, have lengths l_e and l_c, and $l_c \geqq l_e$. Part e will then be under the influence of extension forces and part c of compression forces. These forces will be in the direction of the plane of the fabrics. Any bending moment at the joints is disregarded. It is now of interest to see what will happen to the system when $l_c > l_e$.

If a thin plate is compressed in the direction of the plane of the plate, it will buckle if the force exceeds the critical buckling force [2, 3, 4]. Part c would then separate from e as in Figure 3, and cause puckering. To avoid this, the compressional force in c must be below the critical buckling force [5]. It is assumed that the fabric behaves like a completely elastic material and that there is a rectilinear relation between load and extension and also

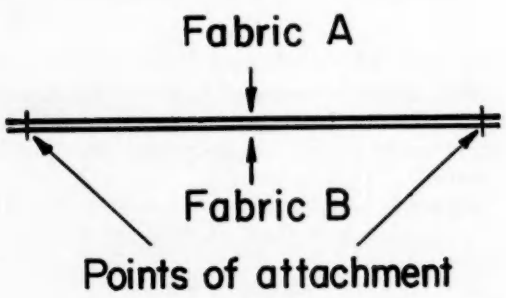

Fig. 1.

Fig. 2.

between load and compression. To simplify the problem it is assumed that any contraction or extension in the other direction can be neglected. It is further assumed that the buckling load for the fabric follows Euler's equation for buckling of bars rigidly supported at both ends. The critical buckling load, P_{cr}, is

$$P_{cr} = \frac{4\pi^2 b_c}{l_c^2}$$

where b_c is the bending stiffness of part c or

$$P_{cr} = \text{const.} \cdot b_c$$

since l_c can be regarded as constant. Figure 4 shows a buckling curve for an ideal case.

As can be seen from the curve, the fabric can be compressed a distance B before it buckles. This distance is called the buckling compression. If the stiffness for extension and compression are equal and denoted by T_c, the buckling compression

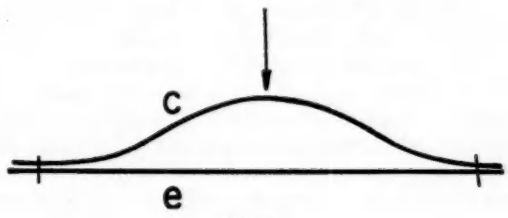

Fig. 3.

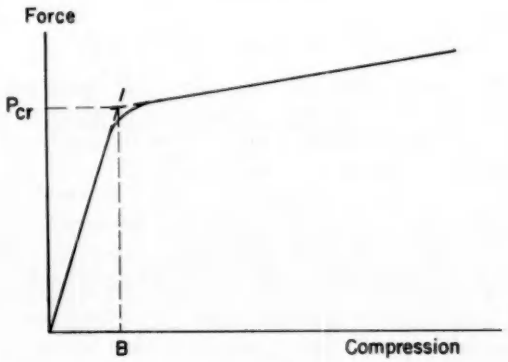

Fig. 4.

can be written:

$$B = \frac{P_{cr}}{T_e} = \text{const.} \cdot \frac{b_c}{T_c}$$

But

$$b_c = E_b \frac{t^3 h}{12}$$

and

$$T_c = E_T t h$$

where E_b and E_T are the moduli for bending and extension–compression respectively, t the thickness and h the width of the fabric. We then have

$$B = \frac{\text{const.}}{12} \cdot \frac{E_b}{E_T} t^2$$

The expression $\frac{b_c}{T_c}$ can be defined as the formability of the fabric [5] and is denoted by F. $B = \text{const.} \cdot F$. We then have

$$F = \frac{b_c}{T_c} = \frac{E_b}{E_T} \cdot \frac{t^2}{12}$$

For a homogenous isotropic material the formability is directly dependent on the thickness.

Dimensional Changes in the System

Assume that c and e are two different materials with bending stiffnesses of T_c and T_e and formabilities F_c and F_e, all values relating to the direction in which the forces in the system are acting. It is further assumed that the total change of length in c and e that could occur in different ways, including mechanical compression, is Δl_c and Δl_e. Shrinkage and compression give negative values. The lengths of c and e after these changes are then

$$l_c + \Delta l_c = l_c'$$

and

$$l_e + \Delta l_e = l_e'$$

We now have the following criteria for the appearance of the system: $l_c' > l_e'$ gives buckling of c; $l_c' < l_e'$ gives buckling of e. (The indexes should then be reversed.)

$l_c' = l_e'$ gives a smooth system. It should be noted that a very slight difference between l_c' and l_e' will give noticeable buckling. The only condition of interest here is $l_c' = l_e'$. We then have

$$l_c + \Delta l_c = l_e + \Delta l_e$$

or

$$l_c - l_e = \Delta l_e - \Delta l_c$$

This equation could be expressed in relative, instead of absolute, measures. By introducing the definitions

$$\alpha = \frac{l_c - l_e}{l_e}; \quad D_c = \frac{\Delta l_c}{l_c}; \quad D_e = \frac{\Delta l_e}{l_e}$$

into the equation above, it becomes

$$\alpha = D_e - (1 + \alpha) D_c$$

In most cases α is small and therefore

$$\alpha = D_e - D_c \tag{1}$$

which only expresses the rather self-evident fact, that the difference between the changes of length of c and e must be equal to the initial difference in length of c and e in order to get a smooth system.

Different Types of Dimensional Change

It is possible to distinguish between three different types of length change in the system.

1. The length of any part may be changed by means of external mechanical forces. This change of length is noted by Δl_{cP} and Δl_{eP}. There will be internal tension in the system.

2. The change in length may be caused by relaxation of tensions, or a setting operation in the compressed or extended state. The change is noted by Δl_{cS} and Δl_{eS}, and this change should be measured when the internal tension of the fabric is zero.

3. A change of length, which may occur before, during, or after any setting processes, caused by swelling, delayed recovery, or release of temporary set. The change is noted by Δl_{cD} and Δl_{eD}.

These different types of length change will generally occur in different combinations in systems in which the two parts may or may not have the same lengths from the beginning. In all cases, however, except when the system is set and there is a complete relaxation of internal stresses, Case 1 will be prevalent. This case will therefore be treated first.

Effect of External Mechanical Forces

Such forces are produced either by deliberately making the two parts in the system of different length or by length changes taking place in the system.

We have

$$D_c = D_{cP}; \quad D_e = D_{eP}$$

and

$$-T_c D_{cP} = -P_c$$
$$T_e D_{eP} = P_e$$

and as there is force equilibrium between c and e

$$P_c = -P_e \quad \text{and} \quad T_c D_{cP} = -T_c D_{cP}$$

These expressions can be combined with Equation 1 thus

$$\alpha = -D_{cP}\left(1 + \frac{T_c}{T_e}\right)$$

In order to have a smooth system it is necessary to fulfill the condition

$$-D_{cP} \leqq B = kF_c \quad (k = \text{const.})$$

that is, the compression must not exceed the buckling compression. Therefore

$$\alpha \leqq kF_c\left(1 + \frac{T_c}{T_e}\right) \tag{2}$$

If the two fabrics are equal, $T_c = T_e$, and we have

$$\alpha \leqq 2kF_c \tag{3}$$

These formulas will determine the precision with which two fabrics need to be stitched together. Due to shortcomings on the part of machines and operators there will always be some length differences between two fabrics either along one seam or between two neighboring seams. The formulas also may be used for a fabric and a sewing thread forming the other part of the system.

Subsequent Dimensional Changes in the Fabric System

In Case 3 a number of causes for dimensional changes in fabrics were mentioned. Whatever the causes for changes are, excessive changes will cause puckering and cockling of garments, which will impair the appearance. As a result of dimensional changes stresses will be produced in the two parts of the system. Therefore, Case 3 will be treated in combination with Case 1.

We can write

$$D_e = D_{eP} + D_{eD} \quad \text{and} \quad D_c = D_{cP} + D_{cD}$$

Equation 1 takes the form

$$\alpha = D_{eP} + D_{eD} - D_{cP} - D_{cD}$$

If the expression above is combined with Equation 2 we obtain

$$\alpha \leqq kF_c\left(1 + \frac{T_c}{T_e}\right) - (D_{cD} - D_{eD}) \tag{4}$$

or for two equal fabrics

$$\alpha \leqq 2kF_c - (D_{cD} - D_{eD}) \tag{5}$$

If the changes of length in both fabrics are equal in sign and value, the appearance of the system will not be affected.

This is important to note because sometimes the opinion is put forward that moderate shrinkage of cloth will help in tailoring.

A very common special case is when $\alpha = 0$. We then have

$$D_{eD} - D_{cD} \leqq kF_c\left(1 + \frac{T_c}{T_e}\right) \tag{6}$$

This expression gives the tolerance limits for the change of length in a two-component system, for instance, in a shirt collar.

A shirt collar generally is made up of a stiffening interlining and the outer fabric. It is not uncommon for the collar to be deformed by puckering or cockling after the first washing, which might cause the dimensional changes. By c and e we have indicated only which fabric takes up the compression or the extension. If we indicate one of the fabrics by a prime mark we can have two cases for Equation 6.

$$D_{eD}' - D_{cD} \leqq kF_c'\left(1 + \frac{T_c'}{T_e}\right) \tag{6a}$$

and

$$D_{cD} - D_{eD}' \leqq kF_c\left(1 + \frac{T_c}{T_e'}\right) \tag{6b}$$

depending on which fabric is compressed. Since $F_c = \frac{b_c}{T_c}$, we can also write

$$D_{eD}' - D_{cD} \leqq kb_c'\left(\frac{1}{T_c'} + \frac{1}{T_e}\right)$$

and

$$D_{cD} - D_{eD}' \leqq kb_c\left(\frac{1}{T_c} + \frac{1}{T_e'}\right)$$

Since it was assumed that $T_e' = T_c'$ and $T_e = T_c$ we can divide the equations above and obtain

$$\frac{D_{eD}' - D_{cD}}{D_{cD} - D_{eD}'} = \frac{b_c'}{b_c} \tag{7}$$

The tolerance limits for acceptable appearance depend on the direction of the relative change and have the same ratio as the bending stiffnesses of the two fabrics. It is evident from this expression that the relative change of length must occur in such a way that the stiffer fabric is compressed [5].

By having the outer fabric, for instance, in a shirt collar shrink moderately it may be possible to obtain a tight fit over the interlining, which might help to eliminate irregularities in tailoring.

Fullness and Setting

A common technique in the heavy clothing industry is to introduce fullness along the seams and then to ease in this fullness by pressing. This means that the two parts, originally of different length, are made to coincide during the sewing operation, either by an overfeed, or by stretching the shorter one. Puckering will occur in the longer part when the system is released. These puckers are removed by steam pressing, which is a form of setting.

One example, typical for this type of operation, is how the roundness of the shoulders is obtained in making a jacket. The opening of the sleeve is cut wider than the hole in the body. The two parts are stitched together using an overfeed technique. The fullness thus created is removed by pressing, and consequently a certain roundness is obtained. It is quite obvious from the example given that the exact pattern to which the sleeve should be cut will depend on the degree of overfeed one decides to use. Since these patterns are made up sometimes even before the cloth is bought, it will be of major importance to know or be able to specify fabric properties influencing the result of the operation described here. It is only under certain conditions, namely, that it is possible to make the fabric smooth. The simplified model should now be used to analyze these conditions.

The degree of fullness will be denoted by the symbol α, which has been defined previously. We can now write Equation 1.

$$\alpha = D_{eP} + D_{eS} + D_{eD} - D_{cP} - D_{cS} - D_{cD}$$

where

$$D_e = D_{eP} + D_{eS} + D_{eD}$$

and

$$D_c = D_{cP} + D_{cS} + D_{cD}$$

The symbols D_{cS} and D_{eS} indicate how much of the compression or extension can be set. The value of D_{cS} and D_{eS} will, however, depend on the amount of compression or extension before setting.

It is therefore convenient to introduce another definition of setting. Thus, settability is the ratio between the change of length given the fabric before setting, Δl_b, to the change of length retained after setting and releasing, Δl_a. If the settability is denoted by S_c and S_e we have

$$S_c = \frac{\Delta l_{ca}}{\Delta l_{cb}} \quad \text{and} \quad S_e = \frac{\Delta l_{ea}}{\Delta l_{eb}}$$

In general, setting of a fabric will, in itself, cause a change in dimensions even if the fabric is free from tension [1]. This change can be determined if the fabric is set tensionless. The value of Δl_a obtained when setting in a compressed or extended state should be corrected for the value obtained when setting tensionless. This latter value should be included in the term D_D. The settability may then be regarded as a material constant depending primarily on the type of fiber.

Assume that c and e differ so much in length that c has buckled. A pressure perpendicular to the plane of the system is now applied (Figure 3). Part c will then be compressed and e extended until they are equal in length and the system is flat (if α is not too large). Assume further that there is a force equilibrium between c and e in the compressed flat state, and that the compression and extension are D_{cx} and D_{ex}. We then have

$$S_c = \frac{D_{cS}}{D_{cx}} \quad \text{and} \quad S_e = \frac{D_{eS}}{D_{ex}}$$

If α is the difference between c and e when they are joined together, and there is a change of length before setting, it is necessary to split up D_{eD} and D_{cD} into D_{eDb} and D_{cDb}, which denote changes before setting, and into D_{eDa} and D_{cDa}, which denote changes after or during setting. We then have

$$\alpha + (D_{eDb} - D_{cDb}) = D_{eP} + D_{eS} + D_{eDa} - D_{cP} - D_{cS} - D_{cDa} = D_{ex} - D_{cx}$$

Now we assume that the stiffness for extension and compression before setting are T_{cb} and T_{eb}, and after setting are T_{ca} and T_{ea}. At force equilibrium we have

$$-T_{cb}D_{cx} = -P_c; \quad T_{eb}D_{ex} = P_e; \quad -P_c = P_e$$

We can now obtain

$$D_{eS} - D_{cS} = \frac{\alpha + (D_{eDb} - D_{cDb})}{1 + \frac{T_{cb}}{T_{eb}}} \left(S_c + S_e \frac{T_{cb}}{T_{eb}} \right)$$

and as before

$$D_{eP} - D_{cP} \leqq kF_c \left(1 + \frac{T_{ca}}{T_{ea}} \right)$$

These expressions can be combined to

$$\alpha \leqq \frac{\left(1+\frac{T_{cb}}{T_{eb}}\right)\left[kF_c\left(1+\frac{T_{ca}}{T_{ea}}\right)-(D_{cDa}-D_{eDa})\right]}{(1-S_c)+(1-S_e)\frac{T_{cb}}{T_{eb}}} - (D_{cDb}-D_{eDb}) \quad (8)$$

If the fabrics are equal

$$S_c = S_e; \quad T_{cb} = T_{eb}; \quad T_{ca} = T_{ea}; \quad D_{cDb} = D_{eDb}$$

and we obtain the following special case

$$\alpha \leqq \frac{2kF_c - (D_{cDa} - D_{eDa})}{1 - S} \quad (9)$$

which gives the relation between degree of fullness, formability, settability, and dimensional stability, when two equal fabrics are joined together.

If $S \to 1$, $\alpha \to \infty$. The value of α, however, is limited by the amount of compression and extension c and e can take up when the system is pressed flat. This upper limit depends on the formability and maximum pressure the fabric can stand before surface changes take place.

If the assumptions about the linearity of the load-elongation and compression curve and the absence of larger hysteresis effects are correct, Equation 8 may be used to predict the degree of overfeed or fullness that can be used with any particular cloth and accordingly the exact pattern that should be cut for any particular garment.

It was assumed previously that there was force equilibrium between c and e when c was pressed down before setting, and the derivation of Equation 8 was based on this assumption. It is, however, not certain that such a force equilibrium exists. Friction against the support may prevent extension of e and the system may also be deliberately stretched during pressing and setting. A flat system could even be produced by stretching alone. A change in the length of the system is equal to a change in e. This change ought to be easily determined. As previously it is denoted by D_{ex}. We then have

$$D_{eS} - D_{cS} = \alpha + (D_{cDb} - D_{eDb}) - D_{ex}(S_c - S_e)$$

and Equation 8 takes the form

$$\alpha \leqq \frac{kF_c\left(1+\frac{T_{ca}}{T_{ea}}\right)-(D_{cDa}-D_{eDa})-D_{ex}(S_c-S_e)}{1-S_c} - (D_{cDb}-D_{eDb}) \quad (10)$$

This equation gives the interesting information that, if the settabilities of the two fabrics are equal, the result is independent of the force equilibrium. The settabilities are assumed to be independent of the degree of deformation.

Conclusion

Very little of a scientific nature has been written in the field of clothing technology, and most textile scientists and technologists seem to be rather unaware of the problems in this field, although the garment field represents the biggest outlet of fabrics.

This paper does not claim to be a thorough study of the field. Its purpose is to show how simple fabric mechanics can be used to explain and better understand certain problems in garment making. If we take for instance, Equation 9 and assume that the values for D are zero, two fabrics with the same settability, but one only half as thick as the other, will, according to the expression given for the formability, give an α four times as high for the thicker fabric than for the thinner. This explains from a theoretical point of view the well-known fact that thinner fabrics are more difficult to tailor than thicker ones. But the equations also indicate what may be done, still from a theoretical point of view, to improve the performance of thin fabrics.

It is hoped that this paper will stimulate further theoretical and experimental work in this very important field.

Acknowledgment

My thanks are due to Dr. Bertil Olofsson for helpful suggestions and advice regarding the mathematical derivations.

Literature Cited

1. Cednäs, Margareta, to be published.
2. Dahlberg, B., TEXTILE RESEARCH JOURNAL **31**, 94–99 (1961).
3. Dahlberg, B., and Eeg-Olofsson, T., *Meddelande från TEFO*, Nr. 2, 1958.
4. Lindberg, J., Behre, B., and Dahlberg, B., TEXTILE RESEARCH JOURNAL **31**, 99–122 (1961).
5. Lindberg, J., Waesterberg, L., and Svenson, R., *J. Textile Inst.* **51**, T1475–T1491 (1960).

Manuscript received October 4, 1960.

Letters to the Editor

Further Simplifications of the Vibraweigh Method

G. F. Bush Associates
Box 175, Princeton, N. J.
January 6, 1961

To the Editor
TEXTILE RESEARCH JOURNAL

Dear Sir:

The Vibraweigh Method [1] of calibrating a fiber vibroscope [1] without use of expensive microbalances or frequency oscillators, but only by the use of the instrument itself, that is, "self-calibration," depends primarily on the equation

$$w = k_s(R_2 - R_1) \qquad (1)$$

where w is linear density in g./cm., $k_s = k_c/(2f)^2(L_2^2 - L_1^2)$, R_2 and R_1 are vibroscope dial readings, L_2 and L_1 are fiber specimen gauge lengths for the R's in cm., f is fiber frequency, and k_c is fiber load/dial division.

By such self-calibration, the calibration curve of Figure 1 may be obtained so that the vibroscope may then be used for direct, linear determination of linear densities as small as 10^{-6} g./cm. (1 denier approximately).

A brief explanation of the Vibraweigh Method is as follows. Two readings, R_2 and R_1, of the same fiber at two different lengths, L_2 and L_1 (readily set by simple precision gauges), ideally give the linear density, w, directly and quickly. Two such determinations of w ideally, but three preferably, will produce the desired calibration curve of Figure 1.

In his original paper [1] the author recommended the determination of three R's and a plot of Figure 2 to establish more accurately the straight-line relationship of Equation 1. Now, because of a new simplification, namely the more accurate determination, by calculation, of R_0, only one R is required ideally instead of two. That is to say only one R is required ideally, but two are recommended for greater accuracy, whereas for the calibration curve of Figure 1 ideally two and preferably three were required; thus a considerable economy of time and errors obtains.

R_0 may be calculated as follows. From

$$P = P_0 + k_c R$$

where P_0 is the load in g. at $R = 0$, write

$$P_{50} = P_0 + k_c R_{50}$$

where P_{50} is the load in g. at $R = 50$, then

$$R_0 = -P_0/k_c = -P_{50}/k_c + R_{50}$$

For 0.0086 g./link of loading chain and 50 links load at $R = 50$ (a mere coincidence of numbers) and the additional weight of clamp unit equivalent to one link, $P_{50} = (0.0086)(980)(51) = 430$ dynes. For $k_c = 2.79$ dynes/division of dial, $R_0 = -430/2.79 + R_{50} = -104$.

The calculated value of R_0 is quite accurate, in fact more accurate than the straight-line points of

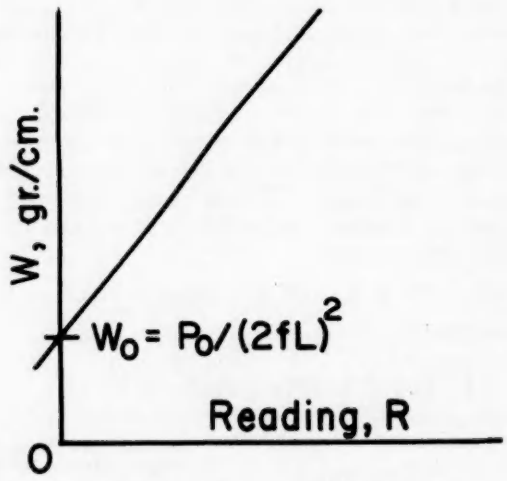

Fig. 1. Vibroscope calibration.

[1] A vibroscope is an electromechanical instrument for measuring rapidly the linear density of a single fiber or strand by vibrating it at its natural fundamental frequency, as for a string. Either length, load, or frequency may be varied in the approximate Equation 2, $w = P/(2fL)^2$ where w is the linear density in dynes/cm., P the load (or tension) in g., f the frequency in cps, and L the gauge length in cm.

Figure 2, which are more susceptible to instrument and personal errors.

It is again pointed out that all graphs of *any* linear density pass through R_o of Figure 2. This means, among other things, that this is a property common to *all* materials, but is subject, of course, to the assumptions inherent in the originating Equation 2. (One of the major assumptions is that the fiber is perfectly flexible, an assumption which is fairly tenable.)

In obtaining by the Vibraweigh Method the two or three points needed for the calibration curve of Figure 2, a check on the related plots of Figure 1 can be made by referring to the relationship

$$w_x = w_s(y_x/y_s) \qquad (3)$$

where w_x is the unknown linear density, w_s is a known, correct linear density, and the y's, as shown, are the ordinates of the graph for some constant length, L. For example, if it is known that the value of, say, 15 denier for w_s is correct (say as a standard, etc.), then the sloped line for a finer fiber, say of 7.5 denier, should pass through the midpoint of the ordinate, as shown in Figure 2.

Another observation not to be neglected is that all of the above applies if f, the frequency, and L, the length, are interchanged, i.e., instead of the frequency, f, being held constant while the length L is varied, the length L may be held constant while the frequency is varied. This will not apply linearly to the load, P, and either L or f.

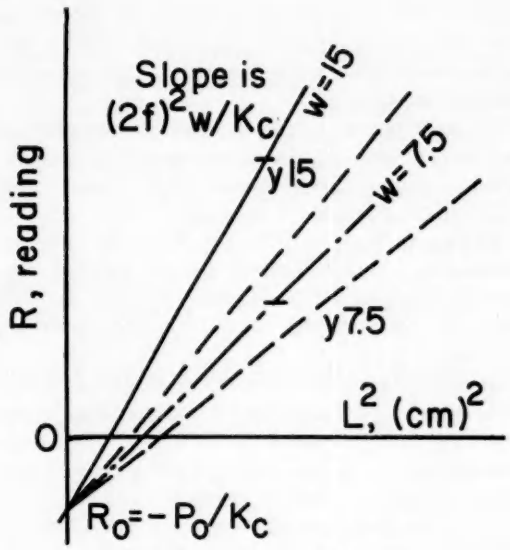

Fig. 2. R versus L^2.

Further developments, extending from the above, will be presented in a later paper.

Literature Cited

1. Bush, G. F., TEXTILE RESEARCH JOURNAL **28**, 89 (1958).

G. F. BUSH

Some Aspects of the Wash-and-Wear Problem

North Carolina State College
Raleigh, North Carolina
March 8, 1961

To the Editor
TEXTILE RESEARCH JOURNAL

Dear Sir:

The most important part of the wash-and-wear problem is what happens to the fabric or garment during the washing and drying process. An analysis of this particular problem throws some doubt on the crease recovery as being the only important factor in this respect.

I will deal only with the washing process, including the washing per se, dewatering, and any necessary after-treatment such as ironing or mangling. A number of changes in fabric or garment properties may occur during the washing process, but here I shall discuss only mussiness and seam puckering.

Mussiness and seam puckering can be defined as deviations from the smooth state of the fabric. There are two distinctive and different causes for mussiness in a fabric [5].

1. When inherent internal stresses in the fabric are released by heat and moisture, the fabric will pucker and become uneven if the internal stresses are unevenly distributed over the fabric. This is normally the case, because of imperfections in material and processing. The fabric will always tend to

attain a state of minimum potential energy. Thus, the aim must be to make the smooth state or any other desired state of the fabric that of the minimum potential energy.

In order to achieve this, internal stresses must be permanently relaxed, that is, permanently for conditions prevailing during the washing process. This elimination of stresses I shall call setting.

Drying in itself will largely "freeze-in" internal stresses by a cohesive setting, but on rewetting, this setting disappears [4]. Cohesive setting is what happens during ironing, which is, in effect, a drying process.

It is quite obvious that it is imperative to remove permanently all unevenness in stress distribution over the fabric, whether produced by the textile manufacturer or by the maker of the garment (generally produced in multicomponent systems). Because of the nature of the processes, it is exceedingly difficult to avoid uneven stress distribution during both textile manufacture and garment manufacture. Therefore, a simple setting process is needed that can be applied to the material more than once, that is, during both fabric manufacture and garment manufacture.

The type of mussiness described above will appear even when no mechanical treatment is involved, though such treatments will probably further it. This means, in effect, that this phenomenon is completely independent of the crease-recovery properties of the fabric and will need a different test method for evaluation.

2. When a fabric is subjected to mechanical deformation and fails to return to its original state, creases will appear which contribute to the mussiness of the fabric. The crease recovery for any particular fabric will depend first on the degree of deformation, and second on temperature, moisture, and recovery properties of the particular fabric.

The degree of deformation will depend on external conditions during the washing process and on the mechanical properties of the fabric, that is, on the extent to which the fabric itself can avoid taking up localized high strains. The mechanical properties that are of importance in this respect are bending stiffness and shearability. It should be noted that these properties may be changed very much in the change from a dry to a wet state [2].

The crease recovery of a fabric, with respect to the more or less permanent crease obtained, will depend largely on the degree to which the elastic forces of the fibers can overcome the restraining frictional forces [2]. Frictional forces and elastic forces are influenced by changes in temperature and moisture, and changes in these conditions will therefore affect the crease recovery. The elastic forces will depend on degree of deformation of fibers and on fiber stiffness, but since the fiber recovers from a higher to a lower deformation, the relevant stiffness will be that obtained by infinitely slow loading rate [2].

A very interesting observation was made last year at TEFO, Gothenburg, regarding crease recovery. If a creased fabric is dried, the creases are cohesively set and will remain set as long as temperature and humidity are not changed. If, however, the creased fabric, whether cohesively set or not, is taken through a number of moisture cycles, the creases will largely disappear [1]. Moisture cycles assist in the recovery from any deformation of a fabric and bring the fabric back to an equilibrium state along an exponential curve [3]. This method may provide a simple means for eliminating wrinkles introduced during the washing process, that is, the part of the mussiness discussed under 2 above. However, moisture changes will release frozen-in internal stresses and will produce the type of mussiness discussed under 1 above.

From the above discussion, it is obvious that the important thing is to set the fabric permanently to avoid mussiness of type 1. Whether any other changes of the fabric, like those produced by crease-resistant treatment, are needed depends on end-use, construction, and so on.

Most methods of treatment for producing crease resistance will involve permanent setting of fabrics apart from changing the mechanical properties of fibers. It can therefore be confusing to use crease-recovery measurements to evaluate wash-and-wear performance.

In short, my arguments can be summarized as follows:

1. New test methods are needed which can distinguish between mussiness of types 1 and 2.

2. Mussiness of type 1 is the more important and should be studied first. Such a study would involve different setting methods.

3. Recovery properties of fabrics during moisture cycles should be studied.

4. The relation between mechanical properties of fabrics and the actual deformation of fabrics under

certain external conditions, specifically random mechanical action, is important.

5. The significance for crease recovery of fiber stiffness at an infinitely slow loading rate should be investigated.

Literature Cited

1. Farnworth, A. and Lindberg, J., TEXTILE RESEARCH JOURNAL, accepted for publication.
2. Lindberg, J., Behre, B., and Dahlberg, B., TEXTILE RESEARCH JOURNAL **31**, 99 (1961).
3. Lindberg, J., Waesterberg, L., and Svenson, R., *J. Textile Inst.* **51**, T1475 (1960).
4. Olofsson, B., *J. Textile Inst.*, accepted for publication.
5. Williams, C. R., *Am. Dyestuff Reptr.* **48**, No. 13, 27 (June 29, 1959).

JOEL LINDBERG

Effects of Buffers on Formaldehyde-Curing of Amidoximate Hydrochloride of Partially Cyanoethylated Cotton

Faculty of Technology
Gumma University
Kiryu, Japan
March 8, 1961

To the Editor
TEXTILE RESEARCH JOURNAL

Dear Sir:

In the previous publications from our laboratory, it was reported that the hydrochloric acid scouring of the amidoximation products of partially cyanoethylated cotton fabrics not only prevents discoloration but brings about a catalytic action in the formaldehyde-curing by forming the amidoximate hydrochloride salt [1, 2]. However, there is some possibility that part of the amidoxime or hydroxamic acid groups between which the long intermolecular cross-links have been considered to be formed is subjected to hydrolysis by the split hydrochloric acid during the curing [3]. Moreover, a strong catalyst such as hydrochloric acid may cause unfavorable effects such as the formation of short formal cross-links between cellulose–OH groups or the hydrolyzing of the cellulose molecular chains. In the present study,

TABLE I. Effects of the Use of Buffers in Formaldehyde-Curing on Tensile Strength and Elongation

Sample	Nitrogen content, %	pH of padding solution	Tensile strength, Kg./cm.	Elongation, %
Unmodified cotton		uncured	7.88	13.2
Cyanoethylated cotton	2.62	uncured	9.08	13.5
Amidoximate acid-scoured subsequently, formaldehyde-cured	2.96	uncured	7.42	14.0
without buffer		7.00	5.57	12.7
with buffer				
sodium oxalate		6.16	6.08	14.7
sodium tartrate		6.60	5.95	12.6
sodium formate		6.45	5.80	13.0
sodium acetate		6.85	6.28	13.5

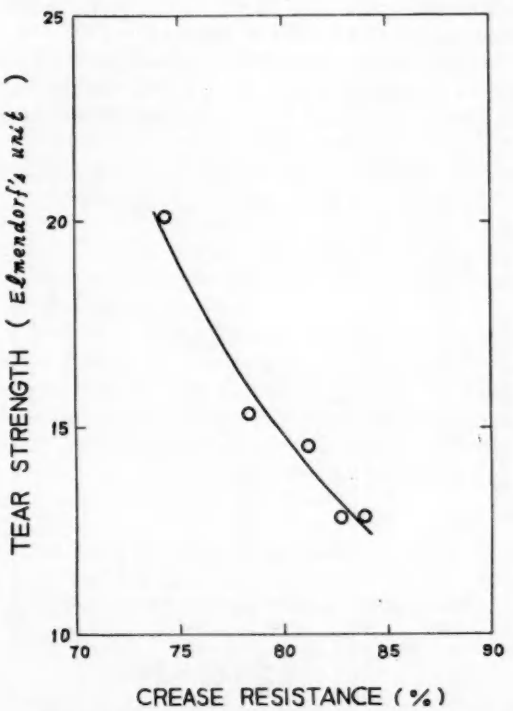

Fig. 1. Relation between tear strength and crease resistance.

TABLE II. Effects of the Use of Buffers in Formaldehyde-Curing on Tear Strength and Crease Resistance

Sample	Nitrogen content, %	Electrolytic dissociation constant of acid component in buffer salt at 20–25° C.* K_1	K_2	Tear strength, Elmendorf's unit	Crease resistance, %
Unmodified cotton		uncured		31.2	47.6
Cyanoethylated cotton	2.35	uncured		29.0	52.8
Amidoximate acid-scoured	2.83	uncured		22.3	62.8
subsequently, formaldehyde-cured					
without buffer				12.8	83.8
with buffer					
sodium oxalate		5.90×10^{-2}	6.40×10^{-5}	12.8	82.8
sodium tartrate		1.04×10^{-3}	4.55×10^{-5}	14.5	81.1
sodium formate		1.77×10^{-4}	—	15.3	78.3
sodium acetate		1.75×10^{-5}	—	20.1	74.3

* Cited from the "Chemical Handbook" (Chemical Society of Japan, 1958).

in order to obtain further improvements in the physical properties of cured fabrics, the moderation of the catalytic action of hydrochloric acid was attempted by adding 0.5% buffers to the neutralized 12% formaldehyde solutions used for padding before curing. As buffers, sodium salts of oxalic, tartaric, formic, and acetic acids were used. These 0.5% buffer solutions are 0.052–0.075 *N* solutions.

At first, using the partially cyanoethylated cotton fabrics containing 2.62% nitrogen, the partial amidoximation was carried out in the neutralized aqueous hydroxylamine salt as described in the previous report. The reaction products were washed with water, scoured by 0.3% hydrochloric acid (25° C., 30 min., and 200 liquor ratio) and then washed thoroughly with water. The nitrogen content of the products was 2.96%. The subsequent formaldehyde-curing was performed exactly as in the previous paper (10 min. and 115° C.). The tensile strength and elongation of the cured fabrics were measured and are shown in Table I. It appears that the pres-

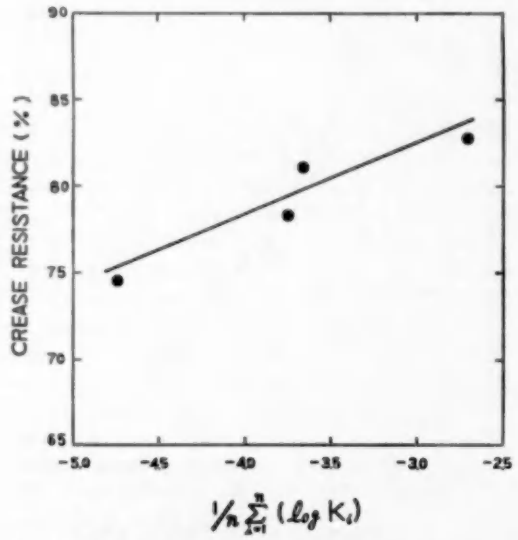

Fig. 2. Relation between crease resistance and log of geometric mean of electrolytic dissociation constants.

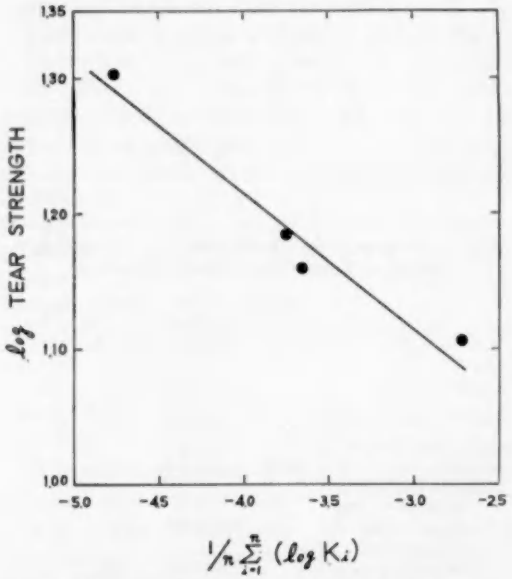

Fig. 3. Relation between log tear strength and log of geometric mean of electrolytic dissociation constants.

ence of buffers gives a little improvement in tensile strength.

Next, using 2.35% N cyanoethylated cotton fabrics, the partial amidoximation was carried out as above. The nitrogen content of the acid-scoured amidoximate was 2.83%. The tear strength by the Elmendorf's pendulum tester and the crease resistance by the T.B.L. method were determined and are shown in Table II and Figure 1. It is noteworthy that as the electrolytic dissociation constant K of the acid component in the buffers decreases, the tear strength is improved at less sacrifice of crease resistance. It is considered probable that the buffers might act to diminish the hydrolysis of amidoxime or hydroxamic acid groups and the formation of the short formal cross-links as expected.

In addition it is interesting to note that when the crease resistance and the log of the tear strength are each plotted against the log of the geometric mean of K, expressed by

$$1/n \sum_{i=1}^{n} (\log K_i)$$

where n is basicity of acid, linear relationships as shown in Figures 2 and 3 are found.

Literature Cited

1. Negishi, M., Itō, H., and Aida, N., TEXTILE RESEARCH JOURNAL **29**, 990 (1959).
2. Negishi, M., Itō, H., and Takahashi, K., TEXTILE RESEARCH JOURNAL **30**, 999 (1960).
3. Schouteden, F. L. M., *Makromol. Chemie* **27** (3), 246 (1958).

MICHIHARU NEGISHI
HEIHACHIRO ITŌ
TOSHIYUKI KURAMOCHI

Book Reviews

Soviet Research on the Swelling of Cellulosic Materials 1949–1956. New York, Consultants Bureau Enterprises, Inc. [1960]. v + 262 pages. Price $25.00.

Reviewed by Dr. L. Rebenfeld, Texile Research Institute, Princeton, New Jersey

This paper bound volume is a collection of translated Russian articles, pertaining to the swelling of cellulosic materials, which were selected and organized by Dr. Harold Tarkow of the Forest Products Laboratory, U. S. Department of Agriculture. The papers were chosen from previously translated, pertinent articles appearing between 1949 and 1956 in the following Russian journals: Bulletin of the Academy of Sciences of the USSR, Colloid Journal, Journal of Applied Chemistry, Journal of General Chemistry, and Proceedings of the Academy of Sciences of the USSR (Chemistry Section).

The contents of this volume are divided into four sections. The first, entitled "Basic Science," consists of 24 papers dealing with the kinetics and thermodynamics of the sorption and swelling processes. Several of these papers deal with polymeric materials other than cellulose, but these are included because of their obvious relationship to a study of cellulose swelling. Particular emphasis in this section is on papers dealing with heats of wetting of polymeric materials. The second section, entitled "Chemical Effects," consists of 13 papers which deal with subjects where chemical reactions clearly take place. The papers in this section might better be classified as dealing with the reactivity of cellulose and related polysaccharides. The third section, entitled "Industrial Considerations," is a group of six papers where it was felt that distinct industrial applications might arise. The final section, "Techniques," is composed of three papers in which special techniques for studying swelling are discussed.

In view of the importance of swelling of textile fibers during processing and use, the value of a thorough understanding of this physico-chemical phenomenon is undisputed. The papers in this volume are a distinct contribution to the available literature, and the publishers have performed a service in making them available in a single volume.

Biological Degradation of Cellulose. J. A. Gascoigne and Margaret M. Gascoigne. London, Butterworths, 1960. 257 pp. Price $8.00.

Reviewed by Dr. L. Rebenfeld, Textile Research Institute, Princeton, N. J.

The biological decomposition of cellulose is of both scientific and practical significance. As is well

pointed out in the preface to this book, biological decomposition of cellulose has direct bearing on the textile, wood, paper, and fermentation industries. The authors have performed a distinct service to these industries as well as to the research man in summarizing in this volume the enzymological background to the biological decomposition of cellulose.

The first chapter is a review of the chemistry and physics of cellulose and cellulose derivatives, and also contains a brief discussion and classification of enzymes. This introduction, while quite superficial, undoubtedly is sufficient to introduce the reader to the further study of biological decomposition. The second chapter discusses in a general manner the enzymes which are involved in chemical reactions of β-glycosides with particular attention to β-glucosidase. The next four chapters, comprising the bulk of this book, consider the sources, purification, properties, and modes of action of cellulolytic enzymes. An extensive table indicates the sources of cellulase and classifies these materials according to their origin: animal, plant, fungal, and bacterial cellulases. In these chapters on cellulolytic enzymes attention is given to both the organic and physical chemistry of such systems, and consideration is given to enzymic decomposition of cellulose and cellulose derivatives.

A brief chapter is devoted to the occurrence and action of hemicellulases with particular emphasis on pentosanases, which have received most rigorous attention from research.

The last chapter is concerned with the industrial significance of cellulases. The degradation of cellulosic textiles, particularly cotton, and the chemistry of the biological decay of wood and wood products are considered.

This short book contains more up-to-date information on the subject than is available from any other single source. It is a most worthwhile addition to the scientific literature and fills an important gap. An extensive bibliography to the original scientific literature, at the end of each chapter, makes this a particularly useful reference book for the beginner as well as the seasoned researcher in the field of biological decomposition of cellulose and cellulose derivatives.

Cellulose Research Symposium, II—1958. New Delhi, India, Council of Scientific and Industrial Research [1960]. ii and 156 pp. Price sh. 20/–.

This publication comprises some twenty-three review papers presented in 1958 at Dehra Dun at the Second Symposium organized by the Cellulose Research Committee of the C.S.I.R. The papers are grouped in five sections: Structure and Physical Properties of Cellulose (8 articles), Chemistry and Technology of Cellulose (6 articles), Chemical Pulp and Rayon Industry (2 articles), Mechanical Pulp with Special Reference to Paper Industry (4 articles), and Microbiological Studies on Fibre Degradation (2 articles). One article in Cellulose Physics deals with the structure and mechanical properties of cellulose.

While some of the papers contain original contributions, most of them represent accounts of the progress of cellulose research accomplished in the past years, and are available in the original literature.

Information for Contributors

Subject Matter

There are five principal classes of contributions suitable for the JOURNAL: (1) fundamental research articles, presenting important new information and data in any area of science related to the textile field; (2) technical papers describing development work, engineering advances, and innovations in manufacture and processing; (3) laboratory techniques with sufficient experimental data to illustrate the utility of methods or equipment described; (4) Letters to the Editor, seldom exceeding 1000 words, which are intended for prompt publication of new discoveries or observations, or for informative comment on papers previously published in the JOURNAL; (5) review articles of an authoritative and critical nature on a topic of major importance.

With the exception of Letters to the Editor, all submitted manuscripts are sent to qualified persons for review and critical comment. The names of reviewers are not disclosed without their consent.

Preparation of Manuscripts

Arrangement—Any logical arrangement of the subject matter is acceptable.

Style—The JOURNAL's style guides are "Webster's Unabridged Dictionary" and the "Government Printing Office Style Manual."

Authors' Names and Affiliations—This information should be given exactly as it is to appear in print. If the author is no longer with the company where the work was done, his new affiliation should be given in a footnote.

Typing—Manuscripts should be typed, *double-spaced; two copies must be submitted.*

Abstract—A brief abstract (about 150 words) should accompany each paper.

Equations and Formulas—Equations are numbered in parentheses to the right; they are referred to in the text as Equation 2, Equation 11a, etc. (no parentheses). All equations should be checked carefully by the author to avoid costly alterations which require hand-setting of type. Exponents and subscripts should be legible and properly positioned. There should be a clear distinction between small and capital letters, between 1 (one) and l (el), and between the letter O and zero. Fairly simple structural formulas can be set in type; complicated ones should be lettered in *India ink* on a separate sheet of paper, from which a plate will be made. Greek letters should be written clearly; it is helpful to spell out the name of an unfamiliar symbol in the margin.

Illustrations—Drawings and graphs should be in *India ink* on white paper or blue tracing cloth, or clear glossy photographic prints of such drawings. Engravings cannot be made of drawings in blue ink. It is essential that all lines be strong and solid; when the drawing is reduced the lines become thinner and discontinuities are accentuated. Lettering must be large enough to accommodate reduction; the following guide will be helpful:

Size of Original	Height of Letters
4 × 5	2–3 mm.
8 × 10	4–5 mm.
10 × 16	8+ mm.

Titles should not appear on the drawings; they will be set in type below the figures and should be submitted together on a separate sheet. Any legible reproduction of the figures may accompany the second copy of the manuscript.

Photographs—Photographs should be glossy prints, clear, sharp, and with as much contrast as possible without loss of detail. Identification of the figures should be made very lightly on the back with a soft pencil.

Literature Cited—All references cited in the text should be given in brackets, e.g., [2] by numerals corresponding to a numbered list, *arranged alphabetically by author,* at the end of the paper. The information should be given in the following order: authors' names, initials, name of publication, volume number, (place of publication and publisher for a book), inclusive page numbers, and year of publication. Abbreviations of journal titles follow those used by *Chemical Abstracts.*

In Coming Issues

Studies in the Light Absorption of Dyes. Part IV: The Relation of Transmission and Reflection of Light by Diffusing Materials to Concentration of Color. *C. H. Giles, S. M. K. Rahman, and D. Smith*

Lightfastness Studies of Basic Dyes on Acid-Modified "Dacron" Polyester Fiber. *S. B. Maerov and H. Kobsa*

Stress-Strain Relationships in Yarns Subjected to Rapid Impact Loading. Part VII: Stress-Strain Curves and Breaking-Energy Data for Textile Yarns. *Jack C. Smith, Paul J. Shouse, Josephine M. Blandford, and Kathryn M. Towne*

Wool Fabric Stabilization by Interfacial Polymerization. Part I: Polyamides. *R. E. Whitfield, L. A. Miller, and W. L. Wasley*

Adsorption of Direct Cotton Dyes by Chemically Modified Celluloses. *E. H. Daruwalla, P. J. Kangle, and G. M. Nabar*

Twist and Tension as Factors in Yarn Characteristics. *K. Sreenivasan and K. S. Shankaranarayana*

The Theory of Shrinkproofing of Wool.

Part II: A Method for Determination of the Force on a Fiber During Felting. *J. H. Bradbury and H. Groll*

Part III: Chemical Modification of the Fiber Surface and Its Effect on Felting Shrinkage, Friction, and Microscopic Appearance. *J. H. Bradbury*

The Influence of Changes in Moisture Content on the Wrinkle Recovery of Fabrics, Parts I and II. *A. J. Farnworth and Joel Lindberg*

A Study of Reactions between Cotton Cellulose and Difunctional Epoxides. *Ruth R. Benerito, Beverly G. Webre, and J. B. McKelvey*

FRL ENVIRONMENTAL TEST CHAMBER

MODEL CS-90

FOR
ELEVATED
AND
REDUCED TEMPERATURE TESTING
IN THE
INSTRON TENSILE TESTER

The FRL Chamber was designed in 1955 by Fabric Research Laboratories, Inc., Dedham, Mass., for use in extreme temperature studies of filamentous materials.

Accuracy: ±2°F.

Atmosphere: Air or inert gas.

Range: −90°F to +750°F (standard); broader ranges available.

Stabilization time: To 500°F in one-half hour; To −90°F in one hour.

Size: Volume approx. 3,000 cu. in.; Maximum throw with Instron jaws is 18 in.; Special attachment permits 23½ in. throw and adapts unit for compression testing.

Versatility: Chamber (which fits any type Instron) is self-contained on hydraulic-lift dolly, easily moved by one person, and can be used in any location independent of the Instron.

Note: Chambers for other units or applications built to order.

Brochures and Price Upon Request

CUSTOM SCIENTIFIC INSTRUMENTS, INC.
541 DEVON ST. KEARNY, N. J.
Tel. WYman 1-6403